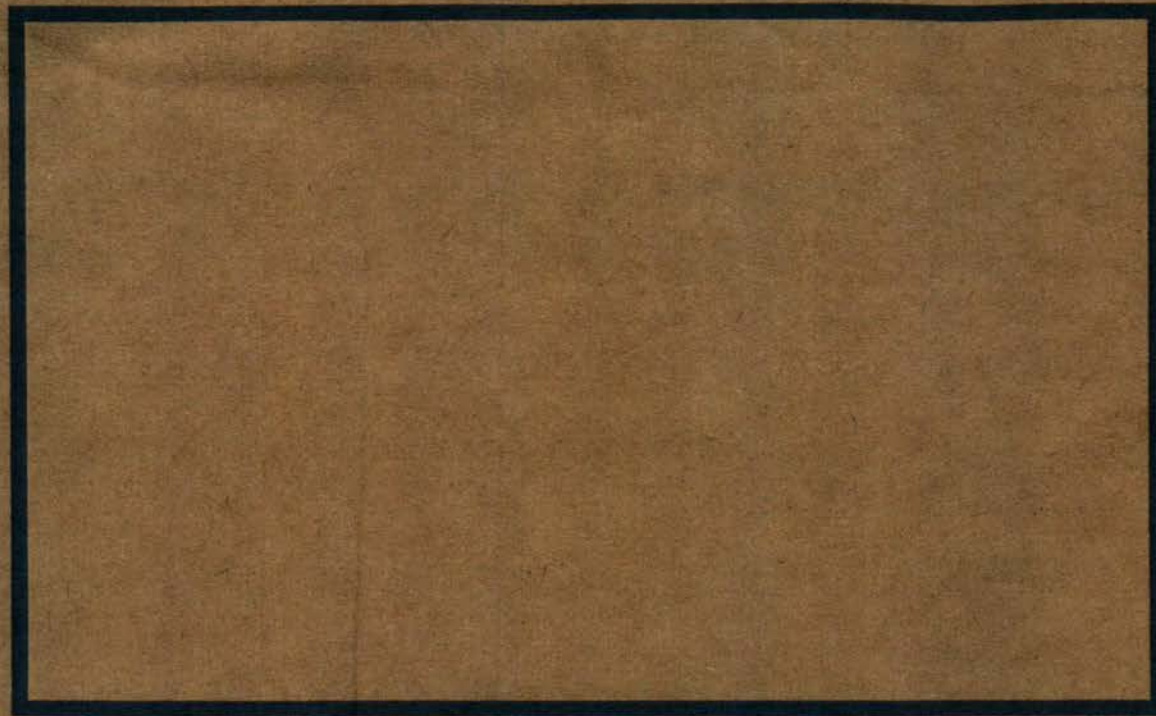


ENG 339-(EQC 2002/SP3)

On improving the seismic performance of precast concrete frames

John B Mander, Department of Civil Engineering, University of Canterbury



ENG
339

Final Report to EQC

Project No 6RSF1C2

**ON IMPROVING THE SEISMIC PERFORMANCE OF
PRECAST CONCRETE FRAMES**

By

John B. Mander

Principal Investigator

Department of Civil Engineering

University of Canterbury

Christchurch, New Zealand

February 2006

GENERAL ABSTRACT

Background

In New Zealand, over the past three decades there has been a complete shift away from constructing buildings using cast-in-place concrete. Nowadays, to speed up the construction process, most multi-storey buildings are constructed using various precast concrete systems. It is therefore not surprising that following the 1994 Northridge earthquake in California, there was much consternation amongst structural engineers as quite a number of the structures that collapsed in that earthquake were of the precast concrete variety. Thus research programmes commenced at both Auckland and Canterbury Universities to investigate whether such a problem would exist with the New Zealand style of precast concrete construction. At the University of Canterbury, work focused on the hollow-core system through a series of full-size super-assembly experiments coupled with companion analysis.

Initial work focused on conducting experiments on a full-scale slice of a representative precast concrete building with precast hollow-core floors. Based on companion computer simulations, loads and displacements were applied to the physical experimental specimen that in the first instance were representative of an earthquake that is likely to be seen within the lifetime of such a structure. This was then followed by a more extreme loading, less likely to occur within the lifetime of the structure, but nevertheless possible. Normal design objectives for these two types of loading are that the structure should survive the first with some repairable damage, and not collapse leading to loss of life in the second.

This original experimental specimen failed to survive both types of applied earthquake loading criteria. Indeed, the collapses seen in the field in California were replicated in the laboratory. Companion analysis confirmed that some 20 percent of such buildings would be expected to collapse in the rare but strong earthquake event.

Research Methods

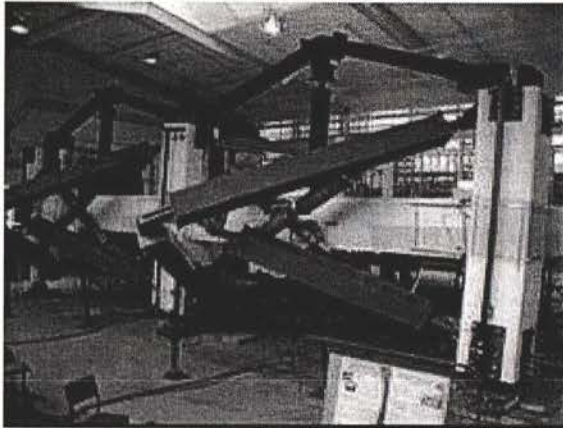
As failures in the existing form of precast concrete construction were confirmed both experimentally and through advanced computer simulation, it was thus considered necessary to investigate what remedial actions and design improvements were necessary for the new generation of precast concrete structures with hollow core floor systems. Based on consultation with the design and construction fraternities, several detailing improvements were proposed for experimental investigation. As a result, two further large-scale experiments were conducted.

The first of these, which was partially supported by EQC funding, investigated a simple (flexible) floor-to-support beam connection. The second experiment, which was essentially fully funded by EQC, investigated a reinforced (rigid) hollow core floor-to-support beam connection. For both experiments, a more onerous loading protocol was adopted to ensure the most adverse form of seismic loads and displacements could be resisted.

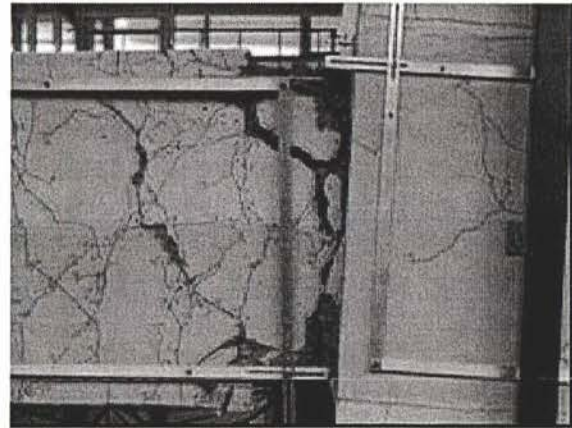
Experimental Results

Both experimental specimens performed well under the imposed simulated seismic loading. Although damage was observed, it was of the sort one would expect for a well designed cast-

in-place concrete structure. Through post-experiment analysis it was shown that all of the damage patterns were explainable and could be predicted using customary engineering theories. For both proposed construction details it was confirmed that the ultimate goal of achieving life-safety in extreme earthquake events was met, as the specimens were capable of deflecting well beyond the most adverse design limits. An example of the appearance of the last experiment, while under test, at an extreme limit is shown in the figures below.



(a) Super-assemblage specimen at +5% interstorey drift.



(b) Damage at the southeast beam-column interface (plastic hinge zone) at +5% interstorey drift

Damage near the end of the super-assemblage test specimen

Research Outcomes

On the strength of the research conducted, the New Zealand Concrete Design Specification (NZS3101:1995) has been officially amended (Amendment 3; 2004). Within that specification there are now improved seating and detailing requirements for precast concrete hollowcore floor systems. These details are also included in a forthcoming re-issue of this specification. The reinforcing design and construction details are of a nature that are deemed to be “acceptable solutions” because they have been specifically validated through large-scale research.

Conclusions

Based on this research (EQC Project No 6RSF1C2) the following main conclusions are drawn:

- Precast concrete buildings possessing hollow-core floor systems built prior to 2004 are liable to possess deficient details that lead to poor seismic performance. The expected annual loss due to on-going seismic activity may be of the order of \$16,000/ \$1million of asset value. Moreover, due to the significant probability of structural collapse, the loss to life and limb may be unduly high.
- It is possible to mitigate the adverse seismic performance of precast concrete structures with hollow-core floors by paying particular attention to specifying acceptable floor-to-support beam details that toughen the structure and impose controlled deformations that do not lead to collapse. For such a system, the expected annual loss due to on-going seismic activity should be less than \$1,000/ \$1million of asset value. The probability of collapse and/or loss of life should also be acceptably low.

ACKNOWLEDGEMENTS

The work reported herein would not have been possible without the generous support of the Earthquake Commission (EQC). The work was either partially or fully funded by a grant to the Principal Investigator from the Earthquake Commission (EQC) under Project No 6RSFIC2 "*On improving the seismic performance of precast concrete frames.*" The Principal Investigator gratefully acknowledges this support. Any opinions reported herein are those of the authors, and should not be construed to be held as the view of EQC or other sectors of the engineering profession.

The Principal Investigator also wishes to thank his collaborators and co-authors for all their efforts bringing this ongoing project to fruition.

CONTENTS

General Abstract

Acknowledgements

Contents

Preface

Technical Summary

References

- Paper 1: "Economic payback of improved detailing for concrete buildings with precast hollow-core floors," by Dhakal, R. P., Khare R.K., and Mander, J. B.
- Paper 2: "Hollowcore Floor slab performance following a severe earthquake," by Matthews J.G., Bull D.K., and Mander J.B.
- Paper 3: "Prediction of beam elongation in structural concrete members using a rainflow method," by Matthews J.G., Mander, J.B., and Bull D.K.
- Paper 4: "Preliminary results from experiments on hollow-core floor systems in precast concrete buildings," by Lindsay, R., Mander, J., and Bull, D.
- Paper 5: "Experiments of the Seismic Performance of Hollow-core Floor Systems in Precast concrete Buildings," by Lindsay, R., Mander, J., and Bull, D.
- Paper 6: "Reinforced concrete seating details of hollow-core floor systems," MacPherson C.J., Mander, J.B., and Bull, D.K.
- Paper 7: "The seismic fragility of precast concrete buildings," by Matthews J., Lindsay, R., Mander, J.B., and Bull, D.

PREFACE

In New Zealand, over the past three decades there has been a complete shift away from constructing buildings using cast-in-place concrete. Nowadays, to speed up the construction process, most multi-storey buildings are constructed using various precast concrete systems. It is therefore not surprising that following the 1994 Northridge earthquake there was much consternation amongst structural engineers, as quite a number of structures collapsed in that earthquake that had precast concrete hollow-core floor systems. Thus research programmes commenced at both Auckland and Canterbury Universities. At the University of Canterbury, work focused on the hollow-core floor system through a series of full-size super-assembly experiments coupled with companion analysis.

The work reported herein was sponsored by EQC and focuses on the latter part of the overall research programme. This report consists of a series of papers that have been co-written by various investigators associated with the Principal Investigator and published at various fora. The first paper [1], is a general outline of the overall work. It gives a summary of the experimental components reported in the next five papers [2-6] and companion analytical work [7], and then culminates in developing a financial risk assessment to give the expected annual losses for different classes and qualities of structural detailing of precast floor-to-frame connections. These papers are largely based on the work conducted by post-graduate students Matthews [8], Lindsay [9] and Macpherson [10].

The work reported herein was either sponsored in part [1-5, 7-9] or in whole [6, 10] by EQC.

Following this preface is a technical summary of the research. This has been kept deliberately concise as further details may be found in the papers that follow listed also as references [1-7].

TECHNICAL SUMMARY

Introduction

Precast concrete is common place in modern constructed facilities in New Zealand and elsewhere. In particular, precast concrete frames with hollow-core floors have become the norm for the construction of multistory buildings constructed in New Zealand. While precast concrete is used largely because it speeds up the construction process, it also introduces certain vulnerabilities at articulations between components that potentially make the structure vulnerable to damage in large earthquakes [2, 8]. It is therefore not surprising that following the 1994 Northridge earthquake in California, there was much consternation amongst structural engineers as quite a number of the structures that collapsed in that earthquake were constructed using various precast concrete components.

The initial research work in this series was conducted by Matthews [8] who focused on investigating the seismic performance of precast concrete frames system through a series of analyses on 3, 6, 9, and 12 storey buildings. Informed by probable seismic loading demands on precast concrete frames, he then conducted a major experimental test on a full-size super-assemblage precast concrete frame structure that also had a topped hollow-core precast concrete floor system.

Based on an analysis of seismic demands new loading and displacement protocols were derived. The first loading sequence was aimed to represent a Design Basis Earthquake (DBE) that has 10 percent probability of occurrence in 50 years [return period = 475 years]. A second [and final] loading sequence was also derived aimed at representing the expected level of displacements for a Maximum considered Earthquake (MCE) that has a 2 percent probability in 50 years [return period = 2450 years]. Normal design objectives for these two types of loading are that the structure should survive the DBE with some repairable damage, and not collapse leading to loss of life in the MCE.

This original experimental specimen failed to survive both types of applied earthquake loading criteria. Indeed, the collapses seen in the field following the 1994 Northridge California earthquake were replicated in the laboratory. Given that many structures are designed for a drift limit of 2 percent under a DBE, it was experimentally demonstrated that incipient collapse could occur at drifts less than 1.9 percent. Companion probabilistic seismic fragility-based analyses confirmed that some 20 percent of such buildings would be expected to collapse in the MCE event [7, 8]. Moreover, the total probable loss ratio is expected to be some 30 percent for a DBE and exceeds 50 percent for an MCE event [1]. Associated with such losses is the potential for loss of life due to partial or total collapse.

Matthews work concluded that if hollow-core floor systems are to continue as a preferred method of construction in modern precast concrete buildings, then it is imperative that further research be conducted on developing new solutions that would lead to improved detailing and construction practice [2]. To this end further theoretical [1, 3, 7] and experimental studies [4, 5, 6, 9, and 10] have been undertaken as part of the present EQC-supported research and is the subject of the papers that follow this Technical Summary.

Research Hypotheses and Methodology

As field-observed failures in the existing form of precast concrete construction were confirmed both experimentally [2, 3, and 8] and through advanced computer simulation [1, 7 and 8], it was thus considered necessary to investigate what remedial actions and design improvements were necessary for the new generation of precast concrete structures with hollow-core floor systems. Based on consultation with the design and construction fraternities through an *ad hoc* Technical Advisory Group (TAG), several detailing improvements were proposed for experimental investigation. As a result, two further large-scale experiments were conducted [9 and 10].

The first of these experiments [9], which was partially supported by EQC funding, investigated a simple (flexible) floor-to-support beam connection as shown in Figure 1.

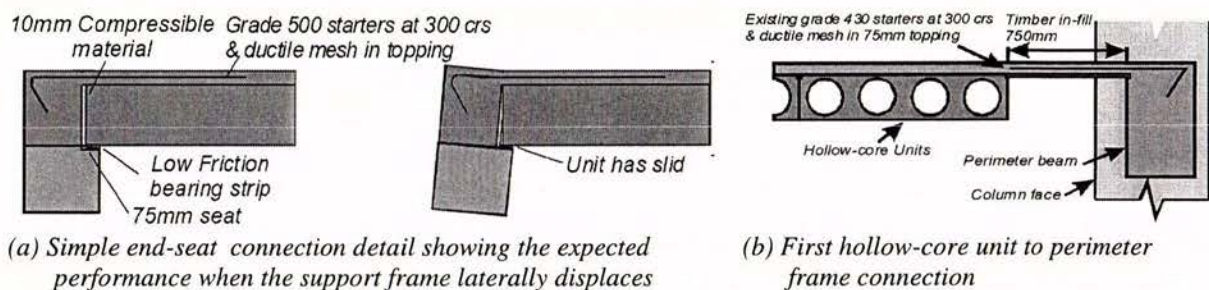


Figure 1. Simple hollow-core seating connection details [4,5 and 9].

The details of the second experiment [10], which was essentially fully funded by EQC, are shown in Figure 2. This experiment primarily investigated a reinforced (rigid) hollow-core floor-to-support beam connection (Figure 2a). Also, based on the results from the first experiment, several detailing improvements were made to the perimeter beam to hollow-core connection (Figure 2b).

For both experiments, a more onerous (proof-testing) type of cyclic loading protocol was adopted to ensure the most adverse form of seismic loads and displacements could be resisted.

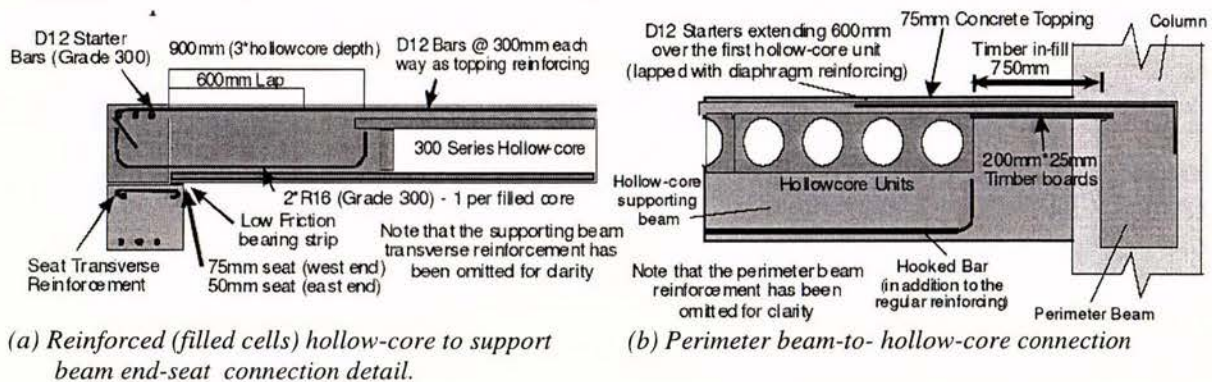
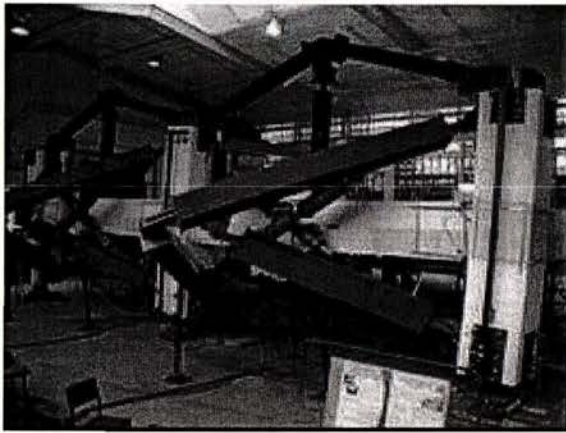


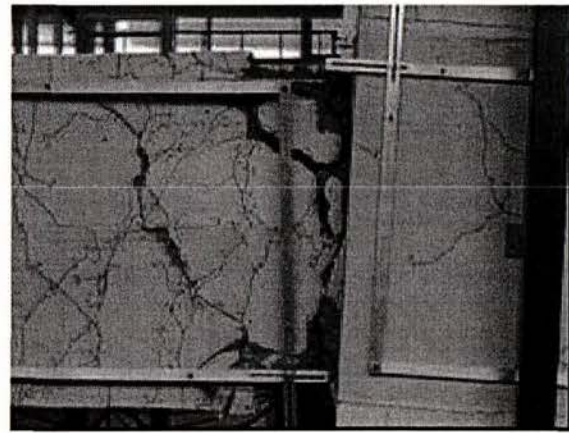
Figure 2. Reinforced hollow-core support connection details [7, 10].

Experimental Results

Both experimental specimens performed well under the imposed simulated seismic loading. Although damage was observed, it was of the sort one would expect for a well designed cast-in-place concrete structure. Through post-experiment analysis [3, 9, 10] it was shown that all of the damage patterns were explainable and could be predicted using customary engineering theories. For both proposed construction details it was confirmed that the ultimate goal of achieving life-safety in extreme earthquake events was met, as the specimens were capable of deflecting well beyond the most adverse design limits. An example of the appearance of the last experiment, while under test, at an inter-storey drift limit of 5 percent—which is well beyond the required 3.5 percent drift limit to survive the MCE—is shown in Figure 3.



(a) Super-assemblage specimen at +5% inter-storey drift.



(b) Damage at the southeast beam-column interface (plastic hinge zone) at +5% inter-storey drift

Figure 3. Damage of the super-assemblage test specimen

Research Outcomes

On the strength of the research conducted, the New Zealand Concrete Design Specification (NZS3101:1995) has been officially amended (Amendment 3; 2004). Within that specification there are now improved seating and detailing requirements for precast concrete hollowcore floor systems, similar to those shown in Figures 1 and 2. These details are also included in a forthcoming re-issue of that specification. The two hollow-core floor to seat design and construction details are of a nature that are deemed to be “acceptable solutions” because they have been specifically validated through large-scale research described in this report.

Follow-up analytical research has investigated the financial losses that may result from the universal set of earthquakes for the pre-2004 and post-2004 hollow-core floor seating details [1]. Results of that study show that the expected annual loss due to on-going seismic activity may be of the order of \$16,000/ \$1million of asset value for building designed and constructed with the faulty pre-2004 details. This is in stark contrast with well detailed systems that conform to the post-2004 details where the expected annual loss due to on-going seismic activity should be less than \$1,000/ \$1million of asset value. Note that these losses are direct structural losses and do not account for non-structural (fittings and contents) damage, downtime, or the effective societal costs resulting from the loss of life and limb.

Conclusions

Based on this research (EQC Project No 6RSF1C2) the following main conclusions are drawn:

1. Precast concrete buildings possessing hollow-core floor systems built prior to 2004 are liable to possess deficient details that lead to poor seismic performance. The expected annual loss due to on-going seismic activity may be considerable. Moreover, due to the significant probability of structural collapse, the loss to life and limb may be unduly high.
2. It is possible to mitigate the adverse seismic performance of precast concrete structures with hollow-core floors by paying particular attention to specifying acceptable floor-to-support beam details that toughen the structure and impose controlled deformations that do not lead to collapse. As a result of this research, concrete design specifications have been enhanced. Thus for such post-2004 modified details, the expected annual loss due to on-going seismic activity is quite low. The probability of collapse and/or loss of life should also be acceptably low; in-keeping with the expectations of current best practice.

REFERENCES

- 1 Dhakal, R. P., Khare R.K., and Mander, J. B., (2006) "Economic payback of improved detailing for concrete buildings with precast hollow-core floors", Bulletin of the NZ Society for Earthquake Engineering, *submitted for possible publication*
- 2 Matthews J.G., Bull D.K., and Mander J.B., (2003) "Hollowcore Floor slab performance following a severe earthquake," fib Conference, Athens, May 2003.
This paper won the "Otto Glogau Award 2004". This was awarded by the NZ Society for Earthquake Engineering. The paper formed the basis for the 2004 Amendment 3 made to the NZ Concrete Standard NZS3101:1995.
- 3 Matthews J.G., Mander, J.B., and Bull D.K., (2004) "Prediction of beam elongation in structural concrete members using a rainflow method" 2004 NZSEE Conference, Rotorua, Paper 27, 8 pp.
- 4 Lindsay, R., Mander, J., and Bull, D., (2004) "Preliminary results from experiments on hollow-core floor systems in precast concrete buildings" 2004 NZSEE Conference, Rotorua, Paper 33, 8 pp
- 5 Lindsay, R.A., Mander, J.B., and Bull, D.K., (2004) "Experiments of the Seismic Performance of Hollow-core Floor Systems in Precast concrete Buildings" 13th World conference on Earthquake Engineering, Vancouver, Canada, August 1-6, CD ROM paper No. 585.
- 6 MacPherson C.J., Mander, J.B., and Bull, D.K., (2005) "Reinforced concrete seating details of hollow-core floor systems," 2005 NZSEE Conference, Wairakei, CD ROM Paper Number 24, 9pp
- 7 Matthews J., Lindsay, R., Mander, J.B., and Bull, D., (2005) "The seismic fragility of precast concrete buildings" International Congress on Structural Safety and Reliability ICOSSAR 2005, Rome, Augusti, Schueller and Ciampoli (eds), Millpress, Rotterdam, pp 247-254.
- 8 Matthews, J., (2004) "Hollow-core floor slab performance following a severe earthquake", PhD Thesis, University of Canterbury
- 9 Lindsay R., (2004) "Experiments on the seismic performance of hollow-core systems in precast concrete buildings." ME Thesis, University of Canterbury.
- 10 Macpherson C., (2005) "Seismic performance and forensic analysis of a precast concrete hollow-core floor super-assembly." ME Thesis, University of Canterbury.

ECONOMIC PAYBACK OF IMPROVED DETAILING FOR CONCRETE BUILDINGS WITH PRECAST HOLLOW-CORE FLOORS

R. P. Dhakal¹, R. K. Khare², J. B. Mander³

SUMMARY

A seismic financial risk analysis of typical New Zealand reinforced concrete buildings constructed with topped precast concrete hollow-core units is performed on the basis of experimental research undertaken at the University of Canterbury over the last five years. An extensive study that examines seismic demands on a variety of multi-storey RC buildings is described and supplemented by the experimental results to determine the inter-storey drift capacities. Results of a full-scale precast concrete super-assembly constructed and tested in the laboratory in two stages are used. The first stage investigates existing construction and demonstrates major shortcomings in construction practice that would lead to very poor seismic performance. The second stage examines the performance of the details provided by Amendment No. 3 to the New Zealand Concrete Design Code NZS 3101:1995. This paper uses a probabilistic financial risk assessment framework to estimate the expected annual loss (EAL) from previously developed fragility curves of RC buildings with precast hollow core floors connected to the frames according to the pre-2004 standard and the two connection details recommended in the 2004 amendment. Risks posed by different level of damage and by earthquakes of different frequencies are examined. The structural performance and financial implications of the three different connection details are compared. The study shows that the improved connection details recommended in the 2004 amendment give a significant economic payback in terms of drastically reduced financial risk, which is also representative of smaller maintenance cost and cheaper insurance premiums.

1. INTRODUCTION

Concrete buildings that use precast prestressed hollow-core floor units have been the dominant form of construction in New Zealand (NZ) over the last three decades. Failures observed after the 1994 Northridge earthquake have raised some concerns regarding the performance of NZ's multi-storey moment resisting RC frame buildings having precast concrete hollow-core floors. This is because NZ construction methods are similar to that used in the US and several of US precast buildings did not perform adequately during the Northridge earthquake. Several buildings in Northridge collapsed as a result of the hollow-core flooring units losing their seating from the supporting beams [1]. Once the beam support was lost, the units collapsed onto the floor below.

Based on their experimental investigations Matthews et al [2] and Lindsay et al [3] integrated aspects of capacity versus demand by developing a series of probabilistic based fragility curves. These curves are further extended in the present work to include financial loss estimation. An earthquake - recurrence relationship is defined to transform spectral acceleration to annual frequency. A loss ratio, which is the ratio of the repair cost necessary to restore the full functionality of the structure to the replacement cost, is then assigned to each damage state observed experimentally. Expected annual loss is calculated using the

extension of the PEER triple integral formulation [4], extended by Dhakal and Mander [5] to a quadruple integral equation. A comparison in the estimated loss of pre- and post-amendment precast concrete buildings of New Zealand is made and discussed. Limitations of the study and sensitivity to various parameters are reported. Comments useful to owners and insurers of the buildings are made from an insurance point of view. Work done by Matthews [6], Lindsay [7] and MacPherson [8] is adopted in the present paper as a basis for this economic analysis.

2. SUMMARY OF PREVIOUSWORK

After observing the failures in Northridge a multi-stage study was undertaken at the University of Canterbury, to determine whether NZ designed and built structures have similar problems, and if so, to what extent these problems exist and what can be done about them.

At first, an extensive study that examined the seismic demands on a variety of precast concrete multi-storey buildings was examined by Matthews [6]. Experimental studies were then performed in two stages to determine the inter-storey drift capacities of multi-storey RC buildings with precast concrete hollow-core floors. A series of large scale experiments were conducted on a full scale super-assembly in order to ascertain the inter-storey drift corresponding to various damage states. Stage 1 of the experimental study examined the then-existing precast

¹ Senior Lecturer, Department of Civil Engineering, University of Canterbury, Private Bag 4800, Christchurch, NZ

² Professor, Department of Civil Engineering, S.G. S. Institute of Technology & Science, Indore - 452003, India

³ Professor, Department of Civil Engineering, University of Canterbury, Private Bag 4800, Christchurch, NZ

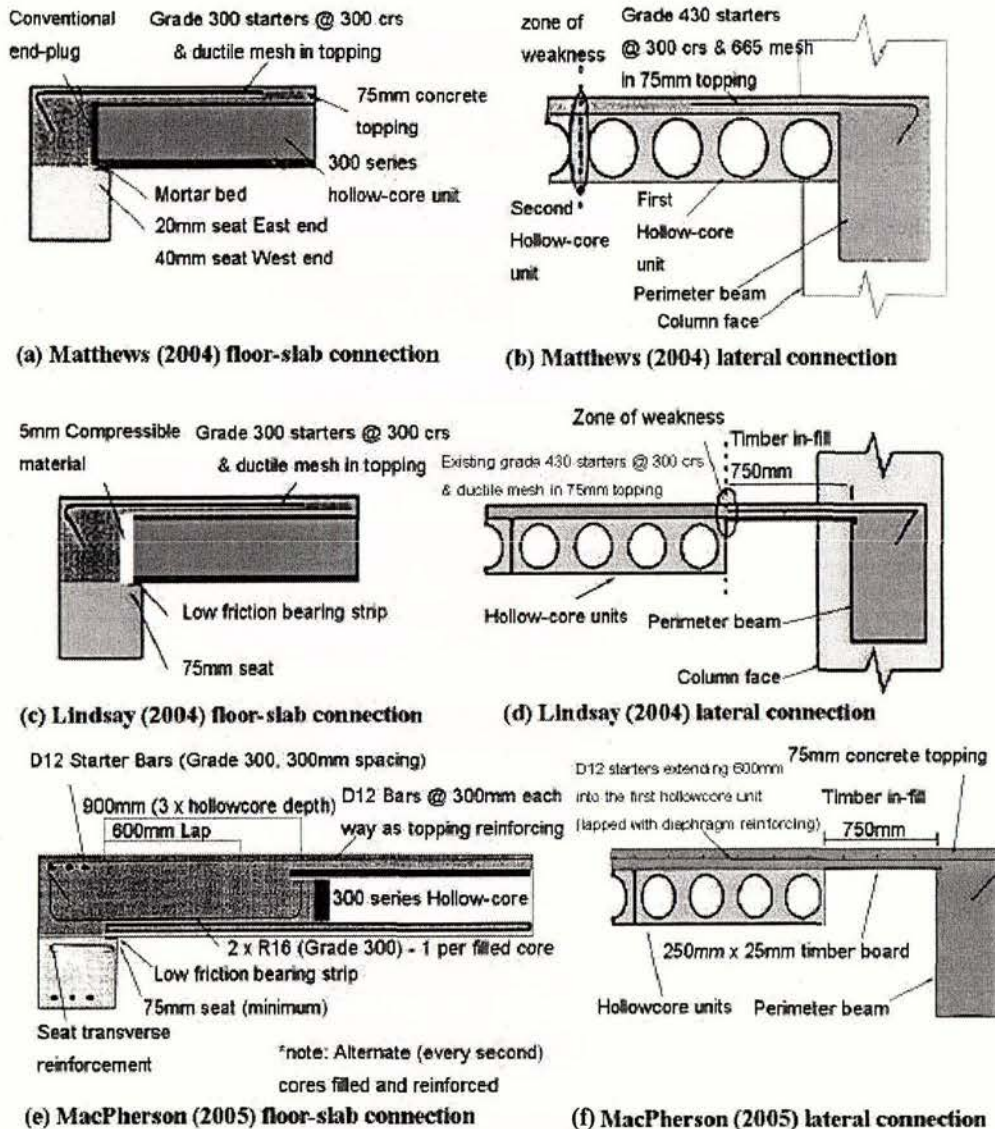


Figure 1: Hollowcore connection details used by Matthews [6], Lindsay [7] and MacPherson [8].

concrete detailing practice in NZ, as recommended by the NZ concrete standard NZS3101:1995 [9]. The collapse of hollow-core units during the tests by Matthews [6] in stage 1 flagged issues over the performance of existing precast concrete frame structures with hollow-core flooring structural systems. In stage 2, Lindsay [7] and MacPherson [8] tested and reported the improved performance of similar super-assembly incorporating the floor-frame connection details as recommended in Amendment No. 3 to the New Zealand Concrete Design Code NZS3101:1995 [9].

2.1 Experimental Assessment of Drift Capacity

A full scale super-assembly experimental set-up was conceived and a new testing methodology was developed to investigate the 3D seismic performance of concrete frames with precast floors. The super-assembly specimen was a two-bay by one-bay section of a lower storey in a multi-storey RC moment resisting frame. The floor units were pre-

stressed precast hollow-core units that were oriented so that they run parallel with the long edge of the building, past a central column. The connection details of hollow-core units used in the experimental programme are shown in Figure 1. The super-assembly was tested in two stages as follows:

Stage 1: Matthews [6] first tested the super-assembly specimen, emulating the 1980's and 1990's construction practice that has historically become the norm in NZ. The reinforcing details were in accordance with NZS3101:1995 [9]. Due to inadequate seating (Figure 1a), as well as displacement incompatibilities between the frame and the floor (Figure 1b), the experiment showed that premature failure of the flooring system can be expected for design basis earthquakes in NZ. It was demonstrated that the floor-to-beam seat connections of existing precast concrete construction are particularly vulnerable.

Stage 2: Lindsay [7] repaired the damaged plastic hinge zones in the frame, and then reconstructed the floor by using modified seating details. Amendment No.3 to NZS3101:1995 [10] provides two details for the connection of hollow-core floor units to the supporting beams. Lindsay [7] reported on the performance of the first of these, with following three specific structural detailing aspects:

1. Improving the seating connection detail between the precast, prestressed hollow-core floor diaphragm and the perimeter reinforced concrete moment resisting frame (Figure 1c).
2. Stopping the central column from displacing laterally out of the building due to an insufficient lateral tie into the building. It was because of this lack of interconnection that the floor slab tore longitudinally due to displacement incompatibility in Matthews test. The central column was not restrained and was able to translate freely outwards in Matthews test.
3. Isolating the first hollow-core unit spanning parallel to the perimeter beams from the frame to avoid displacement incompatibility (Figure 1d). This displacement incompatibility was caused by the units being forced to displace in a double curvature manner due to being effectively connected to the edge of the perimeter beam, when hollow-core units are not designed for such displacement profiles.

The second detail of NZS3101:1995 [9] specifies a reinforced connection that rigidly ties the floor into the supporting beam (Figure 1e). MacPherson [8] investigated the effectiveness of this solution by testing large-scale three-dimensional specimen. The super-assembly tested by MacPherson included the following details:

1. A reinforced connection that rigidly ties the floor into the supporting beam (Figure 1e).
2. An articulated topping slab portion cast on a timber infill that runs parallel to and connects the hollow-core units and edge beams (Figure 1f).
3. Specially detailed supporting beam plastic hinge zones to reduce potential damage to the hollow-core units
4. Grade 500E reinforcing steel used in the main frame elements
5. Mild steel deformed bars in the concrete topping in lieu of the customary welded wire mesh.

2.2 Classification of observed building damage

A common form of damage classification is to use a numerical indicator format as adopted by HAZUS [11]. As given in Table 1, numbers from one and five that refer to increasing level of damage are used

Table 1 HAZUS classification of damage states following an earthquake [11]

Damage State	Damage Descriptor	Post-earthquake Utility of Structure
1	None (pre-yield)	Normal
2	Minor / Slight	Slight Damage
3	Moderate	Repairable Damage
4	Major / Extensive	Irreparable Damage
5	Complete Collapse	

Based on post-earthquake utility and life-safety considerations, the drift limit states for different level of damage are summarised in Table 2. The values of drifts corresponding to different damage states listed in the 2nd, 3rd, and the 4th columns of Table 2 have been decided based on experimental results [6-8]. Similarly, the drifts corresponding to different level of damage of the seismic frames stipulated in the last column of Table 2 have been decided based on the requirements of NZ standard [9, 10].

Table 2 Damage state classification for the super-assembly

Damage State	Inter-storey drift based on:			
	Historical [Ⓐ] floor detailing practice	Modern [Ⓝ] detailing practice for floors and their connections		Historical [Ⓐ] and current [Ⓝ] frame detailing practice
		Detailing 1	Detailing 2	
2	0.3%	1%	1%	1%
3	0.35%	2%	2%	2%
4	1.9%	2.25%	4%	4%
5	2.5%	5%	5%	6%

[Ⓐ] 1985-2003 details to NZS 3101
[Ⓝ] 2004 Amendment 3 to NZS 3101:1995

Note that the drift values given in Table 2 are the global inter-storey drift which would have caused different level of damage in the specified component (floor, frame) provided that the other components of the building remain perfect. Hence, the inter-storey drifts corresponding to frame damage (final column of Table 2) are immaterial in buildings with precast hollow-core floors as the floor or the floor-to-frame connections (prior to the frame) would damage to a similar or larger extent at the same global inter-storey drift. Nevertheless, these values help realize the extent of weakness the floors with different connection detail impart to the building.

For example, it is apparent that the building would have minor or no damage until 2% drift if the floors were not included or if the floors and the connections were perfect. But the inclusion of precast hollow-core floor with pre-2004 connection detail weakens the building to such an extent that it would be severely and irreparably damaged at 2% drift. Despite implementing the improved detailing 1, performance of the building with floor will still be weaker compared to that of building with no floor or perfect floor. As can be seen in Table 2, the building with improved floor-frame connection using detailing 1 would have extensive or irreparable damage at 2.25% drift, whereas at the same level of drift similar buildings with perfect/no floor would experience repairable moderate damage only. Further improvement of the floor-frame connection using detailing 2 would bring the building performance almost on par with the frames; in other words, floors with detailing 2 will not impair the building performance.

2.3 Assessment of Drift Demand

Matthews [6] used the approach developed by Cornell et al [12] for steel structures and further extended by Lupoi et al [13] for the seismic design of reinforced concrete structures for probabilistic assessment of drift demand on a family of seismically vulnerable multi-storey concrete buildings with precast hollow-core floor units designed and constructed in

NZ during the period from 1985 to 2003. To assess the expected seismic demands on a concrete structure, nonlinear time history analyses were undertaken. In order to simulate the likely seismic performance of the test buildings, a suite of earthquake records was chosen for the time history analysis. The dimensions of the "prototype buildings" investigated were based on a representative sample of buildings idealised from professional practice in NZ from the 1980's through 1990's. Results of the time history analyses were normalised so that all the various forms of earthquake motions had a common variable. Results were plotted in the form of cumulative distribution versus drift index proportionality parameter 'a = Drift / Spectral Acceleration ($F_v S_1$)' as shown in Figure 2.

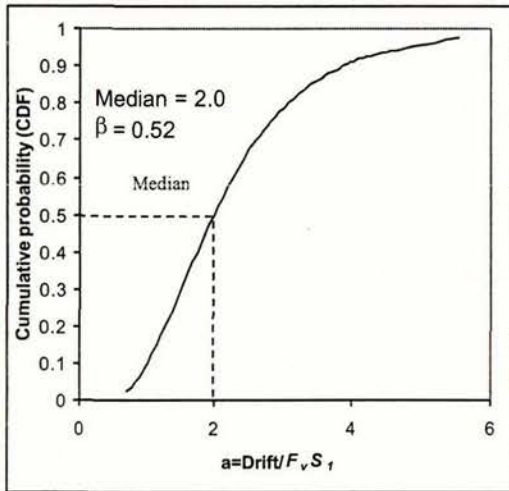


Figure 2: A cumulative function plot for the New Zealand concrete buildings.

It was shown that the results conformed quite well to a cumulative lognormal probability distribution with a median value of 2.0 and dispersion factor (lognormal coefficient of variation) of 0.52. Hence, the relationship between the median drift and the spectral acceleration can be mathematically expressed as:

$$\tilde{D}_D = 2.0(F_v S_1)_D \quad (1)$$

in which D_D = the median (50th percentile) drift demand as a percentage of the storey height, $(F_v S_1)_D$ = one second spectral acceleration. Inverting Equation (1), the expected value of ground motion demand needed to achieve a given median drift capacity can be calculated as:

$$(F_v S_1)_c = 0.5 \tilde{D}_c \quad (2)$$

where D_c = expected drift capacity of the structure, which is difficult to be determined precisely. Although full-scale experiments may give a good indication of the expected capacity, uncertainties are bound to be associated with this determined drift capacity. Acknowledging this, a lognormal distribution function was assumed for the drift capacity and a lognormal coefficient of variation $\beta_c = 0.2$ was used as suggested by Dutta [14].

When capacity and demand are merged in design, uncertainties of both components need to be taken into account. As explained earlier, the uncertainty in drift demand has a lognormal coefficient of variation of $\beta_D = 0.52$. When merging lognormal distribution [15], the resultant lognormal coefficient of variation can be calculated as:

$$\beta_{C/D} = \sqrt{\beta_c^2 + \beta_D^2 + \beta_U^2} \quad (3)$$

where β_U = dispersion parameter to account for modelling uncertainty, taken here $\beta_D = 0.2$. Applying (3) gives $\beta_{CD} = 0.6$. By using a lognormal cumulative distribution that can be described by a lognormal variate ξ_β (where the median = 1 and the lognormal coefficient of variation, $\beta_{CD} = 0.6$), the distribution of ground motion demands needed to produce a given state of damage can be found by

$$F_v S_1 = 0.5 \tilde{D}_c (DS) \xi_\beta \quad (4)$$

where $D_D(DS)$ = the expected drift (in this case, the experimentally observed drift) corresponding to a given damage state (DS) as listed in Table 2.

2.4 Generation of Fragility Curves

Using the ground motion demand for a median drift capacity calculated from Equation (2) and the resultant lognormal coefficient of variation determined earlier, the probability of building response being within a given drift limit can be calculated. Replacing drift with damage states using Table 2 will then give the fragility curves, which show graphically the probability of different damage states being exceeded in an earthquake. For buildings with floor-frame connections designed to pre-2004 standards and post-2004 amendment (detailing 1 and detailing 2) and for similar buildings with perfect/no floors, fragility curves are shown in Figure 3. Two vertical lines are drawn at 0.4g and 0.72g to represent respectively the design basis earthquake (DBE) and the maximum considered earthquake (MCE) at Wellington, following the seismic hazard reported in the loading standard NZS4203:1992 [16]. The intersection of these vertical lines with the fragility curves gives the probability of different damage states for the corresponding seismic hazard.

Figure 3a shows that due to the poor performance of the precast hollow-core floor with old reinforcing and connection details only 2% of buildings with such details would be expected to sustain slight or no damage (within damage state DS2) during an MCE. The remaining 98% buildings would be expected to experience moderate to severe damage (above damage state DS2), of these some 32% would be expected to partially or entirely collapse requiring demolition of the building (above damage state DS4). Similarly it is also evident from Figure 3a that even under a DBE, only 4% of these buildings would escape damage whereas some 8% buildings may still be irreparably damaged or collapsed potentially leading to loss of life.

Figures 3b and 3c show the probability of different extent of damage if the buildings performance is classified in terms of the performances of the precast hollow-core floors with detailing 1 and detailing 2 of post-2004 amendment and the frame performance respectively. Figures 3b and 3c indicate that 70% of buildings with improved connection detailing might be expected to sustain either slight or no damage in an MCE. Figure 3b shows that 23% buildings with floor-frame connection detailing 1 would be expected to be severely damaged. On the other hand, probability of severe damage (DS4 or DS5) in an MCE for buildings with floor-frame connection detailing 2 or for similar buildings with perfect/no floor (i.e. damage contributed by the frame only) is only 4% as shown in Figures 3c and 3d. Under a DBE, 93% buildings with post-2004 floor-frame connection details might be expected to sustain repairable damage (see Figures 3b and 3c). This probability is the same in buildings with perfect/no floor (see Figure 3d) because the inter-storey drift corresponding to the DS2 -DS3 boundary is the same in Table 2 for the improved floor-frame connection (both detailing 1

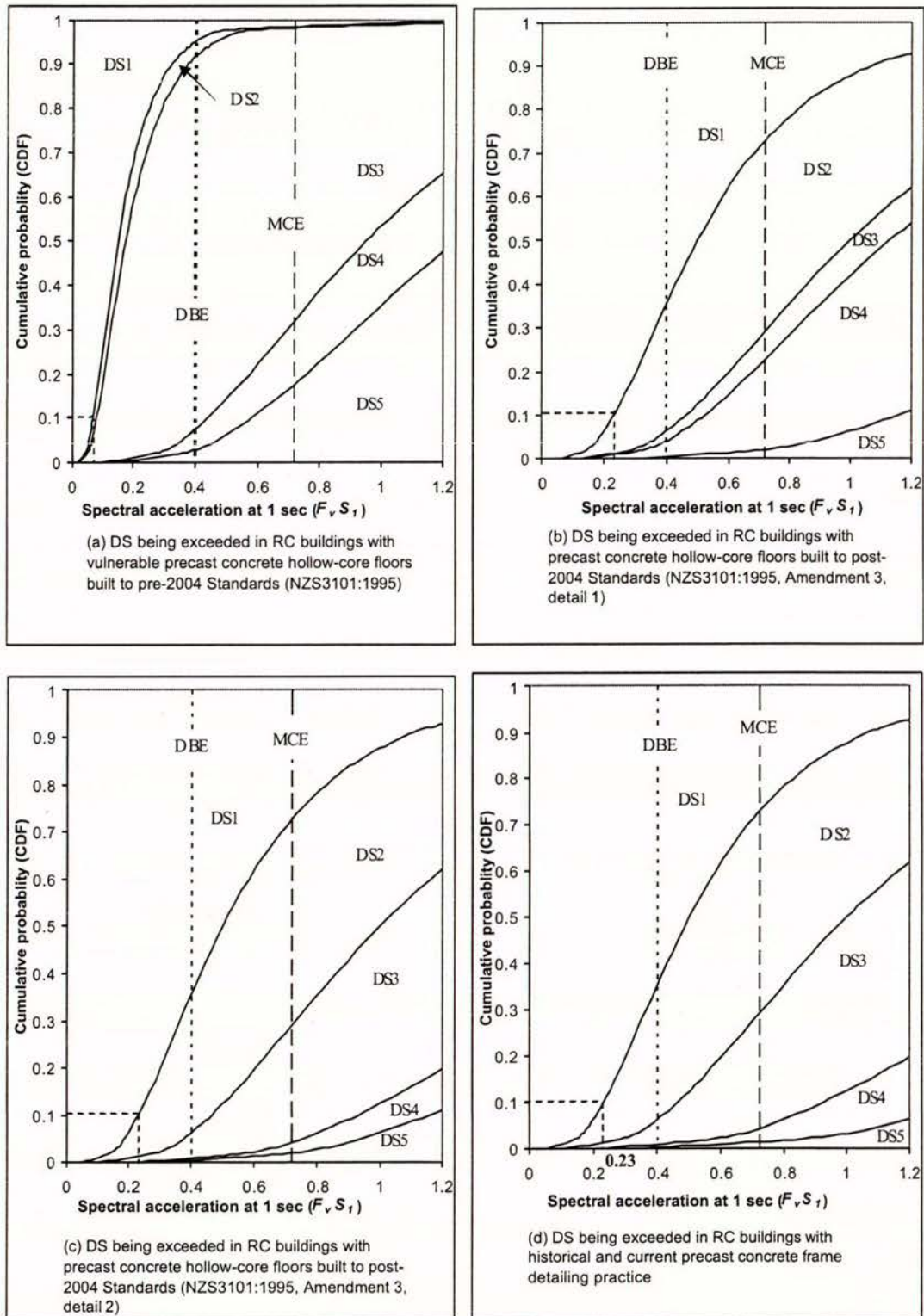


Figure 3: Fragility Curves for New Zealand multi-storey RC buildings related to the HAZUS damage states.

and detailing 2) and for buildings with perfect/no floor. On the other hand, probability of heavy damage leading to partial collapse of buildings with post-2004 connection Detail 1 would be 4%, while only 1% buildings with connection Detail 2 and buildings with perfect/no floor frame detailing would be expected to suffer heavy damage in case of a DBE. Again, this is attributable to the same DS3-DS4 boundary for these two cases in Table 2.

Comparison of Figure 3d with Figures 3b and 3c indicates that the fragility of buildings is not affected adversely by floors with improved connection detail whereas comparison of Figures 3a and 3d informs that the inclusion of floors with the vulnerable pre-2004 connection detail render the building significantly more fragile. Therefore, the overall performance will be governed by the poor performance of the floor in pre-2004 buildings whereas the performance of the post-2004 buildings could be judged by the performance of either the floor (with detailing 2) or the frame as both of these components are found to be equally fragile.

3. FINANCIAL SEISMIC RISK ASSESSMENT FRAMEWORK

Communicating seismic vulnerability to decision makers is an important aspect of performance based earthquake engineering (PBEE). One such communication tool is Expected Annual Loss (EAL) which can be expressed in a dollar value. EAL incorporates the entire range of seismic scenarios, return rate, and expected damage into a median dollar loss. Though there are many methods of quantifying financial risk, EAL is especially useful to decision makers for cost-benefit analysis of design alternatives for new structures or seismic retrofit alternatives for existing structures. Moreover, EAL can easily be accounted for by including into operating budgets.

Recent research at Pacific Earthquake Engineering (PEER) Center on seismic risk assessment has led to a mathematical expression in the form of a triple integral equation [4] that can be used to evaluate the probability of an arbitrarily chosen decision variable exceeding a prescribed limit. The interrelationships used in the triple integration link firstly seismic hazard to structural response, then response to damage, and finally damage to the decision variable. If the decision variable is expressed in terms of economic consequences, the triple integral equation can be used to estimate the total probable loss due to an earthquake. Dhakal and Mander [5] have extended the PEER framework formula to a quadruple integral by including time, thereby enabling the quantification of seismic risk in terms of EAL. The quadruple integral formulation is given as:

$$EAL = \int_0^1 \int_0^1 \int_0^1 \int_0^1 L_R \cdot dP[L_R | DM] \cdot dP[DM | EDP] \cdot dP[EDP | IM] \cdot d_f[IM] \quad (5)$$

in which, IM = intensity measure; $f_d[IM]$ = annual probability of an earthquake of a given intensity IM; EDP = engineering demand parameter; DM = damage measure; L_R = loss ratio (i.e. decision variable); $P[A|B]$ = shortened form of $P[A = a | B = b]$; and $dP[A|B]$ = derivative of the conditional probability $P[A|B]$ with respect to A.

Equation (5) provides a foundation from which the following subtasks can be performed evaluating the probability of seismic hazard analysing structural fragility; damage assessment; and loss estimation. Implicit in the formula is a probabilistic analysis, which incorporates a number of uncertainties to be combined in accordance with the total probability theorem [15] as described by Equation (3).

As is evident from Figure 1, Intensity measure (IM) used in this study is $F_v S_1$ (the spectral acceleration at 1 second). The EDP considered is maximum inter-storey drift, which can be associated with damage in a global sense in terms of partial/complete collapse and in a local sense in terms of yielding spalling, and bar buckling. To quantify damage, damage states defined according to HAZUS [11] are adopted, classifying damage into 5 distinct categories, as summarized in Table 1. In order to relate EDP with the damage measure (DM), drifts causing different damage states are specified as listed in Table 2. For calculating EAL using Equation (5), two more variables namely loss ratio (L_R) and annual probability (f_a) need to be defined and their correlation with one of the three previously defined parameters (IM, EDP and DM) need to be established. The interrelationships between f_a and IM and between L_R and DM are explained in the following sections.

4. ASSESSMENT OF HAZARD SURVIVAL PROBABILITY

4.1 Earthquake Recurrence Relationship

Note that the fragility curves shown in Figure 3 are plots of $P[DM|IM]$ (which is the product of $P[DM|EDP]$ and $P[EDP|IM]$) against IM ($F_v S_1$ in this study). In order to use these curves as a part of Equation (5), the horizontal axis needs to be annual probability (f_a) rather than the hazard intensity. Hence, it is necessary to define a relationship between the annual probability of earthquakes and their intensity.

Based on historical earthquake data, relationship between the peak ground acceleration (PGA) of earthquakes (denoted as a_g) with their annual probability of occurrence (f_a) has been established as:

$$a_g = \frac{a_g^{DBE}}{(47.5 f_a)^q} \quad (6)$$

where a_g^{DBE} is the PGA of the DBE (10% probability of occurrence in 50 years) and q is an empirical constant found to be equal to 0.33 for seismic hazard in NZ [16].

As the IM used in this study is the spectral acceleration at 1 sec ($F_v S_1$), relationship between spectral acceleration and PGA is desirable to utilize Equation (6). In constant velocity region of the design spectra, which spans through 1 sec and covers a range in which the natural periods of most structures are likely to fall, the equation of the spectral acceleration curve is:

$$S_T = \frac{a_g}{T \cdot S} \quad (7)$$

where T is the natural period of structures (in sec); S_T is the spectral acceleration at that period; and S is soil factor. Assuming firm soil for which the soil factor S is unity, the spectral acceleration at 1 sec period is hence equal to the PGA; i.e. $F_v S_1 = a_g$.

It is to be noted that, as investigated by Der Kiureghian [17], earthquakes are discrete, rather than continuous events, and should be modelled as a Poisson process. In this case, the hazard-recurrence formula given above, though conservative, is strictly correct when $f_a > 0.01$. In order to compensate for this shortcoming to some extent, the contribution of frequent earthquakes (i.e. $f_a > 0.1$) is not included in this study.

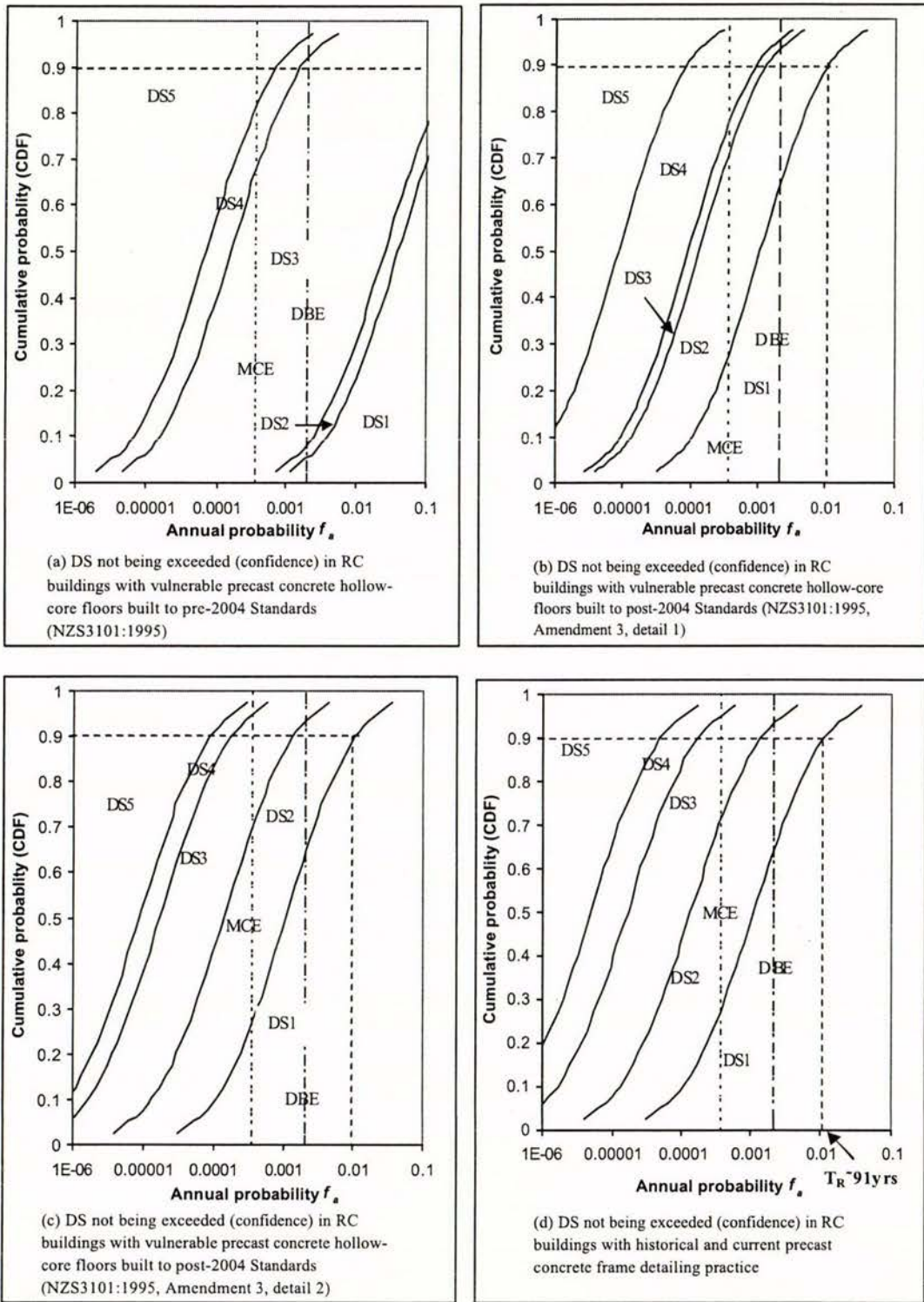


Figure 4: Hazard Survival Curves for New Zealand multi-storey RC buildings related to the HAZUS damage states.

Table 3a Probability of not exceeding different damage states for buildings built to pre-2004 standards with vulnerable precast concrete hollow-core floors

P[DS = DS _i]					
f_a	i=1	i=2	i=3	i=4	i=5
0.1	0.7	0.78	1	1	1
0.01	0.22	0.3	1	1	1
0.001	0.02	0.04	0.85	0.93	1
0.0001	0	0	0.4	0.58	1
0.00001	0	0	0.06	0.14	1
0.000001	0	0	0	0	1

Table 3b Probability of not exceeding different damage states for buildings with improved connections built to the 2004 amendment (Detailing 1)

P[DS = DS _i]					
f_a	i=1	i=2	i=3	i=4	i=5
0.1	1	1	1	1	1
0.01	0.89	1	1	1	1
0.001	0.49	0.87	0.9	1	1
0.0001	0.1	0.44	0.51	0.92	1
0.00001	0	0.08	0.11	0.54	1
0.000001	0	0	0	0.12	1

Table 3c Probability of not exceeding different damage states for buildings with improved connections built to the 2004 amendment (Detailing 2)

P[DS = DS _i]					
f_a	i=1	i=2	i=3	i=4	i=5
0.1	1	1	1	1	1
0.01	0.89	1	1	1	1
0.001	0.49	0.86	1	1	1
0.0001	0.09	0.44	0.84	0.92	1
0.00001	0	0.08	0.4	0.54	1
0.000001	0	0	0.06	0.12	1

Table 3d Probability of not exceeding different damage states for ideal buildings with perfect/no floor; i.e. damage contributed by the frame only

P[DS = DS _i]					
f_a	i=1	i=2	i=3	i=4	i=5
0.1	1	1	1	1	1
0.01	0.89	1	1	1	1
0.001	0.49	0.87	1	1	1
0.0001	0.09	0.44	0.84	0.95	1
0.00001	0	0.08	0.4	0.65	1
0.000001	0	0	0.06	0.19	1

Table 4a Probability of being in a given damage state (confidence interval) for buildings built to pre-2004 standards with vulnerable precast concrete hollow-core floors

P[DS = DS _i]					
f_a	i=1	i=2	i=3	i=4	i=5
0.1	0.7	0.08	0.22	0	0
0.01	0.22	0.08	0.7	0	0
0.001	0.02	0.02	0.81	0.08	0.07
0.0001	0	0	0.4	0.18	0.42
0.00001	0	0	0.06	0.08	0.86
0.000001	0	0	0	0	1

Table 4b Probability of being in a given damage state (confidence interval) for buildings with improved connections built to the 2004 amendment (Detailing 1)

P[DS = DS _i]					
f_a	i=1	i=2	i=3	i=4	i=5
0.1	1	0	0	0	0
0.01	0.89	0.11	0	0	0
0.001	0.49	0.38	0.03	0.1	0
0.0001	0.1	0.34	0.07	0.41	0.08
0.00001	0	0.08	0.03	0.43	0.46
0.000001	0	0	0	0.12	0.88

Table 4c Probability of being in a given damage state (confidence interval) for buildings with improved connections built to the 2004 amendment (Detailing 2)

P[DS = DS _i]					
f_a	i=1	i=2	i=3	i=4	i=5
0.1	1	0	0	0	0
0.01	0.89	0.11	0	0	0
0.001	0.49	0.37	0.14	0	0
0.0001	0.09	0.35	0.4	0.08	0.08
0.00001	0	0.08	0.32	0.14	0.46
0.000001	0	0	0.06	0.06	0.88

Table 4d Probability of being in a given damage state (confidence interval) for ideal buildings with perfect/no floor; i.e. damage contributed by the frame only

P[DS = DS _i]					
f_a	i=1	i=2	i=3	i=4	i=5
0.1	1	0	0	0	0
0.01	0.89	0.11	0	0	0
0.001	0.49	0.38	0.13	0	0
0.0001	0.09	0.35	0.4	0.11	0.05
0.00001	0	0.08	0.32	0.25	0.35
0.000001	0	0	0.06	0.13	0.81

4.2 Hazard Survival Curves

Fragility curves of Figure 3 can now be re-plotted by changing the horizontal axis from IM to f_a using the earthquake recurrence relationship established earlier. Such curves are called hazard-survival curves and they show the probability of damage being within a limit state when an earthquake of a given annual probability strikes. Figures 4a-4d show the hazard survival curves for the buildings with precast floors designed to pre-2004 standards and post-2004 amendment (detailing 1 and detailing 2) and similar buildings with perfect/no floor so that the performance of the buildings is governed by the seismic frames. Two vertical lines representing the annual probabilities of DBE ($f_a \sim 0.002$) and MCE ($f_a \sim 0.0004$) are also shown in the plots for reference. The intersections of any vertical line through a value of f_a with the hazard survival curves give the probability of these damage states not being exceeded in earthquakes of that annual probability of occurrence. Thus obtained damage state survival probabilities in earthquakes of different frequencies are shown in Tables 3a-3d for buildings with the three different floor-frame connection details and an ideal building with perfect/no floor. Similarly, Tables 4a-4d show the probabilities of being in a given damage state (confidence interval) for the four cases. For example, the second row in Table 3a means that if an earthquake of annual frequency of 0.01 (i.e. return period of 100 years) strikes, the probability of DS1 not being exceeded in buildings with the vulnerable pre-2004 connection detailing is 22%; and the corresponding probabilities for other damage states (DS2 and DS3) are 30% and 100% respectively. Similarly the second row of Table 4a means that when an earthquake with an annual frequency of 0.01 (i.e. return period of 100 years) strikes, there is a 22% chance that the damage state of these buildings will be DS1, 8% chance that the damage will be in the range of DS2 and so on.

5. FINANCIAL IMPLICATION OF EARTHQUAKES

5.1 Loss Model

To quantify financial loss, a loss model must be established to relate damage measure (DM) to a dollar value. In this study, the financial implication of each damage state is represented by a *loss ratio* (L_R), which is the ratio of the cost necessary to restore the structure to full working order to the replacement cost. Deciding the cost implication of each damage state is a subjective process and the accuracy of the decided value will depend largely on the amount of time devoted to researching repair costs and their variation by extent of damage, location of building, etc.

Table 5 Loss ratios for different damage states

	DS1	DS2	DS3	DS4	DS5
Likely Range	0	0.05-0.15	0.2-0.4	1.0-1.2	1
Assumed L_R value	0	0.1	0.3	1	1

The assumed values and likely range of loss ratios for different damage states are shown in Table 5. As no damage or repair is expected in pre-yield damage state DS1, no financial loss is incurred and the loss ratio for DS1 is therefore zero. Loss ratio for DS2 is likely to fall between 0.05 and 0.15 to account for minor repairs due to slight but tolerable damage, and $L_R = 0.1$ is assumed for DS2. The loss ratio for DS3 may vary from 0.2 to 0.4 for repairing the

incurred moderate damage to restore functionality, and a representative value of 0.3 is adopted in the present analysis. "Irreparable damage" under DS4 demands complete replacement as repair may be uneconomic; hence the loss ratio of 1 is used here. Similarly for DS5, which is complete failure/collapse the value of loss ratio is 1.

It has been shown [5] that the financial risk is sensitive to the values of loss ratios, especially L_R for DS2 and DS3. Hence, good judgement should be applied in deciding these values. However, the objective of this study is to compare the financial risk of different detailing schemes and a constant set of L_R values will not have considerable impact on the final comparative outcome.

5.2 Probable Loss in an Earthquake

Using the assigned loss ratios, the contribution of different damage states to the financial loss can be estimated. Table 6 lists the probable financial loss (as fraction of the total replacement cost) due to different damage states when earthquakes with annual frequencies of 0.1, 0.01, 0.001, 0.0001, and 0.00001 strike. The values in Table 6 are the product of the probability of being in a given damage state in earthquakes of different annual frequencies (obtained from corresponding Tables 4a-4d) and the assumed loss ratio for the corresponding damage state (obtained from Table 5). Graphical versions of Table 6 (i.e. economic hazard probability curves) are shown in Figures 5a-5d, which exhibit the contributions of different damage states and the total probable loss in the form of bar charts.

As expected, DS1 does not incur any financial loss as it does not need any repair. Similarly, the financial loss incurred by earthquakes of 0.1 or higher annual probability in case of buildings designed and built to post-2004 standards is also nil as such frequent events do not incur any damage requiring repair or replacement (DS2 or higher damage category). However some financial loss (up to 7% of the total cost) is expected due to repairable damage in buildings with vulnerable detailing of pre-2004 standards even by smaller earthquakes of 0.1 or higher annual probability. As shown in Table 5, the loss ratio L_R is higher for DS4 and DS5 than for other damage states. As confidence intervals of higher damage states are multiplied by higher loss ratio, the higher damage-states contribute more to the probable loss although the likelihood of the earthquake-induced damage falling into these severer categories is not high. Again in case of buildings designed to pre-2004 standards, repairable moderate damage (DS3) contributes most to the financial loss when earthquakes of 0.001 or higher probability (i.e. with return period of 1000 years or less) strike.

The total financial loss due to earthquakes of a given probability shown in the last column of Table 6 is the sum of the contributions of the five damage states. Figures 6a-6d plot the total loss ratio against the annual probability. These curves give information on what would be the financial loss if an earthquake of a given annual probability strikes once. As expected the larger and rarer the event the greater the financial loss. Conversely for frequent, but low intensity events, the single-event loss is small.

Two vertical lines corresponding to DBE and MCE are also shown in the figures. It is evident from Figure 6a that a building with pre-2004 connection details is likely to lose about 30% and 50% of its value due to damage incurred by a DBE and an MCE, respectively. Even a small earthquake with 0.1 annual frequency (return period of 10 years) is likely to incur 7% loss to these buildings. Obviously, maintenance of such buildings in a seismic zone would be costly. On the other hand, as can be seen in Figures 6b and 6c, buildings with improved post-2004 detailing will remain almost intact

Table 6 Probable financial loss analysis

	f_a	L_R [DS1]	L_R [DS2]	L_R [DS3]	L_R [DS4]	L_R [DS5]	Total L_R
a) Pre-2004 Standard [Matthews]	0.1	0	0.004	0.066	0	0	0.07
	0.01	0	0.004	0.21	0	0	0.214
	0.001	0	0.001	0.243	0.06	0.07	0.374
	0.0001	0	0	0.12	0.135	0.42	0.675
	0.00001	0	0	0.018	0.06	0.86	0.938
	0.000001	0	0	0	0	1	1
b) Post-2004 (Detailing 1) [Lindsay]	0.1	0	0	0	0	0	0
	0.01	0	0.0055	0	0	0	0.0055
	0.001	0	0.019	0.009	0.075	0	0.103
	0.0001	0	0.017	0.021	0.3075	0.08	0.4255
	0.00001	0	0.004	0.009	0.3225	0.46	0.7955
	0.000001	0	0	0	0.09	0.88	0.97
c) Post-2004 (Detailing 2) [MacPherson]	0.1	0	0	0	0	0	0
	0.01	0	0.0055	0	0	0	0.0055
	0.001	0	0.0185	0.042	0	0	0.0605
	0.0001	0	0.0175	0.12	0.06	0.08	0.2775
	0.00001	0	0.004	0.096	0.105	0.46	0.665
	0.000001	0	0	0.018	0.045	0.88	0.943
d) Ideal (perfect/no floor) Frame detailing	0.1	0	0	0	0	0	0
	0.01	0	0.0055	0	0	0	0.0055
	0.001	0	0.019	0.039	0	0	0.058
	0.0001	0	0.0175	0.12	0.0825	0.05	0.2700
	0.00001	0	0.004	0.096	0.1875	0.35	0.6375
	0.000001	0	0	0.018	0.0975	0.81	0.9255

(losing only 0.5% of its value) in a once in 100 years earthquake ($f_a \sim 0.01$). In a DBE and an MCE, these buildings with detail 1 will incur a loss of about 5% and 22% respectively, which are drastically smaller than those for pre-2004 buildings. This loss will further reduce for buildings with detail 2 being about 3% and 13% in DBE and MCE respectively. As can be seen in Figure 6d, these values are very close to those for idealised buildings with perfect/no floor (i.e. money needed to repair frame damage only); indicating that the floor with improved post-2004 detailing do not cause any additional financial burden in terms of maintenance.

6. SEISMIC ANNUAL FINANCIAL RISK

6.1 Calculation of Expected Annual Loss (EAL)

At this point, each component of the probabilistic analysis process has been established. Relationships have been generated to relate IM to EDP (Figure 2), EDP to DM (Tables 1 and 2), and DM to L_R (Table 5). The total expected annual loss can now be calculated using Equation 5 by integrating the loss ratio over all possible annual frequencies of the seismic hazard; i.e. between 0 and 1. This general equation in continuous form can be expressed as:

$$EAL = \int_0^1 L_R df_a \quad (8)$$

In discrete form, the expected annual loss (EAL) can be calculated as:

$$EAL = \sum_{all l_i} \left(\frac{l_{r,j} + l_{r,i+1}}{2} \right) (f_a[L_R = l_{r,j}] - f_a[L_R = l_{r,i+1}]) \quad (9)$$

in which $f_a[L_R = l_i]$ is the annual probability of the loss ratio being equal to a given value l_i , which can be obtained from the economic hazard probability curves (Figure 6). Table 7 shows the annual loss of the buildings with the three different floor-frame connection details and similar building governed by the frame. First, the probable loss due to earthquakes of

annual probability within a range is calculated which is the area subtended by the economic hazard curves (Figures 6a-6d) between two points on the x-axis. Then the losses contributed by the earthquakes with different ranges of probability are added together to obtain the total expected annual loss (EAL). It can be noted that the annual probability is plotted in logarithmic scale in Figures 6a-d, and the absolute value of the interval between any two points on the x-axis decreases by an order of ten towards the left. Accordingly, the absolute value of the area covered is also decreasing rapidly in that direction (i.e. direction of decreasing probability) in spite of a higher value of the loss ratio. As can be observed from Table 7, the EAL of the buildings built to post-2004 improved connection detailing is approximately 5%-7% of that of buildings built to the vulnerable pre-2004 detailing. For comparison, total loss ratio of pre-2004 buildings with the pre-2004 vulnerable connection details is plotted as dotted line in Figures 6b, 6c and 6d. The large difference in the total loss ratio between pre- and post-2004 buildings with precast concrete floors for different earthquakes can be noted in these figures.

As mentioned earlier, this model overestimates the EAL by over-emphasising the contribution of frequent events ($f_a > 0.01$; i.e. return period of less than 100 years). The error can be compensated by truncating the data above a certain threshold. This threshold is found by locating the IM at which there will be no damage, say with 90% confidence. For example, to induce damage to the ideal buildings with perfect/no floor, earthquakes with $F_v S_1 < 0.23g$ (return period of approximately 91 years) will have 90% probability of not inducing any damage (see Figures 3d and 4d). Contribution to EAL of earthquakes below this threshold, if not considered will have a considerable effect on the final result. The EAL for these ideal multi-storey RC buildings with perfect/no floor is found to be about 34% lower after truncating the data below this threshold. The reduction of EAL by ignoring the contribution of earthquakes below similarly decided thresholds for buildings designed after the 2004 amendment is 24% and 34% for detailing 1 and detailing 2, respectively.

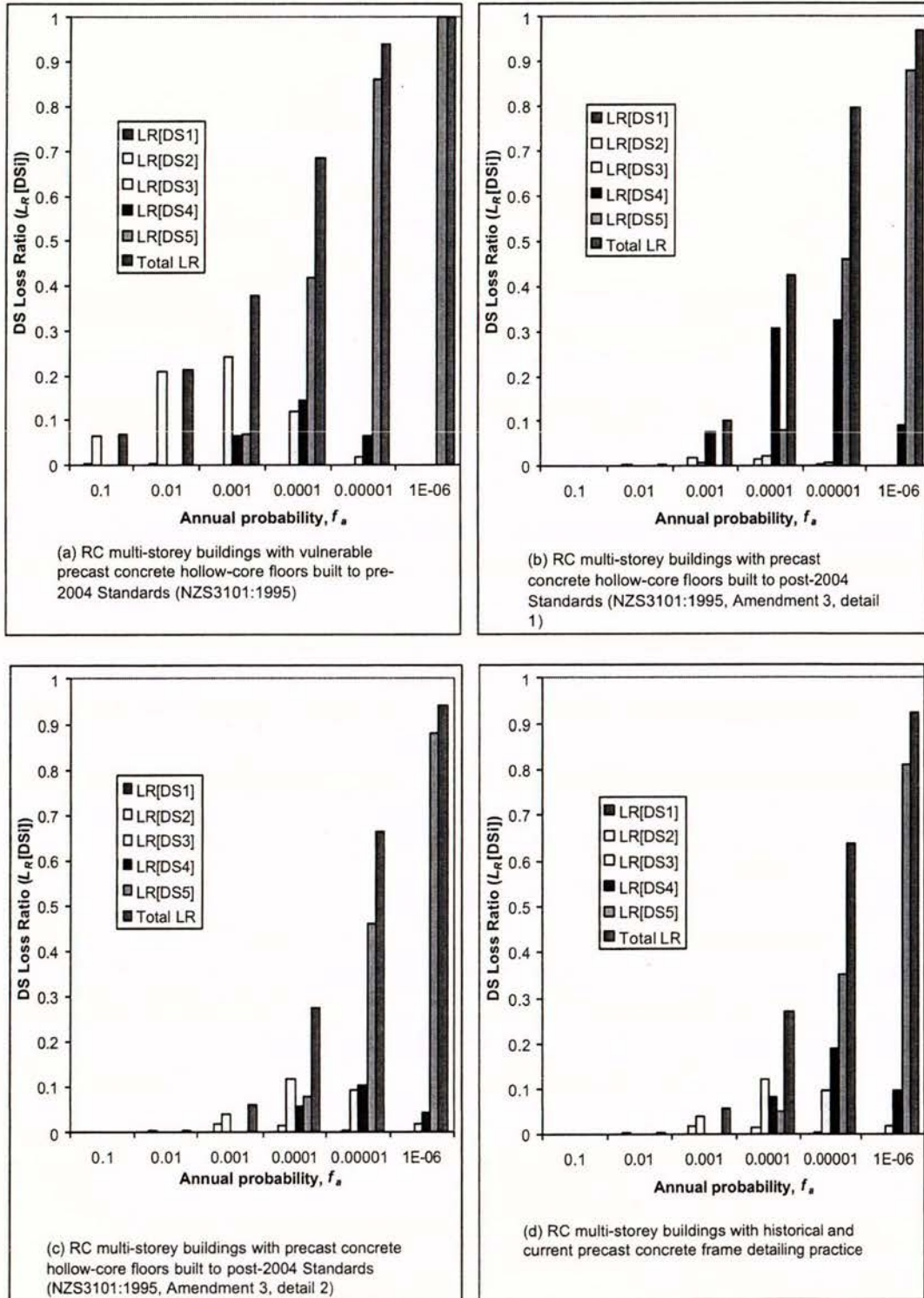


Figure 5: Economic Hazard Probability Curves (Bar Charts) for New Zealand multi-storey RC buildings related to the HAZUS damage states

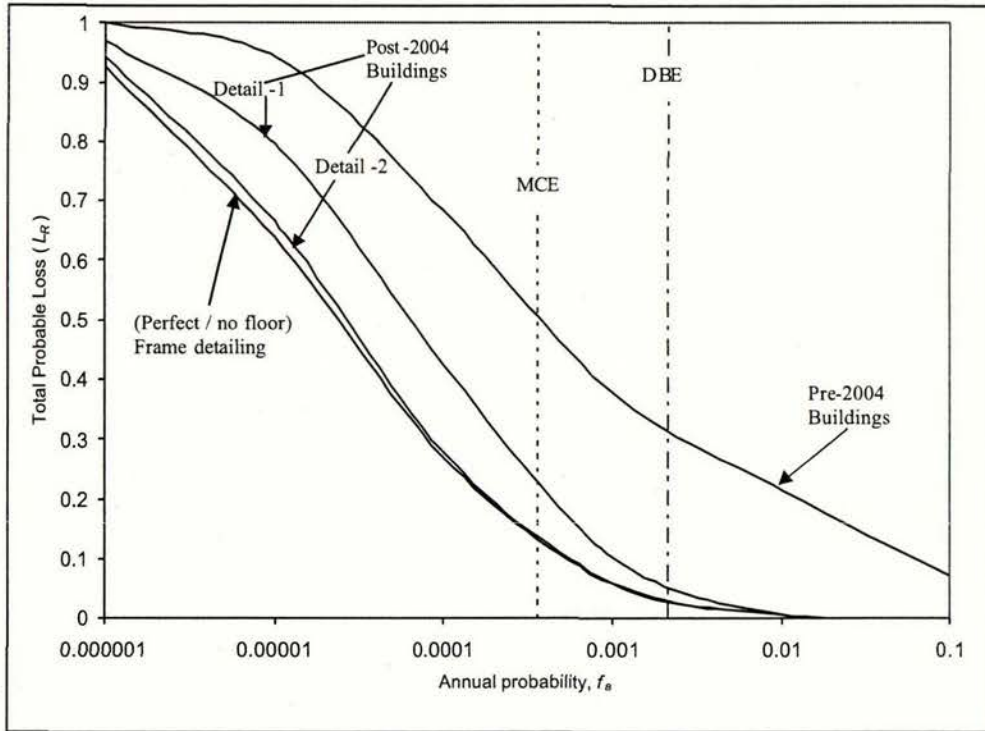


Figure 6: Economic Hazard Probability Curves for New Zealand multi-storey RC buildings

Table 7 Annual financial risk for buildings

f_a	EAL (per \$1 million)							
	Pre-2004 standards [Matthews]		Post-2004 (Detailing 1) [Lindsay]		Post-2004 (Detailing 2) [MacPherson]		Ideal (perfect/no floor) Frame detailing	
	L_R	ΔEAL	L_R	ΔEAL	L_R	ΔEAL	L_R	ΔEAL
0.1	0.07		0		0		0	
		12780		248		248		248
0.01	0.214		0.0055		0.0055		0.0055	
		2646		488		297		286
0.001	0.374		0.103		0.0605		0.058	
		472		238		152		148
0.0001	0.675		0.4255		0.2775		0.27	
		72.6		55		42.4		40.8
0.00001	0.938		0.7955		0.665		0.6375	
		8.72		8		7.24		7.03
0.000001	1		0.97		0.943		0.9255	
Total EAL		16000		1037		746		729

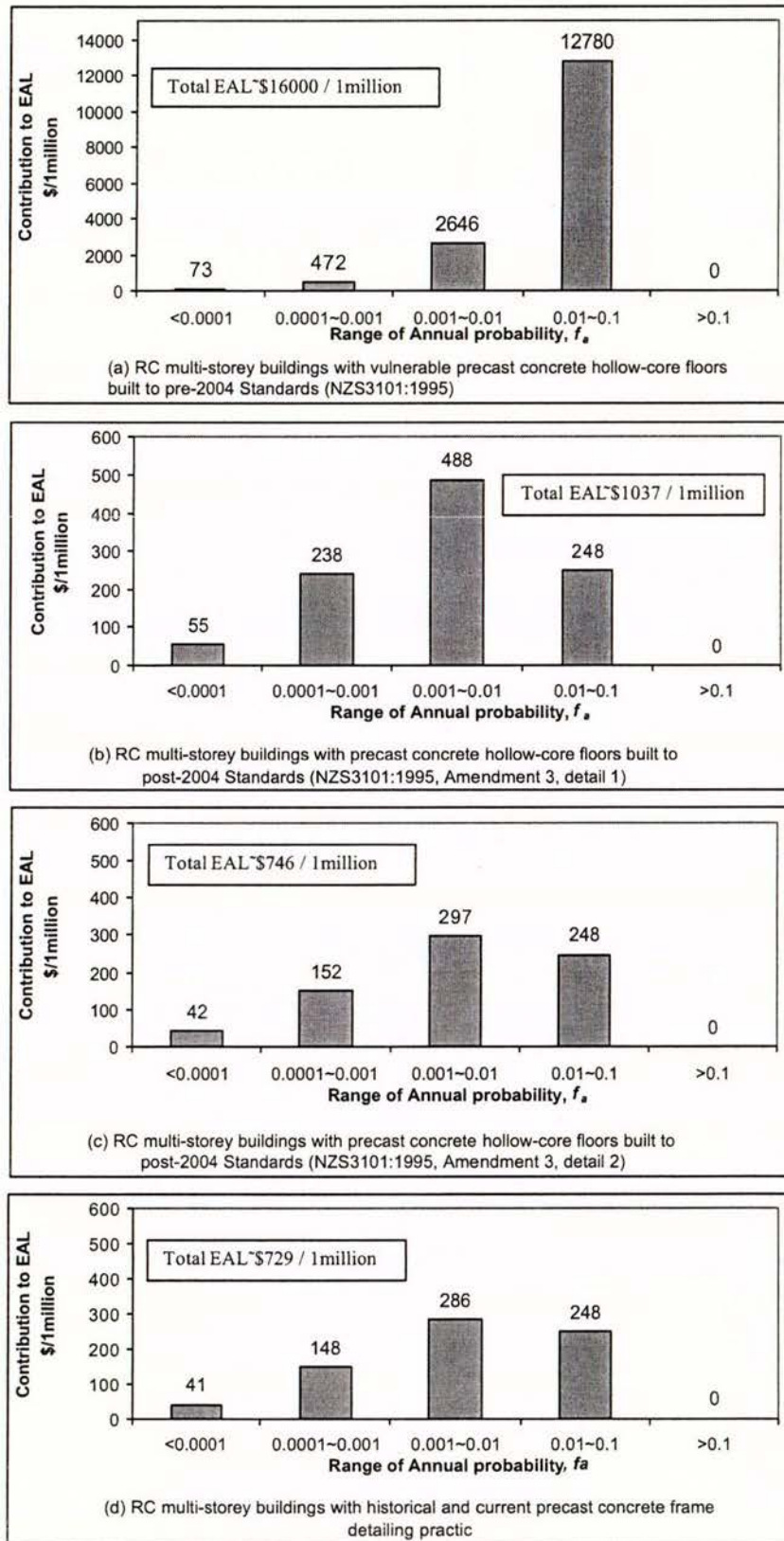


Figure 7: Annual financial risk for New Zealand multi-storey RC buildings due to earthquakes of different probability.

The buildings with vulnerable precast concrete floors with pre-2004 details, however, will have an increase in EAL if 90% confidence level is considered for truncation. As can be noticed in Figure 4a, the horizontal line through 0.9 in the vertical axis (i.e. indicating a 90% confidence) does not intersect the hazard survival curve separating DS1 and DS2 within the plotted range of annual probability. In other words, the annual frequency of earthquakes having a 90% probability of no damage is more than 0.1, data below which were not included in the calculation. Obviously, if the contribution of earthquakes with annual frequency more than 0.1 is included, the ultimate value of EAL would increase significantly. As the threshold frequency for the other three cases is less than 0.1 and hence the truncation will reduce the EAL, which otherwise includes the frequency range from 0.000001 to 0.1. This further widens the gap between the financial risk of buildings with vulnerable pre-2004 and improved post-2004 connection details.

Note in Table 7 that EAL of ideal buildings with perfect/no floor is in the same range as that of the buildings with precast concrete hollow-core floors built to post-2004 connection detailing 2. This demonstrates the effectiveness of the recommendations made in the Amendment No. 3 of NZS 3101:1995 regarding seating and connection details of precast concrete floors used in moment-resisting reinforced concrete frame buildings.

6.2 Implications to Owners and Insurers

A vertical ordinate of the economic hazard probability curves (Figures 6a-6d) gives the total probable loss of a building due to earthquakes for a given annual probability. Hence, they represent the financial risk to owners of individual buildings. Evidently, smaller and more frequent events pose a small risk to owners of buildings with post-2004 improved floor-frame connection details. Consequently, owners may be prepared to bear the risk of these frequent earthquakes by themselves. In the worst case, they may need to spend a small sum (less than 1% of the building value) to repair the damage (if any) incurred if and when these moderate earthquakes strike. On the other hand, the consequences of rarer but stronger earthquakes may be disastrous, often incurring 50% or more loss thereby rendering the repair uneconomical, necessitating replacement. Building owners would obviously be more inclined to pass this risk to insurers.

Note that the insurer's risk encompasses all insured buildings and all possible hazards. In other words, the integration of the economic hazard curve (Figures 6a-6d) represents insurer's risk. As EAL is the area subtended by the economic hazard curve, it represents insurer's risk and is directly related to an annual insurance premium for a building if all levels of seismic hazards are covered. The contribution of earthquakes of different frequency ranges to the total EAL is also graphically depicted in Figures 7a-d. Looking at the trend in Table 7 and Figures 7a-d, it is apparent that the earthquakes with annual frequencies smaller than 0.0001 (return period of more than 10000 years) will pose negligible financial risk. It is the more frequent and smaller events that pose more financial risk, and the large earthquakes amount to very small risks due mainly to their very small annual frequency of occurrence (long return period).

As is evident in Table 7 and Figure 7a, the total annual loss (i.e. the financial risk posed by all earthquakes) of the buildings with vulnerable precast concrete hollow-core floors built to pre-2004 standards amounts to about 1.6% of the replacement cost. In other words, the expected annual financial loss is \$16000 per \$1 million of building cost. 80% of this value corresponds to the risk posed by frequent but modest size earthquakes with an annual frequency in the

range between 0.01 and 0.1 (i.e. return periods between 10 and 100 years). On the other hand, only 25% of the annual financial loss expected of the buildings with improved post-2004 connection using detailing 1 (approximately \$1037 per \$1 million of building cost) corresponds to the risk posed by frequent but modest size earthquakes (see Table 7 and Figure 7b). Similarly, as can be seen in Table 7 and Figure 7c, buildings with floor-frame connection detailing 2 and ideal buildings with perfect/no floor are expected to undergo even lesser annual financial loss of approximately \$730-\$750 per \$1 million of building cost (i.e. 0.07% of the replacement cost) and 35% of this value corresponds to the risk posed by frequent but modest size earthquakes.

Insurers would not be so concerned about the small risk posed by these large and rare events as they themselves would re-insure. The loss to owners, however, would be untenable. That is why most insurance policies are targeted to cover the rarer and bigger hazards. In contrast, the smaller and more frequent events will pose a small risk to the individual owners but a significant collective risk to the insurers. If these frequent hazards are excluded from the insurance policy, the EAL and consequently the annual insurance premium will reduce significantly. From an insurance point-of-view, the risk of these smaller and more frequent events should ideally be carried by the owner. This can be achieved by setting an appropriate deductible to the policy and thus keeping the remainder of the insured risk affordable for the owners. Obviously, a higher deductible reduces the insurance premium.

7. CONCLUSIONS AND RECOMMENDATIONS

Fragility curves drawn based on results of full-scale tests on RC frame with precast concrete hollow-core floor slabs have been used to estimate annual financial loss. Expected annual loss (EAL) has been calculated by using a generalised probabilistic financial risk assessment methodology for buildings with precast concrete hollow-core floors designed and built to vulnerable pre-2004 detailing practice in NZ and the two types of improved connection details recommended in the 2004 Amendment No. 3 to NZS3101:1995. The structural performance, fragility, hazard survival probability and the associated financial risk of buildings with these three floor-frame connection details are compared with each other and also against those of an ideal seismic frame building with perfect/no floor to realize the weakness imparted on the building by the floor with different connection detail.

It is concluded that the seismic performance of precast hollow-core floors in buildings designed and built to pre-2004 standards is vastly inferior to the performance of seismic frames. The floor-frame connection of these older structures may be the weakest link and will dictate the extent of losses for such buildings. On the other hand, improving the floor-frame connection detail according to the NZS3101:1995 Amendment No. 3 brings the overall building performance on par with the frame performance. It indicates that the precast floor with improved post-2004 detailing do not noticeably weaken the building. It is found that the buildings with precast floor designed to pre-2004 standards are likely to incur about 30% and 50% loss in a DBE (10% in 50 years event) and an MCE (2% in 50 years event) respectively, whereas the improvement in the connection details according to 2004 amendment will reduce the total probable loss to 3% in a DBE and 13% in an MCE. The EAL of precast concrete structures with hollow-core floor systems built to pre-2004 standards is found to be very high; in the order of \$16,000 per \$1 million asset value, whereas the annual financial risk of similar buildings with improved post-2004 connection details is only about 7% of that of buildings with pre-2004 details.

Based on the discussions presented herein, it can be concluded that very large earthquakes pose almost negligible financial risk due to their very low probability of occurrence although structures are likely to partially or completely collapse if rare earthquakes of such magnitude strike. On the other hand, smaller earthquakes may only cause repairable minor-moderate damage to structures, but these earthquakes pose a big risk as they are likely to strike more often. Calculations showed that earthquakes with a return period between 10 and 100 years would contribute approximately 25% to the annual financial risk in case of RC buildings with precast floors with the improved post-2004 connection details, whereas the share of these frequent earthquakes is a whopping 80% in case of buildings with precast concrete hollow-core floors designed to pre-2004 standards. Thus, the not-so-high risk posed by frequent and moderate earthquakes may be born by the owners of post-2004 buildings, and the risk posed by rare and strong earthquakes may easily be covered by a low-premium insurance policy. However, owners of pre-2004 buildings with precast concrete hollow-core floors may need to insure their buildings even for smaller and more frequent earthquakes, and will subsequently pay a heavy insurance premium.

While this study has given interesting and useful qualitative information on the relative performance and financial implications of the different floor-frame detailing schemes, the dollar values obtained are only representative and are not precise because of the assumptions and approximations that have been made in the process. Although variations in the capacity and demand and the modelling uncertainty have been quantitatively incorporated in the form of corresponding lognormal coefficients of variation, uncertainties in the assumed loss model have not been accounted for. The values assigned in this study to loss ratios and drift ratios for different damage states are somewhat subjective. EAL is very sensitive to the loss ratio corresponding to different damage states; especially those for DS2 and DS3. Hence, more realistic interrelationship between the loss ratio and damage measure is needed. Nevertheless, the objective of this study is to investigate relative performance of the three different connection details, and a constant set of L_R values for different damage states across the three cases will have little effect on their relative position. Notwithstanding, future studies should try to establish more robust damage model and loss model and investigate their uncertainties so that they could be accounted for in estimating the financial risk.

8. ACKNOWLEDGMENTS

The second author wishes his thanks to National Programme on Earthquake Engineering Education (NPEEE) of Ministry of Human Resource Development, Government of India for awarding him a fellowship for conducting this research. He also wishes his gratitude to S. G. S. Institute of Technology and Science, Indore, India and University of Canterbury, Christchurch, New Zealand for allowing and providing him all the necessary facilities.

9. REFERENCES

- 1 Norton, J.A., King, A.B., Bull, D.K., Chapman, H.E., McVerry, G.H., Larkin, T.J., Spring, K.C., December 1994, Northridge Earthquake Reconnaissance Report, Bulletin of the New Zealand National Society for Earthquake Engineering Vol. 27, No.4.
- 2 Matthews, J. G., Lindsay, R., Mander, J. B and Bull, D. 2005. The seismic fragility of precast concrete buildings, ICOSSAR 2005, Millpress, Rotterdam pp 247-254.
- 3 Lindsay, R., Mander, J. B. and Bull, D.K. 2004. Experiments on the seismic performance of hollow-core floor systems in precast concrete buildings, 13th World Conference on Earthquake Engineering, Vancouver, B.C., Canada, August 1-6, 2004, Paper No. 285.
- 4 Krawinkler H. and Miranda E., 2004, *Performance-Based Earthquake Engineering*, Earthquake Engineering: From Engineering Seismology to Performance-Based Engineering, edited by Bozorgnia Y. and Bertero V.V. CRC Press, Boca Raton, FL.
- 5 Dhakal, R. P. and Mander, J. B. 2005. Probabilistic Risk Assessment Methodology Framework for Natural Hazards, Report submitted to Institute of Geological and Nuclear Science (IGNS), Department of Civil Engineering, University of Canterbury, Christchurch, New Zealand
- 6 Matthews J.G. 2004, "Hollow-core floor slab performance following a severe earthquake." Ph.D Thesis, University of Canterbury, Christchurch, New Zealand
- 7 Lindsay, R., 2004, "Experiments on the seismic performance of hollow-core floor systems in precast concrete buildings", ME Thesis, University of Canterbury, Christchurch, New Zealand
- 8 MacPherson, C., 2005. "Seismic performance and forensic analysis of a precast concrete hollow-core floor super-assembly" ME Thesis, University of Canterbury, Christchurch, New Zealand
- 9 NZS3101:1995, Standards New Zealand, 1995, Concrete Structures Standard, NZS 3101, Parts 1 & 2, Standards New Zealand
- 10 NZS3101:2004, Amendment 3 to NZS3101:1995, Standards New Zealand, 1995, Concrete Structures Standard, NZS 3101, Parts 1 & 2, Standards New Zealand
- 11 HAZUS. 1999, *Earthquake Loss Estimation Methodology*. Technical Manual. Prepared by the National Institute of Building Sciences for Federal Emergency Management Agency, Washington, DC.
- 12 Cornell C.A., Jalayer F., Hamburger R.O. and Foutch D.A., 2002, *Probabilistic Basis for 2000 SAC Federal Emergency Management Agency Steel Moment Frame Guidelines*, Journal of Structural Engineering, ASCE, Vol.128 No.4, pp 526-533.
- 13 Lupoi G, Lupoi A and Pinto P.E, 2002, Seismic Risk Assessment of RC Structures with the "2000 SAC/FEMA" Method, Journal of Earthquake Engineering, Vol. 6, No. 4, pp 499-512.
- 14 Dutta A, 1999, *On Energy-Based Seismic Analysis and Design of Highway Bridges*, Ph.D Dissertation, Science and Engineering Library, State University of New York at Buffalo, Buffalo, NY
- 15 Kennedy, R.P., Cornell, C.A., Campbell R.D., Kaplan, S and Perla H.F, 1980, *Probabilistic Seismic Safety Study of an Existing Nuclear Power Plant*, Nuclear Engineering and Design No. 59, pp 315-338.
- 16 NZS4203:1992, Code of practice for general structural loading for buildings, Standards New Zealand, Wellington, New Zealand.
- 17 Der Kiureghian A., 2005, *Non-ergodicity and PEER's framework formula*, Earthquake Engineering and Structural Dynamics, Vol. 34, No. 13, pp 1643-1652.

HOLLOWCORE FLOOR SLAB PERFORMANCE FOLLOWING A SEVERE EARTHQUAKE.

Jeff MATTHEWS¹, Des BULL², John MANDER¹

¹ Department of Civil Engineering, University of Canterbury, Christchurch, New Zealand.

² Holmes Consulting Group & Department of Civil Engineering, University of Canterbury, Christchurch, New Zealand

Keywords: hollowcore, earthquake, elongation, diaphragm, experimental, seismic

1 INTRODUCTION

Precast concrete buildings that use prestressed hollowcore floor units have been the dominant form of construction used in New Zealand over the last two decades. Several failures of hollowcore flooring systems were observed after the Northridge earthquake (17 January 1994), this has raised serious concern regarding the seismic performance and integrity of New Zealand's precast concrete multi-storey moment resisting frame buildings. In Northridge, a collapse resulted due to the hollowcore flooring units losing their seating from the supporting beams [1], see Fig.1. Once the beam support was lost, the units collapsed onto the floor below causing a concertina effect with other floors.



(a) Complete collapse of a floor slab



(b) Partial collapse of a floor slab.

Fig.1 After the Northridge Earthquake (17th January 1994)

Following the observed failures in the 1994 Northridge earthquake a major research initiative has been undertaken at the University of Canterbury, to determine whether New Zealand designed and built structures have similar problems, and if so, to what extent these problem exist in a New Zealand context and what can be done about mitigation.

In order to test the performance of a precast concrete building constructed to the New Zealand Concrete Standard [2], a full size super-assembly of a building was constructed in the University of Canterbury structures laboratory. By constructing a super-assembly, it is possible to recreate the boundary conditions, as they would exist in a real structure. Previous studies carried out at the University of Canterbury only focused on the individual components of a building (e.g. Beam-column subassemblies). This project focuses on investigating the interaction of column-beam-slab performance of the large super-assembly.

The principal aim of this project is to investigate the floor-frame interaction and the effect that beam elongation has on the support for hollowcore floor units. The strength enhancement to the perimeter beam negative moment capacity due to beam elongation will also be examined. The experimental evidence based on determining member capacities at zones of inelastic behaviour (plastic hinge zones) will be integrated into a computational analysis of seismic demands of a selection of low, medium and high rise frames. By investigating the balance between member capacities versus the seismic demands associated with variable hazard exposure it will be possible to make recommendations on seat width requirements for supporting the ends of the units. Moreover, insight will be given into the seismic vulnerability of the existing building stock with precast concrete floor systems.

2 SPECIMEN DETAILS

This test specimen represents a lower storey in a typical precast concrete building. The flooring system consists of 300mm deep hollowcore units with a 75mm cast insitu topping spanning 12m. The hollowcore unit itself spans past the central column, as this is a common detail used in New Zealand, and is seated on the two end beams with a nominal seat width of 50mm. Their actual length is 20mm on the east beam and 40mm on the west beam. These provided seats are to connect the hollowcore unit to the beam were considered to be representative of the range of seat width adopted in the field over the past two decades. Fig.2 shows the super-assembly dimensions. The connection detail used consisted of the unit being placed on a cement-mortar joint and a standard hooked starter bar being placed around the beam steel lapping with the non-ductile topping mesh. The unit itself was not tied to the perimeter frame.

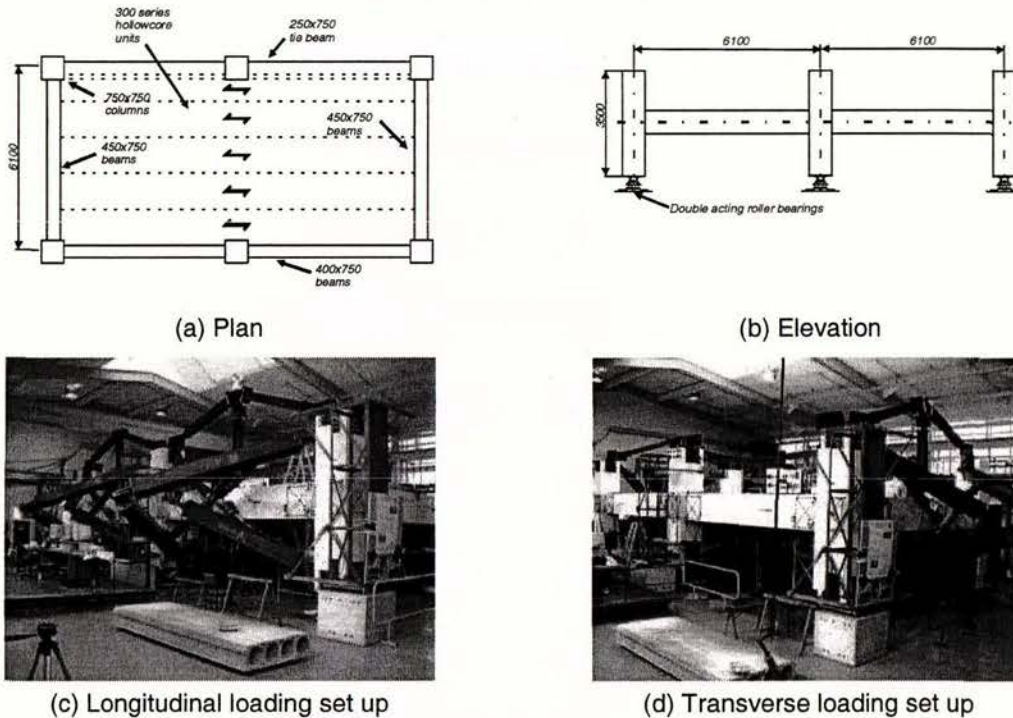


Fig.2 Super assembly dimensions

A complex test rig was developed for this large scale experiment. The test rig was required to apply realistic loads to the structure so that the specimen deforms in the correct manner. Special care was taken to ensure that any beam elongation that develops during the course of the experiment is neither exaggerated nor restrained by the lateral loading apparatus.

Fig.2(c) and 2(d) shows the loading frame set ups for both the longitudinal and transverse loading directions. The two main loading frames are the diagonal frames and they apply the shear forces to the columns. A set of secondary loading frames (that resemble an arrow shape) is provided to enforce displacement compatibility of the adjoining stories. The secondary frames ensure the drift angle on each column is the same.

3 BEAM ELONGATION

During a severe seismic attack, buildings that have been designed in accordance with modern codes behave by a preferred manner whereby a beam sidesway mechanism forms with plastic hinges at each end of the beams. Once plastic hinges form in a beam and the beam undergoes large inelastic rotations, the beam grows in length. This phenomenon has been demonstrated in various experimental studies undertaken by several groups of researchers [3, 4, 5, 6 & 7].

The mechanics of beam elongation can be explained by referring to Fig.3 (Matthews et al [8]). This example describes the elongation for a typical plastic hinge zone where there is more top

reinforcement in the beam than bottom reinforcement. This scenario is common as most beams have a symmetrical reinforcing cage layout. Extra top reinforcement comes from any activated slab reinforcement. For simplicity all the deformations are assumed to be rigid body rotations.

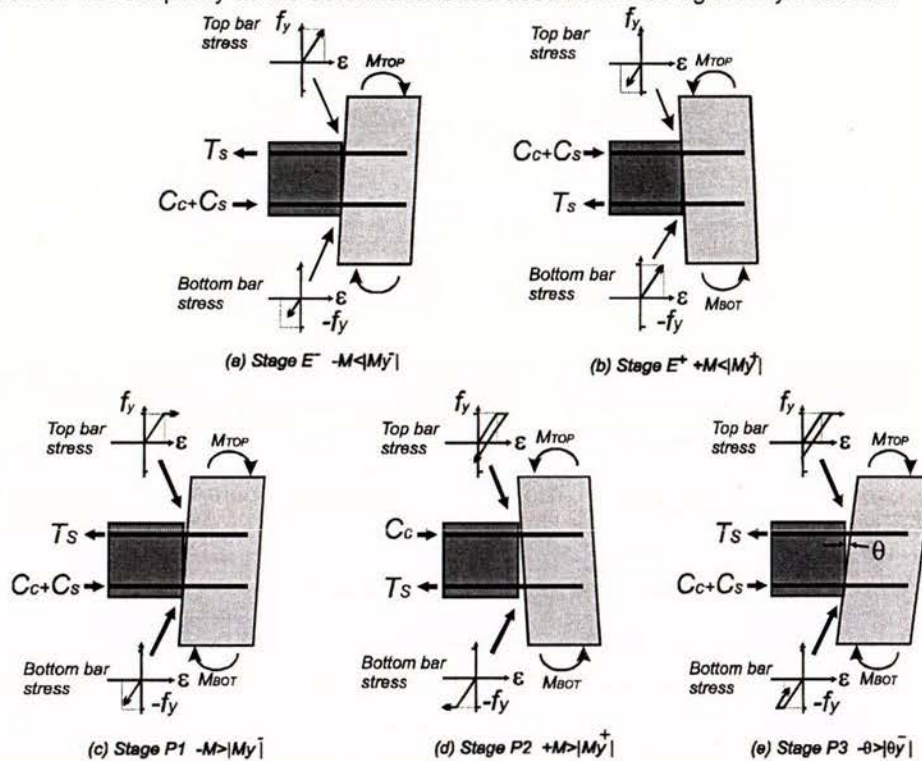


Fig.3 Mechanics behind beam elongation [8]

Stages of load reversal and the effect of cyclic loading are shown in Fig.3. Stages E⁻ and E⁺ are for elastic negative and positive moments, respectively. Stages P1, P2 and P3 are inelastic negative, positive and negative amplitudes where the ductility factors exceed 1. Also shown in Fig.3 are bar stresses that lead to beam elongation. This process continues throughout the duration of the earthquake provided the earthquake imposed displacements are large enough to continue to yield the bars further. The amount by which the plastic hinge elongates depends on the number of inelastic cycles imposed on the beam.

Fenwick & Megget [5] and Restrepo et al [7] have derived mathematical expressions for the magnitude of expected beam elongation. The expression derived by Restrepo for elongation is a function of the amount of rotation the plastic hinge has undergone, the internal lever arm of the beam and the ratio between the column centrelines to the distance between plastic hinges. Typical magnitudes for the elongation have been observed to be 2-5% of the beam depth per plastic hinge. The majority of research conducted on the beam elongation problem to date has not examined the presence of the floor slab system on the beam elongation. The presence of a floor slab is likely to restrain this elongation, but the extent of this restraint is unclear.

4 THE ROLE BEAM ELONGATION PLAYS IN THE SYSTEM

4.1 Hollowcore seating length:

As beam elongation occurs the available seat width for the hollowcore units is reduced. If this length is insufficient to handle the amount of elongation demand then the hollowcore units become unseated. The reliance of bond with the cast in place topping slab to restrain collapse is questionable. Concern has been expressed as to whether this bond is sufficient [9, 10 & 11]. Certain failures observed in the 1994 Northridge earthquake showed that bond is insufficient in providing restraint as shown in Fig.1(b). Concern has also been raised regarding whether the hollowcore unit itself will remain intact during an earthquake.

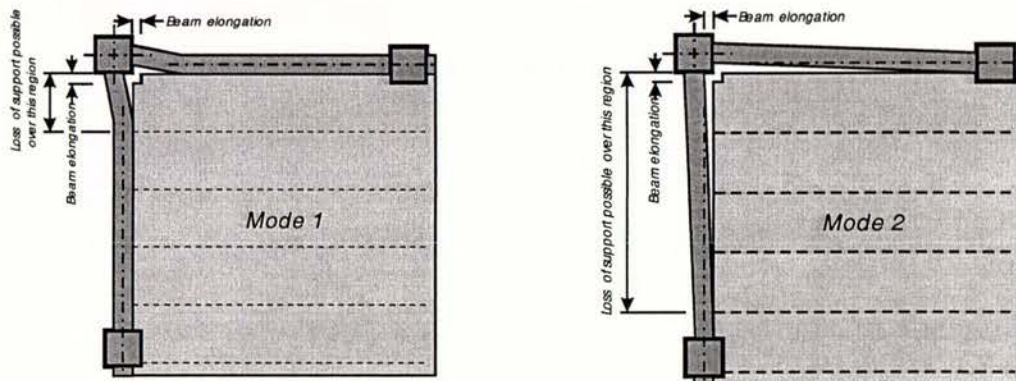
4.2 Negative Moment enhancement:

As beam elongation starts to occur some of the reinforcement within the floor slab becomes activated. This acts as additional beam tensile reinforcement and increases the negative moment capacity of the beam. If this enhancement is significant, there is a chance that the building will not perform in the expected mechanism of a strong column-weak beam as the beams have become stronger than the columns. Researchers [12] have partially investigated this enhancement for monolithic slab construction, but the effect the hollowcore units have on the system has not been studied. If enough columns on a particular floor are damaged then there is a possibility that a soft storey failure could result.

4.3 How does beam elongation affect the displacement of the orthogonal perimeter beam?

As the beams start to elongate the orthogonal beam must start to rotate out-of-plane to account for this beam growth. The way in which this beam displaces will affect the number of hollowcore to lose their seating.

Two possible mechanisms are expected to occur. The first, and most likely, is where the beam rotates out about the plastic hinge zone next to the corner column. If this occurs then the number of units that loose their seating will be low and will only be a problem in the corners of buildings. This is referred to as a "Mode 1" mechanism as shown in Fig.4(a). The second mechanism is where the entire beam rotates as shown in Fig.4(b). The mechanism could lead to more units being pulled off their support. This is referred to as a "Mode 2" mechanism.



(a) Beam plastic hinge rotates to allow for beam elongation

(b) Entire beam rotates to allow for beam elongation

Fig.4 Particular deformation modes to deal with beam elongation.

4.4 Strut and tie solutions for floor diaphragm forces:

Traditionally during a strut and tie analysis for a floor diaphragm of a monolithic frame construction, the corner columns have been used as nodes to allow the compression struts within the diaphragm to be transferred to the perimeter frame [13]. This may not be possible for precast concrete frames because the area around these columns is likely to be extensively damaged. There is a possibility that a large crack occurs along the interface between the floor slab and the column (as shown in Fig.4) not allowing the compression force to be transferred to the perimeter beam.

Another option has been to place a series of 'drag' bars in the floor slab just off the perimeter beams to allow the diaphragm forces to be directed to a relatively undamaged zone in the centre of the beams. This solution may be inappropriate as any additional reinforcing steel placed in the floor slab may unduly enhance the perimeter beam's negative moment capacity causing the beams to become excessively strong and potentially lead to column hinging.

A complete rethink on the strut and tie analysis of floor diaphragms is considered necessary.

5 EXPERIMENTAL APPLICATION OF SEISMIC LATERAL LOADS.

The earthquake simulated loads are applied to the structure as a series of column shear forces to the top and bottom of the columns.

The fundamental component ensuring that beam elongation is not exaggerated nor restrained is the applied column shear forces. A typical shear force diagram is shown in Fig.5(a). These steps in the shear force diagram are due to the floor inertia forces from each floor level. If inertia forces are ignored, as is the case in this testing programme since the floor diaphragm itself is not loaded, then the shear force up the height of the building is constant (Fig.5(a)). Since this testing programme is a pseudo-static test, rather than a real time test, then the assumption of zero floor inertia forces is true. The key issue to allow beam elongation to form naturally is to keep the external applied loads from the column shear forces equal and opposite. This seems to be an area that other researchers have overlooked. If there is an out of balance force between the top and bottom applied shear forces then this elongation is either restrained or promoted. This principle is shown in Fig.5(b).

Since the external applied column shear forces are equal and opposite does not mean that there are no compression or tension fields formed within the beams. As testing proceeds there will be compression fields formed within the beams and these will be equalised by tension fields within the floor diaphragm.

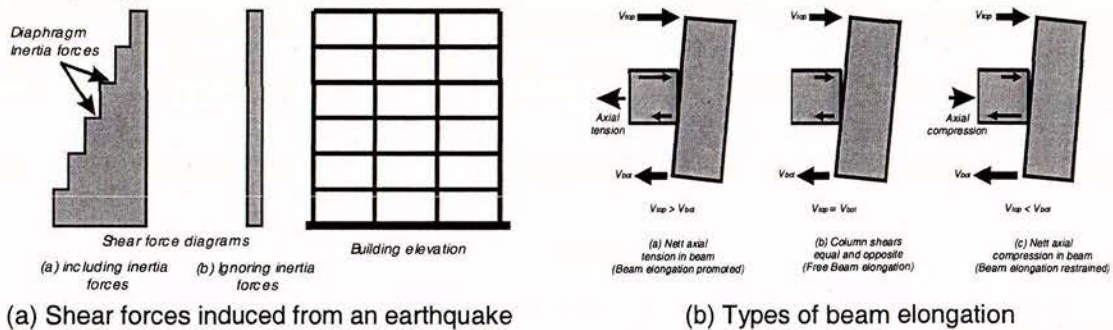


Fig.5 Shear forces induced from earthquake versus potential shear forces induced by experiment

5.1 Time History studies to determine experimental loading protocol.

As recommended by Park [14] the traditional the loading history used to test various concrete elements at the University of Canterbury has required the specimen to be subjected to *two completely reversed loading cycles* at ductility amplitudes of 0.75, 2, 4, 6 and 8. For the present experimental structure whose yield drift is assessed to be 0.5%, this translates into two cycles at $\pm 0.4\%$, $\pm 1.0\%$, $\pm 2.0\%$, $\pm 3.0\%$ and $\pm 4.0\%$. It is considered unrealistic to impose these drifts on the super-assembly as such demands are unlikely to be experienced during a real earthquake. One reason the Park method is considered inappropriate for this experimental programme was because the test being undertaken is one in which existing structural performance is being examined. Therefore the structure should be subjected to a realistic displacement history that can be expected to be experienced, rather than an idealised displacement history aimed at obtaining a conservative dependable performance. When verifying new construction methods, a more conservative experimental protocol is considered acceptable.

Therefore, an analytical study has been undertaken on four different building heights (Fig.6) using numerous earthquake records to determine the expected demand on the sample precast concrete buildings. The earthquake records used in the analytical study have included both near and far field effects. Some records were scaled so that they represented the amount of energy expected from a New Zealand earthquake. From these results it is possible to determine a more realistic loading history that better matches the expected cyclic capacity with the demand.

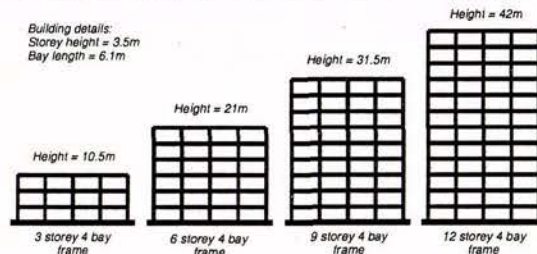
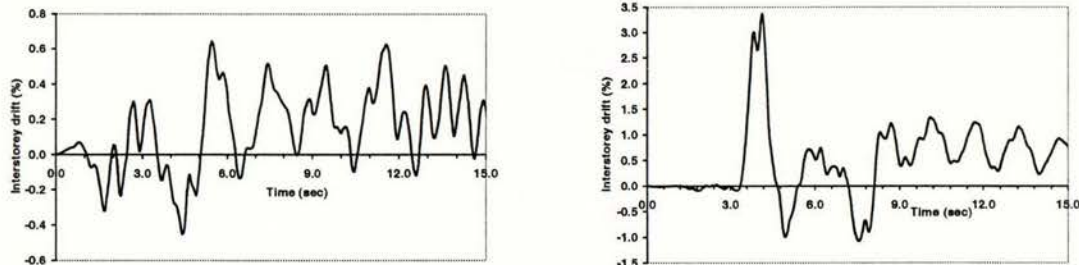


Fig.6 Buildings analysed

The results show that the number of cycles that a structure is likely to experience is significantly less than proposed by Park. Therefore a new loading history was devised based on the time history results.

When examining the results from the time history studies there were two main trends seen. The first was when a far-field type event occurred (1.5xEl Centro 1940). These results showed several cycles of modest amplitudes. An example of the results from this type of earthquake is shown in Fig.7(a). The second trend was seen in a near-field earthquake (Northridge 1994, Syff943) where there was one large pulse and several smaller cycles (see Fig.7(b)). None of the results showed two reversing cycles of increasing magnitude.



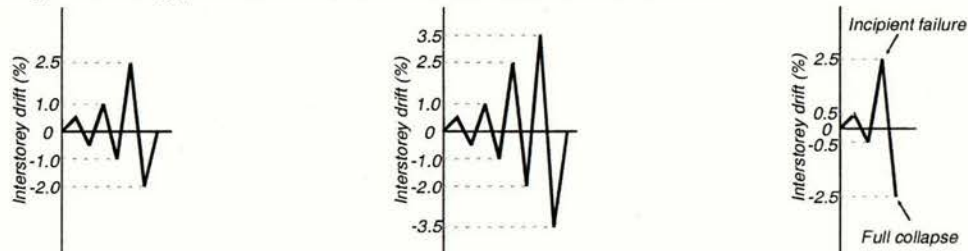
(a) 1.5xEl Centro earthquake, 1940, PGA=0.52G
12 storey structure

(b) Northridge earthquake (Syff943), 1994,
PGA=0.83G, 9 storey structure

Fig.7 Typical time history results.

6 LOAD PATTERN APPLIED.

The finalised loading history to be used to load the super-assembly consisted of three phases (Fig.8). Each phase varied slightly due to the direction of loading but essentially consisted of one completely reversing load cycle at the following interstorey drift levels: $\pm 0.5\%$, $\pm 1.0\%$ and $\pm 2.5\%$ (if a maximum credible event is to be imposed then an additional cycle of $\pm 3.5\%$ is added). Note that this proposed cyclic loading protocol is in stark contrast with the Park method.



(a) Phase I-Longitudinal loading

(b) Phase II-Transverse loading

(c) Phase III-Longitudinal loading

Fig.8 Loading histories applied to the super-assembly.

7 EXPERIMENTAL RESULTS

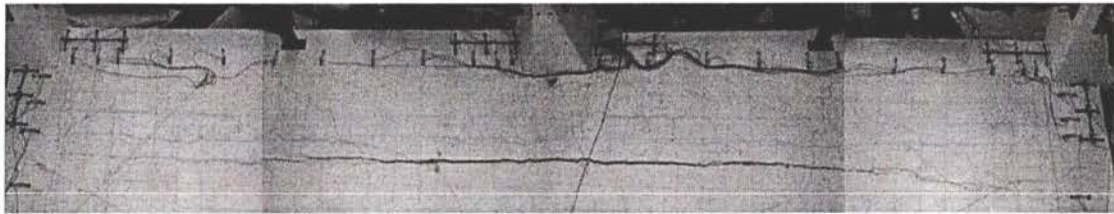
7.1 Phase I: Longitudinal Loading

The results of loading the super assembly are summarised in Fig.9.

As testing progressed the seating detail used to attach the hollowcore floor units to the supporting beams started to crack and show signs of distress from an early stage. The first sign of damage occurred at an interstorey drift of 0.35%, and at a drift of 0.5% ($\mu=1$) this level of damage would be sufficient to cause some economic loss to the building.

Overall the specimen behaved well up to interstorey drifts of $\pm 1.0\%$ ($\mu=2$). However significant cracking in the topping slab developed. As the drift increased this led to a tear forming within the floor slab at a drift of 1.9%. This tear was due to the elongation within the beam causing the central column to translate outwards and taking the first hollowcore unit with it. The reinforcing mesh in the topping slab between the first and second hollowcore units fractured. The tear can be seen in Fig.9(a).

At the completion of the -2.0% cycle, the entire seating for the hollowcore units were damaged (Fig.9(b)), with some of the units dropping 10mm. There was also significant web splitting within the first hollowcore unit. It is considered that when compared to real dynamic earthquake loads, the test was possibly unconservative. This is because if any live load or vertical accelerations had been concurrently applied to the building it would be questionable as to whether the floor would remain suspended. At the completion of the -2.0% drift cycle the central column displaced transverse to the direction of loading by 25mm. This also caused the first floor unit to rise 12mm relative to the rest of the floor. The extent of the crack propagation is shown in Fig.9(c) and (d). The translation was not only due to the elongation of the main beam. The newly formed inverted L shaped beam (beam plus the adjacent floor acting as a flange) contributed to some of this displacement as it tried to bend about its principal axes that were not horizontal or vertical. Since the central column is no longer tied to the floor slab it is possible for the column to fail under buckling. The reason for this is that the floor tear could occur over several floors of the building greatly increasing the columns effective length and hence reducing its load carrying capacity.



(a) Longitudinal tear that formed at 1.9% drift.



(b) Entire seat has been lost at the completion of the Phase I (-2.0%)



(c) Vertical offset after the tear formed (-2.0%)



(d) Longitudinal view of floor slab tear at the end of Phase I (-2.0%)

Fig.9 Observed damage during Phase I testing

7.2 Phase II: Transverse (Short direction) Loading.

Since the major crack had formed within the floor diaphragm it changed the expected performance of the super assemblage during the transverse loading. Initially the expected performance of the diaphragm was for the perimeter beam to rotate relative to the floor units. This was not the case, the first hollowcore unit actually lifted as the beam rotated.

Since the side of the first hollowcore was adequately bonded to the beam, it caused the crack within the soffit of the first hollowcore unit to open some more. This meant that the condition of the hollowcore unit degraded as the transverse loading preceded. The first sizeable piece of concrete fell out around 2.0% drift. This is shown in Fig.10(a). Once the piece of concrete had fallen out of the hollowcore unit it was possible to look at the internal damage within the first hollowcore unit adjacent to the perimeter beam. Extensive damage could be seen to have occurred. Fig.10(b) and (c) shows the extent of the damage. The width of web crack within the hollowcore unit was approximately 25mm. At this stage, the webs of the first hollowcore unit had split halfway along the unit (approximately 6m). For some time now one small triangular shaped piece of concrete was holding the first floor unit up. This small section of concrete could not be relied upon to hold every time. This can be seen in Fig.10(e) at the top of the picture.

It should be noted that the hollowcore unit dropped some 30mm at this stage as shown in Fig.10(d). Fig.10(e) shows the first floor unit after a large piece of floor fell out. At this stage, the floor had dropped by some 60mm.



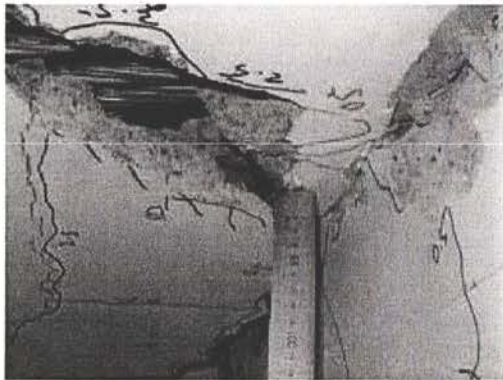
(a) Hollowcore damage



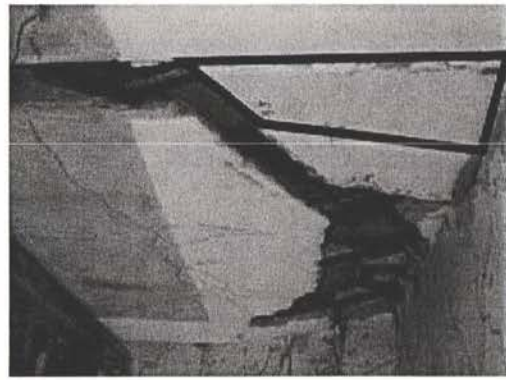
(b) Internal damage looking towards the seat



(c) Internal damage looking away from the seat



(d) Damage to the underside of the west unit.



(e) Damage at 3.0% drift.

Fig.10 Observed damage during Phase II testing

7.3 Phase III: Final Longitudinal Loading

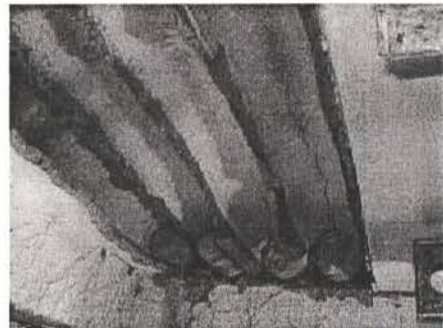
Eventually there was sufficient damage within the first hollowcore unit to allow the entire bottom section to drop as shown in Fig.11 (a) and (b). This failure occurred at an interstorey drift of 2.0%. These photos look very similar to those taken following the 1994 Northridge earthquake [1].

Upon further loading, to the -2.5% drift amplitude, the remainder of the floor failed when the design live load was applied. Again, the photos of this failure (Fig.11) were very similar to that seen in Northridge.

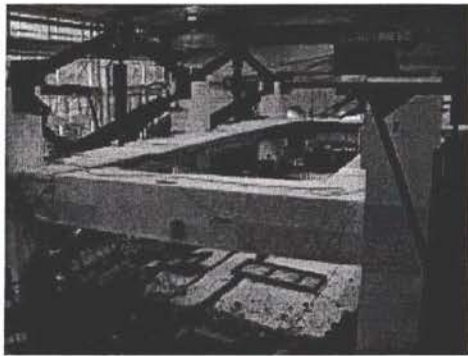
One major point to note is that even though the floor failed, the perimeter frames beams, columns, and beam column joints remained relatively undamaged. Clearly, significantly extra attention is required to be paid to the hollowcore seating details to ensure that this class of precast floor system performs at a level that is not inferior to than that of the structural frame.



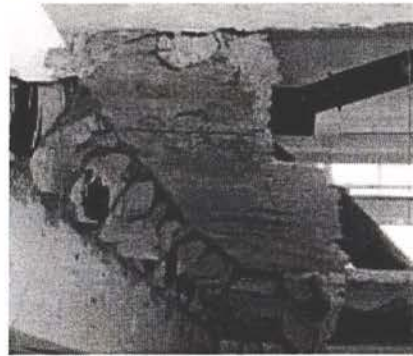
(a) Failure of the first hollowcore unit



(b) Close up looking at the seat damage



(c) The frame after the floor collapsed



(d) The remaining topping and ends of the hollowcore units after collapse

Fig.11 Observed damage during Phase III testing.

8 DISCUSSION

8.1 Seating detail performance.

One major difference between the expected seating performance and the observed performance was the way in which the floor unit moved relative to the beam it was seated upon. In design it is customary to assume that hollowcore units would slide relative to the beam; this was not the case in the experiment. There was enough bond/friction to cause the unit to fracture at the end of the units rather than slide, as shown in Fig.12. The role that beam elongation played in the experiment was not as great as first expected. The reason for this is that this experiment was not exposed to the large number of inelastic rotations that other experiments had been exposed in the past. Also, the role that the floor played in restraining this elongation.

A Technical Advisory Group (TAG) has been formed in New Zealand to discuss these experimental results from the testing programme at the University of Canterbury. The TAG recommended a new connection detail that is expected to perform better than the details currently used. The new detail consists of replacing the dam plug in the end of the unit and placing some compressible material approximately 10mm thick across the end of the unit. The unit will also be placed on a bond breaker, in the form of a low friction (PTFE or equivalent) bearing strip. A sketch of the proposed detail is shown Fig.13 along with the expected improved (damage-free) performance.

Attaching a low friction bearing strip allows the floor unit to slide as previously assumed. The compressible material is added to reduce the compression force applied to the bottom of the unit. The combination of the two details allows the beam to rotate relative to the floor unit without fracturing the end of the floor unit allowing the connection detail to work as assumed.

The thickness of compressible material required is determined by multiplying the thickness of the topping and hollowcore by the maximum expected interstorey drift of the structure. For example, a 300 series hollowcore unit with a 75mm topping requires the compressible material to be at least 13mm thick if the maximum expected interstorey drift is 3.5%.

The initial results from the testing of a sub assemblage using this modified connection detail look promising. This detail is currently being set up for testing in the super assemblage used in this paper. Unfortunately at the time of writing these results are not available for any further discussion.

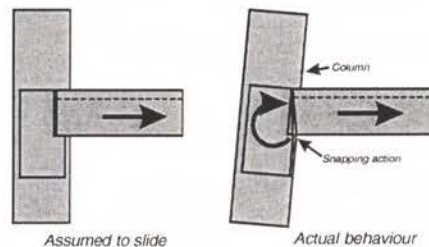


Fig.12 Assumed versus actual hollowcore to beam performance.

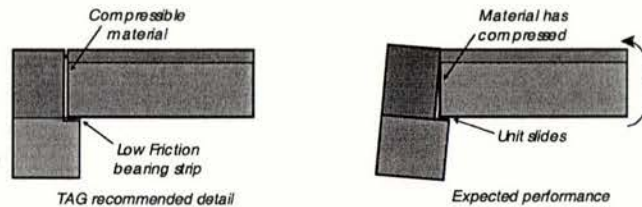


Fig.13 Recommended detail and assumed performance.

Another detail that was tested and performed well in a sub assembly test was one in which two of the cores of the unit had additional reinforcing in the form of a paperclip added. The unit was also seated on a low friction bearing strip. Further work is required on this detail as the sub assembly test made several simplifying assumptions that could mean these results are unconservative. This detail should also be tested in the super assemblage.

8.2 The performance of the first hollowcore unit adjacent to the frame.

A hollowcore floor unit is designed to act as a simply supported one-way floor system. The first unit placed adjacent to the perimeter frame does not act in this manner as it is securely tied not only at its ends but also along its entire length. This leads to the unit being displaced in a quasi-two way manner as the hollowcore unit is forced to undergo the displaced shape of the perimeter beam. This displacement incompatibility between the double curvature of the perimeter beam and the simply supported hollowcore unit causes the hollowcore unit to fail (Fig.14). Since the hollowcore unit has no redundancy in its design the unit fails through web splitting and the bottom half of the hollowcore unit drops.

If the unit was not tied along its length, in other words the hollowcore unit was not forced to undergo the displaced shape of the perimeter beam, then the unit would most probably perform better. If the unit is then detached from the perimeter beam then there are problems with the transfer of the forces from the diaphragm to the perimeter moment resisting frame. This area requires further investigation.

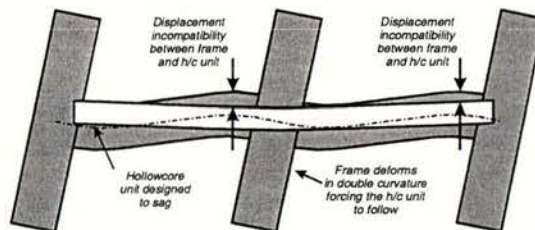


Fig.14 Displacement compatibility between the frame and the hollowcore floor units.

Changing the way in which the first hollowcore unit is connected to the adjacent perimeter beam should allow the unit to perform in the manner in which it was intended by design—that is, a one-way slab. The solution specified involves a timber infill that allows a more flexible interface (Fig.15). Damage is expected within this in-filled section leaving the first hollowcore unit undamaged. This detail is also currently being tested.

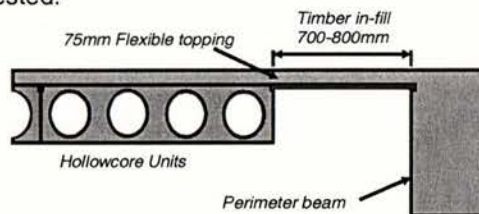


Fig.15 Recommended detail allowing the first hollowcore unit to be separated from the perimeter beam.

8.3 Extra diaphragm tie reinforcement

During the experiment a longitudinal tear formed within the floor diaphragm due to the overloading of the diaphragm reinforcement as floor-frame set up displaced. This tear within the floor now affects the column effective length. If such a tear occurred over several floors in a real multi-storey frame then the column may become unstable.

Another scenario that is not usually considered is that columns at lower levels within buildings need to be adequately tied to the floor diaphragm. These columns need to be tied because as a building displaces in an earthquake all the bottom columns must hinge at ground level. This means that several of the edge columns are being dragged across by floor diaphragm. If the provided tie force is insufficient then the diaphragm will tear due to this displacement incompatibility.

The New Zealand Concrete Standard, NZS3101:1995 [2], states, "additional tie reinforcement must be used to tie the column to the floors at each flooring level. The magnitude of the tie force is equal to the larger of 5% of the maximum total axial compression load on the column or 20% of the column shear force induced by the lateral design forces." The draft joint Australian and New Zealand Structural Design Actions Standard [15] requires that "all parts of the structure shall be interconnected. Connections shall be capable of transmitting 5% of the value of $(G + \psi_c Q)$ for the connection under consideration."

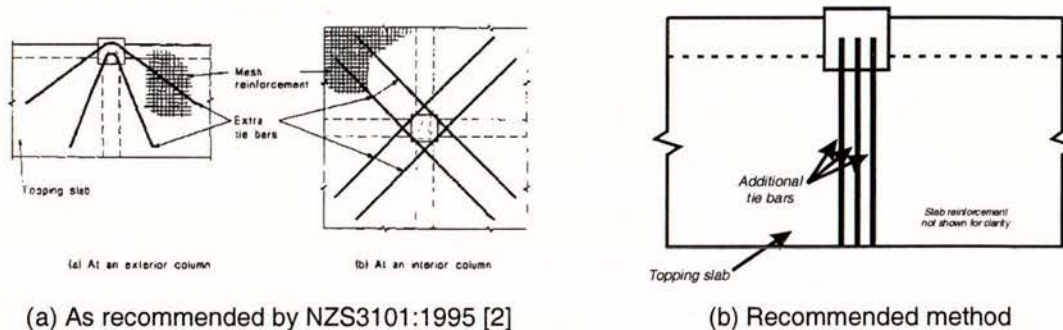


Fig.16 Recommended tie details.

As specified by the NZS3101 the bars should be placed at angles close to 45° . This does help tie the column in but also contributes to the perimeter beams over strength actions. The bars would be better placed transverse to the perimeter beam. These two comparisons are shown in Fig.16.

9 PERFORMANCE IMPLICATIONS

Buildings in New Zealand are commonly designed for displacements of up to $\pm 2.0\%$ interstorey drift. This is for the so-called 10% in 50 year earthquake (500 year return period). However, there is a worldwide trend to use a 2% in 50 year earthquake motion as the principal design event (≈ 2500 year return period). For New Zealand seismicity, considering a limit state of collapse avoidance, this would lead to interstorey drifts in excess of 3.5% for the present building stock.

The experiment conducted as part of this research has demonstrated that for present design basis earthquakes considerable damage to precast flooring systems may be expected and lead to irreparable damage. However, should a larger event occur, such as a maximum credible-like event (2% in 50 years) complete collapse of the precast floor is possible. This violates the life-safety intent of the present design codes.

It is concluded that further work is required on three fronts:

(1) For existing structures retrofit measures need to be explored to enhance floor seating and strength. Provision of limiting interstorey drift may also be considered such as the use of structural walls and/or damping devices.

(2) For structures to be designed in accordance with the present design codes, design drifts should be limited to about 1.2% to ensure life-safety can be maintained. This may have severe economic implications because in order to limit the drifts heavier, stiffer and stronger structures will result.

(3) For future structures, considerable work needs to be undertaken if precast flooring systems are to remain a viable design option. Particular attention needs to be paid to 3D effects and the seating details. In summary a new Damage Avoidance Design (DAD) philosophy needs to be developed for seismic resistant building structures.

ACKNOWLEDGEMENTS

This project would not be possible without the financial support from the following organisations: University of Canterbury, Firth Industries Limited, Stresscrete, Stahlton Prestressed Flooring, Precast Components, Technology New Zealand, Cement & Concrete Association of New Zealand, BRANZ, Earthquake Commission, Construction Techniques and Pacific Steel.

REFERENCES

- [1] Norton, J.A, King, A.B, Bull, D.K, Chapman, H.E, McVerry, G.H, Larkin, T.J, Spring, K.C, 1994, *Northridge Earthquake Reconnaissance Report*, Bulletin of the New Zealand National Society for Earthquake Engineering Vol. 27, No.4, December
- [2] Standards New Zealand, 1995, *Concrete Structures Standard, NZS 3101, Parts 1 & 2*, Standards New Zealand
- [3] Douglas K.T and Davidson B.J, 1992, *Elongation in Reinforced Concrete Frames*, University of Auckland Research Report No.526, October
- [4] Davidson B.J and Fenwick R.C, 1993, *The Seismic Response of Ductile Reinforced Concrete Frames with Uni-directional Hinges*, University of Auckland Research Report No.527, January
- [5] Fenwick R.C and Megget L.M, 1993, *Elongation and Load Deflection Characteristics of Reinforced Concrete Members Containing Plastic Hinges*, Bulletin of the New Zealand National Society for Earthquake Engineering, Vol 26, No. 1, pp 28-41, March
- [6] Fenwick R.C and Fong A., 1979, *The Behaviour of Reinforced Concrete Beams under Cyclic Loading*, Bulletin of the New Zealand National Society for Earthquake Engineering, Vol 12, No. 1, pp 158-167, June
- [7] Restrepo J.I, Park R and Buchanan A, 1993, *Seismic Behaviour of Connections Between Precast Concrete Elements*, Research Report 93-3, Department of Civil Engineering, University of Canterbury, Christchurch, New Zealand.
- [8] Matthews J.G, Bull D.K and Mander J.B, 2001 *Investigating the Loadpaths of floor diaphragm forces following severe damaging earthquakes*, Conference Proceedings Combined Concrete Society and Ready Mix, TR24, pp122-131, Rotorua October
- [9] Mejia-McMaster J.C and Park R., 1994, *Tests on Special Reinforcement for the End Support of Hollow-Core Slabs*, PCI Journal, Vol 39, No. 5, pp. 90-105, September-October
- [10] Herlihy M.D, Park R. and Bull D.K, 1995, *Precast Concrete Floor Unit Support and Continuity*, Research Report 93/103, Department of Civil Engineering, University of Canterbury, Christchurch, New Zealand.
- [11] Oliver S. J, 1998, *The Performance of Concrete Topped Precast Hollowcore Flooring Systems Reinforced With and Without Dramix Steel Fibres Under Simulated Seismic Loading*, Master of Engineering Thesis, Department of Civil Engineering, University of Canterbury, Christchurch, New Zealand, 176 pp.
- [12] Cheung P. C., Park R, Paulay T, 1991, *Seismic Design of Reinforced Concrete Beam Column Joints with Floor Slab Support*, Research Report 91-4, Department of Civil Engineering, University of Canterbury, Christchurch, New Zealand, 328 pp.
- [13] Park, R., Paulay, T. and Bull, D.K, 1997, *Seismic Design of Reinforced Concrete Structures*, New Zealand Concrete Society, pp.5-1 – 5-19.
- [14] Park R., 1989 *Evaluation of ductility of structures and structural assemblages from laboratory testing*, Bulletin of the New Zealand National Society for Earthquake Engineering, Vol. 22, No. 3, September, pp155-166.
- [15] Standards New Zealand, 2003, Draft AS/NZS 1170.3:2002 *Structural Design Actions- Earthquake Loadings*, Standards New Zealand, Wellington

Prediction of beam elongation in structural concrete members using a rainflow method

J.G. Matthews, J.B. Mander

Department of Civil Engineering, University of Canterbury, Christchurch, New Zealand.

D.K. Bull

Department of Civil Engineering, University of Canterbury; Holmes Consulting Group.



2004 NZSEE
Conference

ABSTRACT: The prediction of beam elongation has been studied by various researchers. Results have shown that beam elongation can be predicted by assuming that the elongation varies proportionally with interstorey drift. A Rainflow Counting method is proposed that enables a better understanding of how beam elongation occurs. The method predicts the amount of beam elongation on an individual plastic hinge basis or a frame as a whole. This predictive approach is then validated against the results conducted as part of a current research programme.

1 INTRODUCTION

Beam elongation is a phenomenon that occurs as a result of a structural concrete element forming a plastic hinge and growing in length under reversed cyclic loading. Although the phenomenon of beam elongation has been qualitatively understood for some time, only recently have fundamental theories emerged to predict elongation history as a function of cyclic loading. One recent micro-mechanics based theory has been advanced by Lee and Watanabe (2003). Other investigators, such as Fenwick and Megget (1993) and Restrepo et al (1993) have proposed empirical formulations, adjusted to fit experimental data, to predict total elongation. While the empirical methods are useful for designers in identifying the length of ledges (seats) required to support precast concrete flooring units in multi-storey frames; these lack the rigour and the intellectual appeal in predicting the time history behaviour of beam elongation developed by Lee and Watanabe (2003).

During an earthquake, well designed buildings are expected to behave by ensuring a beam side sway mechanism forms with plastic hinges at beams ends. Once plastic hinges form in a beam and the beam undergoes large inelastic rotations, the beam grows significantly in length. The plastic hinges within a beam which generate beam elongation can be defined as one of two types, either fully reversing or uni-directional (Fenwick and Megget, 1993 and Fenwick et al, 1999). A uni-directional hinge is one that forms within a gravity dominated system in which the positive and negative moment plastic hinges develop in different locations. A reversing plastic hinge is one in which the positive and negative moment plastic rotations develop in the same location.

Beam elongation occurs for two reasons: (1) Recoverable elongation is due to the neutral axis being less than half the member depth and the strain at the mid depth is in tension; (2) Non-recoverable (permanent) beam elongation occurs because $C_s = T - C_c$ where $C_s < T$ from the previous reversal (where C_s = compression force in the reinforcement in one face of the beam; T = tensile force in the reinforcement in the opposite face; and C_c = concrete compressive force), see Figure 1. The plastic strains in tension are not recovered on the compression reversal.

Fenwick and Megget (1993), Restrepo et al (1993) and Lee and Watanabe (2003) have derived equations for determining the amount of expected beam elongation. The experimental programmes that formed the basis for determining these equations did not appear to incorporate a floor slab even though it was evident from the previous investigators work that the role of the floor slab is critical in determining the magnitude of the beam elongation. For a detailed breakdown of the mechanism behind beam elongation refer to Fenwick and Megget (1993) and Restrepo et al (1993).

This paper proposes an analysis methodology for predicting the beam elongation history of structural concrete elements under cyclic loading. The approach is based on a "Rainflow Counting" method adapted from high cycle fatigue counting theory. This theory is then validated against the results from the present super-assembly experiment and includes both individual hinge elongation and gross ledge (seat) width demands based on the elongation of several hinges across the bent. Finally, conclusions are drawn and a recommendation on the seat width demand is given.

2 A Rainflow method for predicting beam elongation

Fenwick and Davidson (1995) stated that beam elongation is caused by two factors. Firstly, when a deformed reinforcing bar yields in tension the region around the bar cracks. This causes the concrete to dilate and aggregate particles get wedged in the cracks so that as the load reverses the cracks do not entirely close as it takes appreciable force to close the cracks and secondly, a flexure shear truss is formed within the beam. These two reasons are not the sole explanation for beam elongation. Herein it will be shown that beam elongation can be explained in terms of plastic flexure alone via rigid body kinematics.

The force-deformation graphs on the right hand side of Figure 1 show that for a positive moment the tension reinforcement has yielded and undergone plastic deformation while the compression reinforcement is at a stress below yield. For the negative moment the top reinforcement recovers the elastic compressive stress and then yields in tension while the bottom reinforcement regains its elastic recovery but has a residual strain at zero stress. Therefore, Figure 1 shows that both a positive and negative moment result in a permanent elongation strain at the centre of gravity of the concrete section (c.g.c) of the beam (refer to the strain diagrams). This permanent elongation strain forms within both elastically and plastically responding structures.

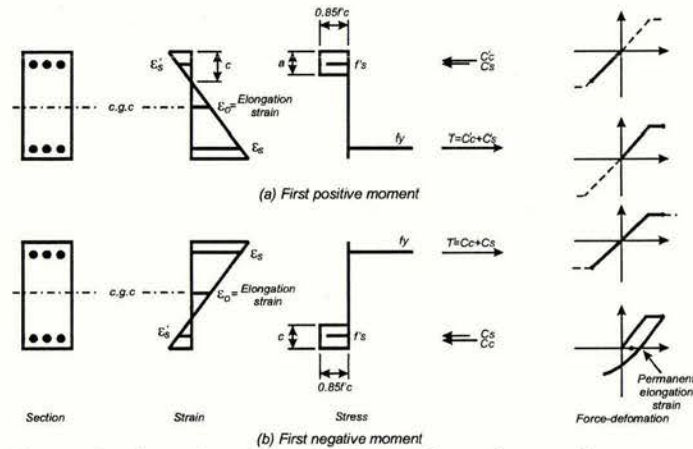


Figure 1 Rigid body kinematics is used to show that beam elongation can be expressed in terms of plastic flexure

The basis of deriving beam elongation history as a result of reversed cyclic loading is summarised in Figure 2. Figure 2(a) shows a typical lateral load deflection behaviour of an inelastic frame system. The maximum cyclic amplitudes are numbered (1 to 5) with the odd numbered cycles representing positive displacement peaks, while the even numbered cycles are for the negative displacement peaks. From the hysteresis plot it is possible to determine the yield drift (θ_y) and the amount of plastic rotation (θ_p) that the plastic hinges undergo.

Beam elongation occurs whenever "new" rotation occurs. "New" rotation is defined as the rotation that occurs at a level of interstorey drift that has not been achieved during a previous load cycle. An example of this is from points 3-5 on Figure 2(a). Figure 2(c) shows that when the load reverses, once it has reached a new maximum, it is assumed that the beam elongation remains constant until some "new" rotation occurs in the opposite direction.

Within the pre-yield phase, only the first half cycle to yield contributes to the beam elongation. This is because when the load reverses the plastic hinge experiences elastic recovery and then elongates in the

opposite direction. Because of the elastic recovery the apparent beam elongation appears to be half that of the first half cycle. In fact, if the elastic recovery and additional elongation are summed this equates to the same beam elongation as in the first half cycle. This elastic recovery and additional elongation has been chosen to be ignored and represented as a horizontal line in Figure 2(c).

The sub-figures shown at points 3-5 represent the actual deformation of the particular plastic hinge zone and the strain states within the beam reinforcement. Prior to point 1 in Figure 2, whenever the load reverses the reinforcing steel in tension partially recovers its elastic deformation and the crack at the beam column interface closes. From the yield point (point 1), to point 3 top steel yields in tension and undergoes plastic deformation. The bearing of the concrete and the bottom reinforcement in compression resists the compressive force. Upon load reversal toward point 4, as there is significantly more top reinforcement (due to the activated slab reinforcement), the bottom reinforcing yields in tension before the top reinforcing is able to yield back in compression. This beam elongation is caused because the top crack has not closed fully and the bottom reinforcement has been pulled out of the beam. The compressive force now is resisted by the compression reinforcement alone. Further as the load reverses towards point 5 the bottom crack essentially closes except for the aggregate wedged into the cracks, as there is sufficient force to yield these bars back in compression due to the large area of top reinforcement. Now the top beam reinforcement undergoes further plastic deformation and the crack width increases. Each of these three points experience new plastic rotation.

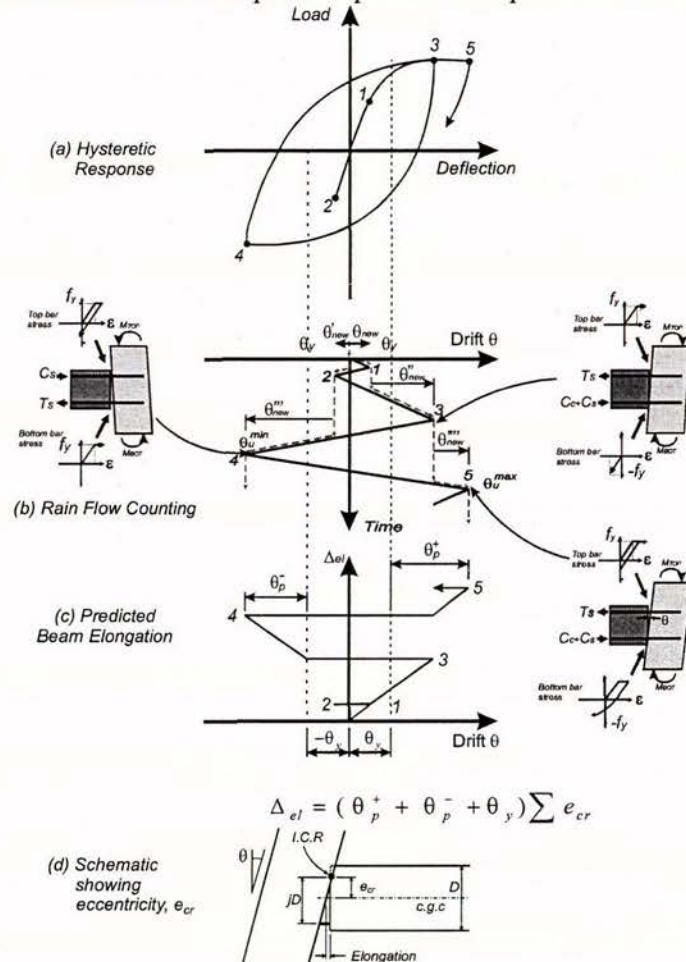


Figure 2 General theory for the determination of beam elongation.

Figure 2(b) shows a time versus drift graph that is used to determine the amount of rotation that contributes to the beam elongation. Beam elongation occurs within both the elastic and plastic ranges of a test. Major beam elongation only takes place when the deformation exceeds the previous peak. Therefore, the technique commonly used herein to identify new segments of drift that contribute to beam elongation is analogous to the method used in high cycle fatigue counting analysis called

“Rainflow Counting” (Dowling, 1972). The solid lines on the time versus drift graph are imagined as a series of pagoda roofs. Droplets of rain, starting from zero rotation are then dropped onto the pagoda roofs and allowed to flow down the slope. The drops are tracked (dashed lines) until it falls off the edge of the roof and then the amount of plastic rotation is counted. Once the total amount of “new” rotation is determined, (i.e. the portions in Figure 2(b) shown by the regions denoted as “ θ_{new} ”) an expression for the beam elongation can be determined. If additional cycles to the same rotation occur the elongation may increase slightly due to the additional aggregate being pulled into the cracks.

The amount that a plastic hinge elongates for a given rotation is expressed by

$$\delta_i^{el} = \theta e_{cr} \quad (2-1)$$

where δ_i^{el} = elongation of the i^{th} hinge; θ = rotation the beam undergoes; and e_{cr} = eccentricity between the c.g.c of the beam and the centroid of the compression force (instantaneous centre of rotation, I.C.R).

A designer is interested in the maximum expected beam elongation for a given frame so that the required ledge (seat) length for a precast element can be determined. This total elongation is expressed in terms of rotation by

$$\delta_{max}^{el} = \left(|\theta_p^+| + |\theta_p^-| + \theta_y \right) \sum_{i=1}^n e_{cri} \quad (2-2)$$

where δ_{max}^{el} = maximum plastic elongation within a frame/bent; θ_p^+ = maximum positive plastic rotation imposed on the structure; θ_p^- = maximum negative plastic rotation imposed on the structure; θ_y = yield drift of the structure (the yield drift, θ_y , herein is assumed to be the same for each direction of loading) and e_{cri} = force eccentricity of the beam depth which is the distance between the beam centreline and the instantaneous centre of rotation (the centroid of the compression force) for the i^{th} hinge.

Equations derived by other researchers, such as Restrepo, were not loading dependent and were based on a symmetric loading pattern whereas the elongation model used to derive Equation (2-2) is loading history dependent so therefore determines beam elongation for any loading history.

3 Validation of theory

The proposed theory has been validated against experimental observation made by previous investigators work (Fenwick et al (1981), Restrepo et al (1993) and Lau (2001)). Full details are reported elsewhere (Matthews (2004)).

Beam elongation was monitored during an experimental testing programme in which a two-bay by one-bay moment resisting frame building that incorporated a hollow-core floor slab. The super-assembly was loaded in three phases as follows: Phase I loading was parallel to the hollow-core floor units; Phase II was loaded transverse to the hollow-core floor units; and Phase III was again parallel to the hollow-core floor units. As there were no new displacements beyond the previous maxima in Phase III, beam elongation only occurred in Phase I and II. The experimental results of these two phases are compared with the theoretical prediction in what follows. For full details on this experimental programme refer to Matthews (2004).

3.1 Total beam elongation

Due to the composition of the frame two types of joints are studied when the super-assembly is loaded parallel to the hollow-core floor slabs (Phase I), the first being the exterior joints and secondly the interior joints. The direction of the cyclic loading plays a role in the amount of elongation that forms. This is because a negative and positive moment for the same plastic hinge has a different internal eccentricity (e_{cr}) due to the different amount of tension reinforcement activated. Since there is significantly more top reinforcement compared to the bottom reinforcement (due to the activation of some slab reinforcement) e_{cr} will also be different. Values of e_{cr} were determined by compatibility and equilibrium analysis and found to be $0.425D$ and $0.475D$ for a negative and positive moment

respectively (in which D is the overall member depth)(Figure 3(a)). During the elastic phase of the experiment a moment-curvature analysis confirmed that the values of $e_{cr}=0.425D$ and $0.475D$ were appropriate. The interior plastic hinge zones on either side of the central column have different e_{cr} values when compared to the exterior plastic hinges. This is because the central column has a hollow-core floor unit spanning past it that has a large number of prestressing strands in the central region of the reinforced concrete beam. The prestress effectively reduced the internal leverarm factor e_{cr} by moving the centre of rotation closer to the beam centreline as well as causing the centroids of the tension reinforcement to be closer to the beam centreline (Figure 3(b)). Based on a compatibility and equilibrium section analysis, the values of e_{cr} were $0.225D$ and $0.275D$ for negative and positive moments, respectively (for both elastic and plastic analysis).

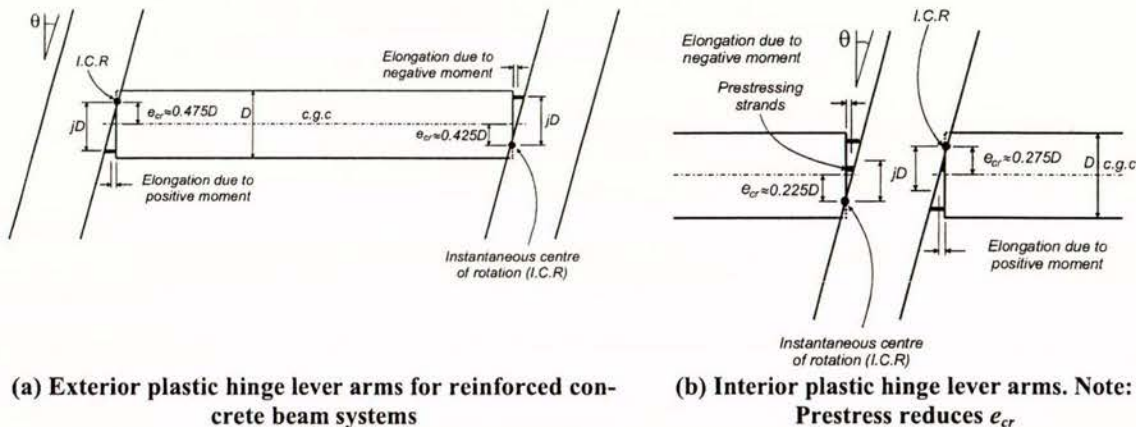


Figure 3 Internal lever arms for an interior and exterior joint

By adding the elongation from the four plastic hinges, it is possible to determine the total beam elongation for Phase I. From this outcome and the time history shown in Figure 4(a) it can be seen that there is satisfactory agreement between the theory and observed results. From the experiment, the observed beam elongation equates to a growth of 35mm. Using Equation (2-2) the predicted maximum elongation is $\delta_{max}^{el} = 41.5\text{mm}$. Figure 4(a) shows that only the first half cycle within the elastic range contributed to the overall elongation of the super-assembly. This elastic elongation was approximately 5mm at 0.5% interstorey drift.

For the Phase II loading only an exterior plastic hinge formed. To compare the theoretical versus experimental results it is best to compare the two beams in which the plastic hinges form. These beams were the East and West beam of the super-assembly. For all the plastic hinges the e_{cr} values were either $0.425D$ for a negative moment or $0.475D$ for a positive moment (Figure 3(a)).

By adding the beam elongation for the two plastic hinges in each of the East and West beams plus the initial beam elongation due to the torsion cracks that formed during Phase I, it is possible to determine the total beam elongation for each beam during Phase II. This growth equates to a 47.2mm and 45.1mm for the East and West beams respectively; giving an average of 46.2mm. This observed average compares well with a predicted result of $\delta_{max}^{el} = 45.7\text{mm}$ given by Equation (2-2).

Figure 4(b) present the total beam elongation for the East beam. Further validation of the assumption that was mentioned in Section 2 that only "new" rotation contributes to beam elongation is evident in Figure 4(b). In between the -2.5% cycle and the 3.5% cycle there was a small cycle to $\pm 0.5\%$ undertaken. Note that this cycle did not contribute to the beam elongation, as predicted, because it did not cause any "new" rotation to occur.

3.1.1 Individual plastic hinge elongation

Phase I

Figure 5 shows both the experimentally observed beam elongation as well as the theoretical predicted beam elongation for the exterior hinges. As can be seen from Figure 5 there is good agreement

between the predicted and observed elongations for the two exterior plastic hinge zones. Because the e_{cr} values were different for each of the two loading directions and the imposed loading cycles were not symmetric, the theoretical elongation for each hinge is slightly different.

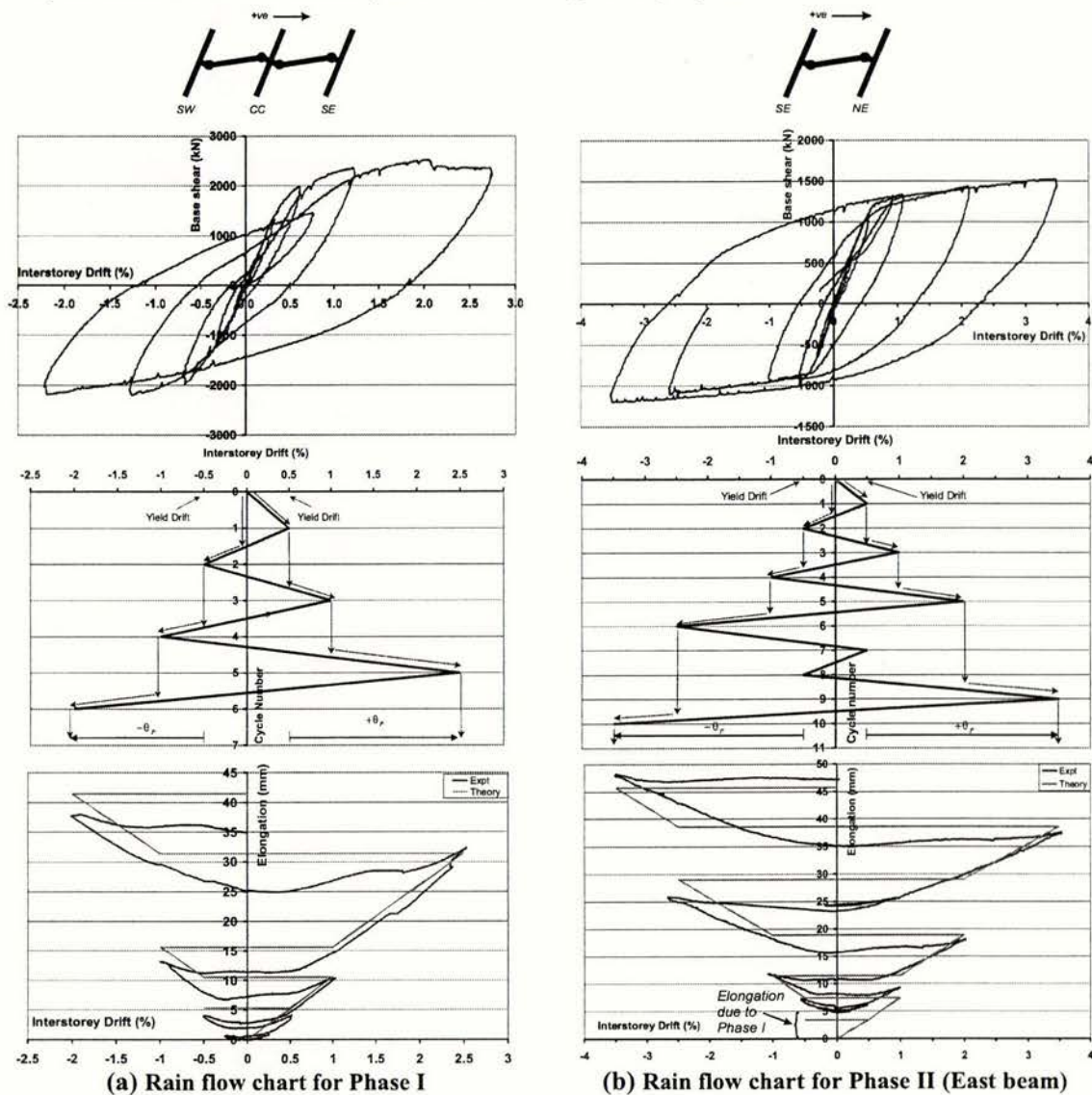
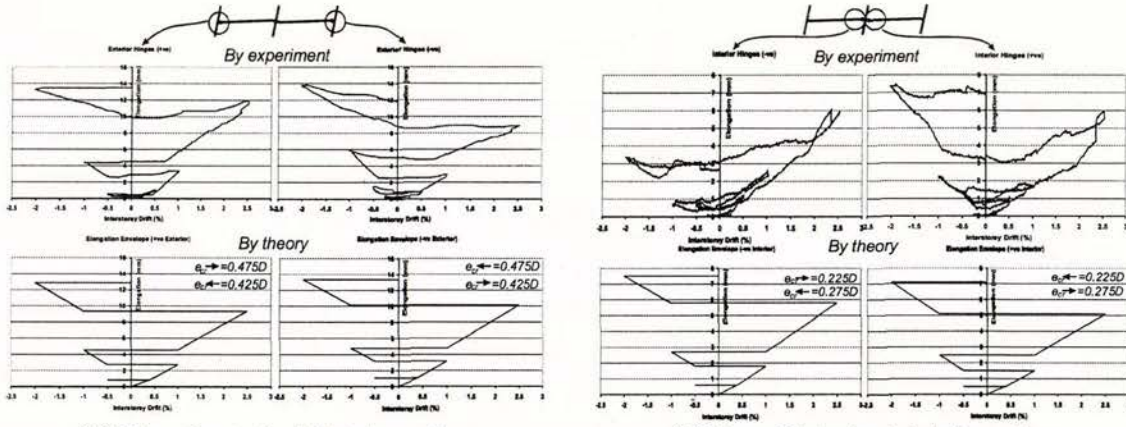


Figure 4 Rain flows charts for Phase I and II: Total Beam Elongation

Figure 5(b) shows good agreement between the predicted and observed elongations for the interior plastic hinges. The left hand interior hinge did not elongate as expected during the cycle to -2% drift. The reason for this is that at this stage during the test the first hollow-core unit had severe web splitting and this affected the hinge performance (in particular the affect the prestressing strands had on the hinge performance).



(a) Phase I exterior joint elongation (b) Phase I interior joint elongation
 Figure 5 Phase I experimental versus predicted beam elongation graphs

Phase II

Figure 6 shows good agreement between the theoretical and experimentally observed elongation for the individual hinges. The initial off set in the observed beam elongation plots was due to the beam elongation that occurred during Phase I in the form of torsion cracks.

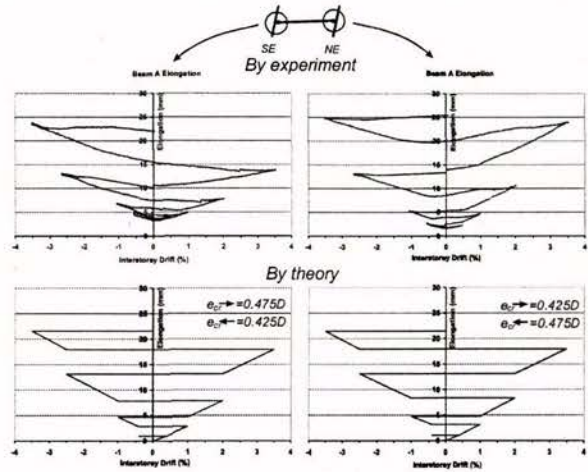


Figure 6 Phase II East beam elongation

4 Design recommendations

Knowing the total amount of beam elongation that occurs in a bent during an earthquake is extremely important when precast floor units are seated on the beams of a moment resisting frame. The required ledge length must be large enough to account for the total beam growth plus construction tolerances. Therefore, the ledge (seat) width demand (for each seat) is given by

$$U_T = U_S + U_D \tag{4-1}$$

where U_T = seat width requirement; U_S = static seat width due to construction requirements; and U_D = dynamic seat width due to beam elongation where U_D is defined as

$$U_D = \frac{1}{2} \delta^{el} = \frac{\omega}{2} n \left\{ |\theta^+| + |\theta^-| \right\} e_{cr} \tag{4-2}$$

where ω = a magnification factor which may be thought of as a factor of safety (a value of 1.5 is suggested here); n = number of hinges within the span of the floor slab under construction; e_{cr} = average beam depth between the beam centreline and the instantaneous centre of rotation (the centroid of the compression force); θ^+ = maximum positive rotation imposed on the beam hinges; and θ^- =

maximum negative rotation imposed on the beam hinges. The value of e_{cr} can be assumed to be $0.475D$ for an exterior positive hinge, $0.425D$ for an exterior negative hinge and $0.25D$ for an interior hinge with prestressing running through the joints (D is the overall beam depth).

5 CONCLUSIONS

This research has shown that beam elongation occurs in both elastically and plastically responding structures. Researchers have predicted beam elongation assuming that the elongation varies proportionally with interstorey drift. By using a rainflow counting method and examining the applied loading history it is possible to more accurately understand the formation of beam elongation on an individual plastic hinge basis or a frame as a whole. This predictive approach, Equation (2-2), developed herein was successfully validated against the experimental results reported by previous researchers, as well as the results conducted as part of the present research.

For the design engineer who wants to be able to predict the amount of elongation and ledge (seat) length required within a building that is being designed it is now possible using Equation (2-2). All the designer requires is the maximum positive and negative drift amplitudes of the structure, the structures yield drift, and the beam details.

ACKNOWLEDGEMENTS:

This project would not be possible without the financial support from the following organisations: University of Canterbury, Earthquake Commission, Cement & Concrete Association of New Zealand, BRANZ Technology New Zealand, Firth Industries Limited, Stresscrete, Stahlton Prestressed Flooring, Precast Components, Pacific Steel and Construction Techniques Ltd.

REFERENCES:

- Centre for Advanced Engineering, 1999, *Guidelines for the Use of Structural Precast Concrete in Buildings*, Centre for Advanced Engineering
- Dowling N.E, 1972, *Fatigue Failure predictions for complicated stress-strain histories*, Journal of Materials, JMLSA, Vol7, No 1, March, pp 71-87
- Fenwick R.C and Davidson B.J, 1995, *Elongation in Ductile Seismic-Resistant Reinforced Concrete Frames*, Recent Developments in Lateral Force Transfer in Buildings, Thomas Paulay Symposium, ACI, pp 143-170
- Fenwick R.C, Dely R. and Davidson B.J, 1999, *Ductility Demand for Uni-directional and Reversing Plastic Hinges in Ductile moment Resisting Frames*, Bulletin of the New Zealand Society for Earthquake Engineering, Vol 32, No. 1, March, pp 1-12
- Fenwick R.C and Megget L.M, 1993, *Elongation and load deflection characteristics of reinforced concrete members containing plastic hinges*, Bulletin of NZNSEE, Vol 26, No. 1, March, pp 28-41
- Fenwick R.C., Tankut A.T. and Thom C.W., 1981, *The deformation of reinforced concrete beams subjected to inelastic cyclic loading-Experimental results*, University of Auckland Report No 268, University of Auckland
- Lau D, B, N, 2001, *The Influence of Precast-Prestressed Flooring on the Seismic Performance of Reinforced Concrete Perimeter Frame Buildings*, Department of Civil and Resource Engineering, University of Auckland, Report No 604
- Lee J.Y and Watanabe F, 2003, *Predicting the longitudinal axial strain in the plastic hinge regions of reinforced concrete beams subjected to reversed cyclic loading*, Engineering Structures, Vol 25 No. 7, June, pp 927-939
- Matthews J.G, 2004, *Hollow-Core Floor Slab Performance following a Severe Earthquake*, Ph.D Thesis, University of Canterbury, Christchurch
- Restrepo J.I, Park R and Buchanan A, 1993, *Seismic Behaviour of Connections Between Precast Concrete Elements*, Research Report 93-3, Department of Civil Engineering, University of Canterbury, Christchurch, New Zealand
- Standards New Zealand, 1997, *Specification for concrete construction*, NZS 3109, Standards New Zealand, Wellington



13th World Conference on Earthquake Engineering
Vancouver, B.C., Canada
August 1-6, 2004
Paper No. 585

EXPERIMENTS ON THE SEISMIC PERFORMANCE OF HOLLOW-CORE FLOOR SYSTEMS IN PRECAST CONCRETE BUILDINGS

Renee A LINDSAY,¹ John B MANDER² and Des K BULL³

SUMMARY

Recent earthquake engineering research undertaken at the University of Canterbury has aimed at determining whether New Zealand designed and built precast concrete structures, which incorporate precast concrete hollow-core floor slabs, possess inadequate seating support details. A full scale precast concrete super-assembly was constructed in the laboratory and tested in two stages. The first stage investigated existing construction and demonstrated major shortcomings in construction practice that would lead to very poor seismic performance. This paper presents the results from the second stage that investigates the efficiency of improved construction details on seismic performance. The improved details consist of a simple (pinned-type) connection system that uses a low friction bearing strip and compressible material for the supporting beams together with a 750mm wide timber infill between the perimeter beams and the first precast floor unit. Test results show a marked increase in performance between the new connection detail and the existing standard construction details, with relatively small amounts of damage to both the frame and flooring system at high lateral drift levels. The results show that interstorey drifts in excess of 3.0% can be sustained without loss of support of the floor units with the improved detailing. The overall performance of the super-assembly is determined in terms of the hysteretic performance and the fragility implications in terms of the drift damage are classified. Recommendations for future design and construction are made based on the performance of the super-assembly test specimen and a probabilistic fragility analysis.

¹ ME Thesis student, Department of Civil Engineering, University of Canterbury, Christchurch, New Zealand and Design Engineer, Holmes Consulting Group, Christchurch, New Zealand

² Professor, Chair of Structural Engineering, Department of Civil Engineering, University of Canterbury, Christchurch, New Zealand

³ Holcim Adjunct Professor in Concrete Design, Department of Civil Engineering, University of Canterbury, Christchurch, New Zealand and Technical Director, Holmes Consulting Group, Christchurch, New Zealand.

INTRODUCTION

This research has followed on from recent work completed at the University of Canterbury's Department of Civil Engineering by Matthews [1]. Overall, the performance of the precast, prestressed concrete floor system in the Matthews (Stage 1) test was poor while the perimeter moment resisting frame behaved well. The testing completed by Matthews showed premature failure of the flooring system can be expected for design basis earthquakes in New Zealand, due to inadequate seating details and displacement incompatibilities between the frame and floor. Outlined in Matthews' thesis are several areas highlighted for future research that have been addressed in the second stage of the testing programme, including:

- Improving the seating connection detail between the precast, prestressed hollow-core floor diaphragm and the perimeter reinforced concrete moment resisting frame,
- Stopping the central column from displacing laterally out of the building due to an insufficient lateral tie into the building. It was because of this lack of interconnection that the floor slab tore longitudinally due to displacement incompatibility in the Matthews test. The central column was therefore no longer restrained and was able to translate freely outwards, and
- Isolating the first hollow-core unit spanning parallel with the perimeter beams from the frame due to displacement incompatibility. This displacement incompatibility was caused by the units being forced to displace in a double curvature manner due to being effectively connected to the edge of the perimeter beam, when hollow-core units are not designed for such displacement profiles.

SUPER-ASSEMBLY REPAIR

The entire experiment set-up was based on the Matthews [1] testing rig with connection modifications to improve the performance of the hollow-core units. The building was a two-bay by one-bay section of a lower storey in a multi-storey precast concrete moment resisting frame. The floor units were pretensioned precast hollow-core and were orientated so that they ran parallel with the long edge of the building, past the central column. The buildings origin along with the layout and dimensions are shown in Figure 1.

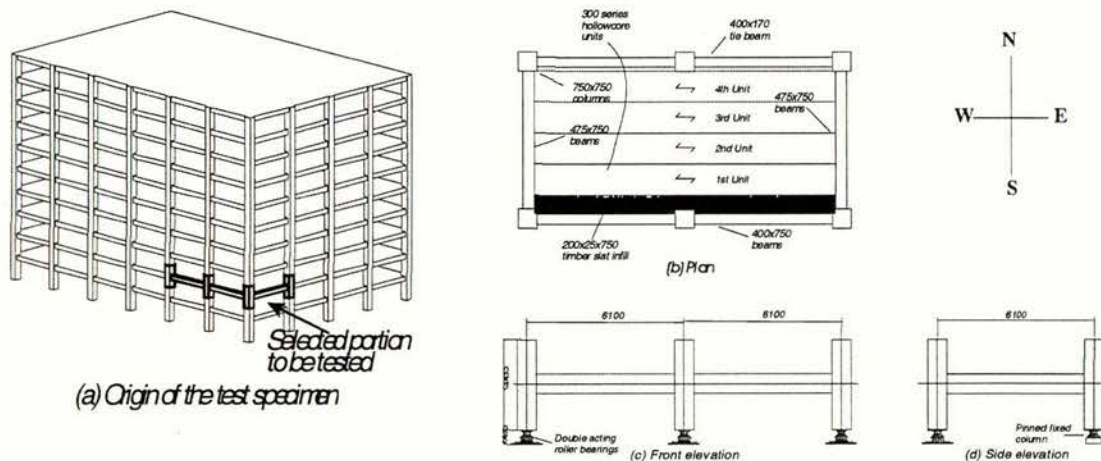


Figure 1. Origin, Layout and dimensions of the Stage 2 (Lindsay) super-assembly.

Following the Matthews testing the super-assembly's frame was cracked but relatively undamaged compared with the collapse of the flooring system. It was decided to repair and re-use the existing structure; the remaining floor sections were removed, the concrete in the transverse beams was removed and the damaged plastic hinge zones in the southern longitudinal beam were removed and reconstructed. As the existing reinforcing bars were being re-used, the bars were heat treated to restore ductility and reduce internal stresses. This was done by heating the reinforcing steel to a temperature around the critical transition point ($\sim 750\text{-}850^{\circ}\text{C}$) and allowing it to cool (Oberg et al. [2]).

NEW CONNECTION DETAILS

Seating Connection Details

The seating connection between the hollow-core unit and the supporting beam consisted of replacing the plastic dam plug in the ends of the unit with 10mm of compressible material fully across the end of the unit and seating the unit on a low friction bearing strip. This detail is shown in Figure 2 along with how the floor unit is expected to rotate relative to the beam. The low friction bearing strip allows the floor unit to slide as designers had previously assumed it would. The compressible material is assumed to reduce the compression forces applied at the bottom of the unit under negative moments as well as restricting concrete from entering the cores of the units. If the large compression force forms between the bottom of the unit and the face of the supporting beam it is transferred at a relatively flat angle to the topping concrete. A perpendicular principle tensile force then forms, causing splitting of the webs at very early stages of the test.

When the unit is seated on a low friction bearing strip, the seat length becomes very important; it must be placed back from the face of the beam so that as the unit tries to rotate it does not dig into the bearing strip. The draft 2003 amendment to the New Zealand Concrete Structures Standard NZS3101:1995 (Standards New Zealand [3]) has amended the required seat length of hollow-core floors to span/180 or 75mm based on Matthews' recommendations. A seat length of 75mm was used in this test.

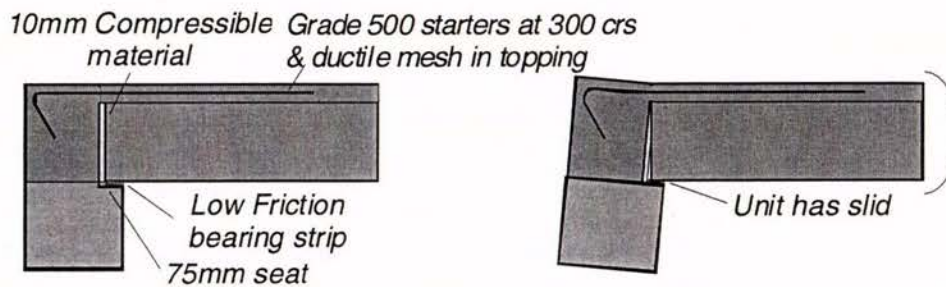
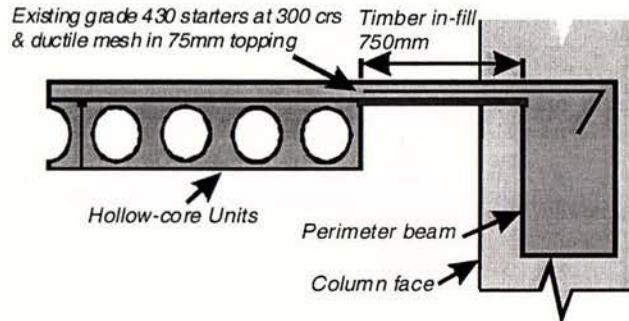


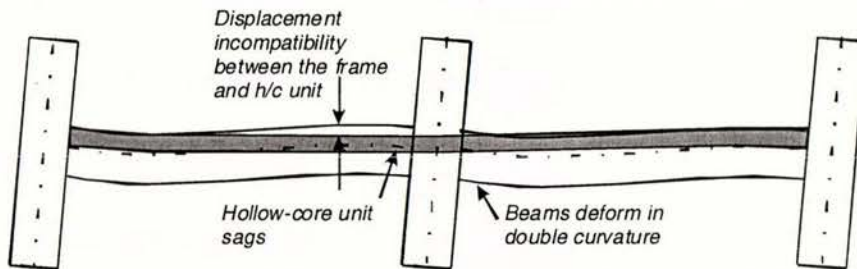
Figure 2. Seating connection detail with expected performance.

Lateral Connection to the Perimeter Frame

This connection consisted of moving the first unit away from the perimeter beam and replacing it with a 750mm timber infill with 75mm insitu concrete topping (Figure 3(a)). The infill allows a more flexible interface between the frame and southern hollow-core unit. Some cracking is expected in this interface due to the displacement incompatibility but it is anticipated that the more flexible interface will accommodate this while allowing the beam to deform in double curvature and the hollow-core unit in single curvature, (Figure 3(b)) leaving the floor essentially undamaged. Ductile reinforcing mesh was used in the topping to aid in the performance of the floor by helping to ensure that any damage and cracking would not result in such an early failure of the floor system.



(a) First hollow-core unit to perimeter frame connection.



(b) Expected displacement incompatibility between the hollow-core floor units and the perimeter frame.

Figure 3. Displacement incompatibility and connection between hollow-core unit and perimeter frame.

Diaphragm Tie Reinforcement

The New Zealand Concrete Structures Standard, NZS3101:1995 (Standards New Zealand, [4]), requires that columns shall be tied at each level of the floor system and be capable of resisting 5% of the maximum total axial compression load on the column. NZS3101 specifies that these bars should be placed at an angle close to 45° to the beam. However, this would contribute to the overstrength actions of the perimeter beams, through flange action, therefore the drag bars were placed perpendicular to the longitudinal beams. Two YD20 ($f_y=500\text{MPa}$) drag bars were required by design and were post-installed into the central column, spanning 5m into the floor.

TEST SET-UP

The super-assembly loading was conducted in drift control. Displacements were applied to the specimen through the form of horizontal shear forces to the top and bottom of each column. The load frame set-up design is explained in Matthews [1]. Three different displacement histories, corresponding to different phases of loading, were applied to the super-assembly as shown in Figure 4.

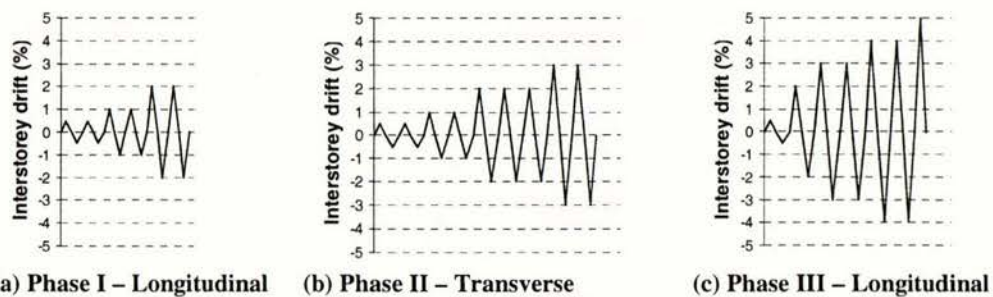
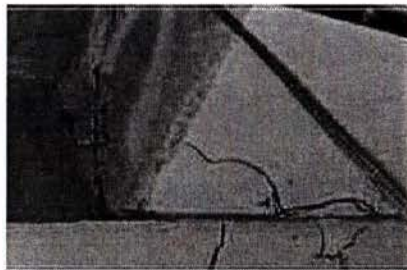


Figure 4. Loading histories applied to the super-assembly.

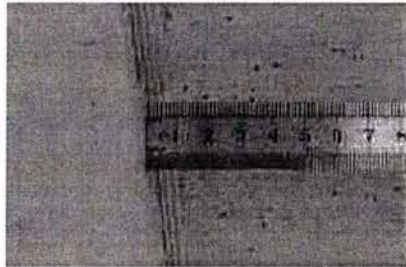
EXPERIMENTAL RESULTS

Phase I: Longitudinal Loading

The super-assemblage performed well in this phase of loading. The yield drift was determined to be 0.5%. The key results are shown in Figure 5. Diagonal cracks in the infill appeared at +1.0% and extended in the second $\pm 1.0\%$ cycle reaching the infill/hollow-core interface and running along the interface for almost the entire floor length, except around the central column where the drag bars appeared to tie the infill and floor together. By the end of Phase I this crack was 2mm wide with a vertical displacement of 2mm, in the west end (Figure 5(c)). A crack in the south corner of the first unit (ref Figure 1 for layout) developed at +2.0% and extended into the second core of the unit. There was 10mm of hollow-core pull-off in the $\pm 2.0\%$ cycle with the low-friction bearing strip sliding out in some places instead of the unit sliding on the bearing strip (Figure 5(a) and (b)). Some spalling occurred in the later cycles of this phase on the seat of the first unit due to the unit bearing on the unreinforced cover concrete. The economic consequences to an owner of a building with damage like this may become an issue. However, the cracks are considered to be repairable with the only permanent damage being the residual interstorey drift of the building (about 0.8% drift).



(a) Corner crack in first hollow-core unit at +2.0%



(b) Bearing strip sliding out at +2.0%

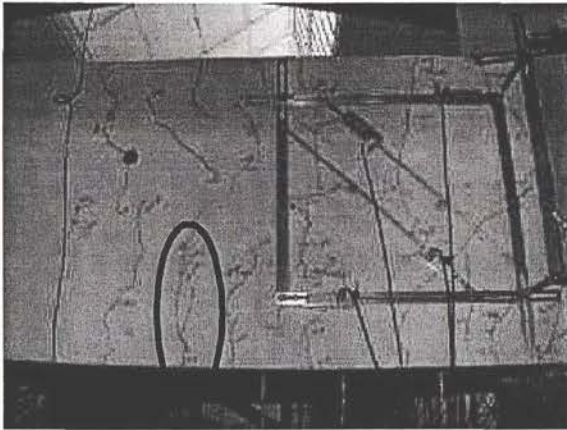


(c) Crack at hollow-core/infill interface at $\pm 2.0\%$

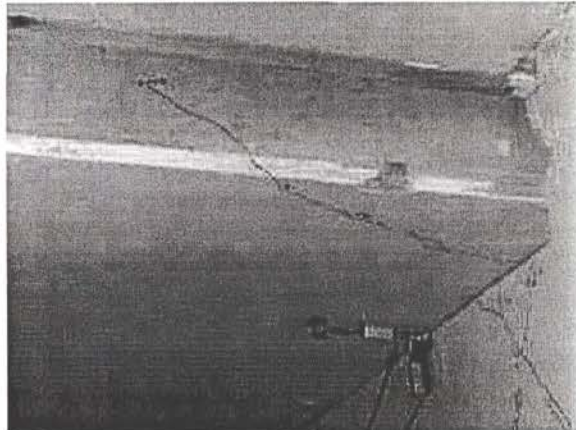
Figure 5. Damage to super-assemblage after Phase I loading.

Phase II: Transverse Loading

Very little new cracking occurred in the early stages of the transverse loading. This was because the transverse beams were pre-cracked from the longitudinal loading and these cracks simply opened during transverse loading. Key behaviour photos are shown in Figure 6. In the $\pm 1.0\%$ cycle a crack (2mm at this stage, opening to 6mm at $\pm 2.0\%$) opened up in the ends of both of the transverse beams about 1.0m from the column face as indicated Figure 6(a). It appeared that the weight of the hollow-core units caused the transverse beams to sag, accentuated by the cracked section, and in turn formed a uni-directional hinge at about 1.0m from the column face at both ends. The north side corner of the fourth hollow-core unit at both ends formed a corner crack at -1.0% drift that progressed up from the bottom of the unit to run along the web (Figure 6(b)).



(a) Large crack forming in transverse beam, 1.0m from column face at +1.0%.



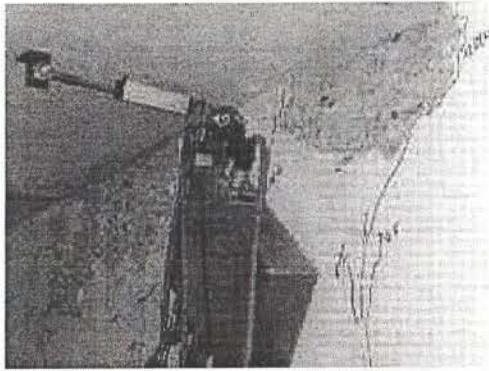
(b) Corner crack in north side of fourth hollow-core unit developing into a web-split at +1.0%.

Figure 6. Significant damage in the transverse loading cycle

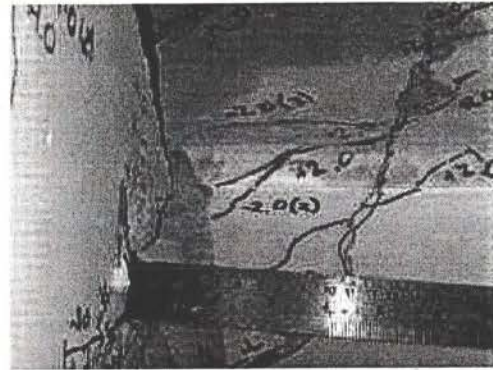
Phase III: Longitudinal Re-Loading

Early in the Phase III testing, beam spalling at the west end of the first hollow-core unit left the unit with almost $\frac{3}{4}$ of its length with at least 20mm of seat spalled off (Figure 7a) and (b)). At +2.25% drift, on the way to +3.0% drift, the first crosswire of mesh fractured at the hollow-core/infill interface about 2m west of the central column. This first fracture was followed by nine others on the way to +3.0%. Once the mesh had fractured it could be seen that the fracture was due to two mechanisms. Firstly, the tear was due to the floor diaphragm restraining the frame from elongating causing a transverse tension force as the beam tries to translate outwards instead; this produced a horizontal east-west dislocation between the infill and topping of the first hollow-core unit (15mm) once the mesh fractured (Figure 7(d)) as well as accentuating the transverse north-south displacement (i.e. crack width, 10mm) (Figure 7(c)). Secondly, the tear was due to the displacement incompatibility. This caused a vertical offset of 10mm once the mesh had fractured (Figure 7(e)). The crack was 3m long at this stage but the central column was still adequately tied into the building. The transverse beams showed significant amounts of torsion due to degradation of the PHZs accentuated by the hollow-core load eccentricity.

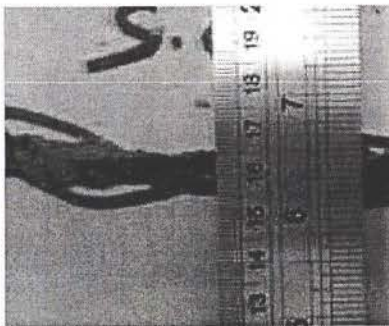
A large section of the unreinforced seat of the fourth hollow-core unit at the west end began to drop away showing the necessity of reinforcing the seat to tie it to the beam. The load carrying capacity of this seat/cover concrete was lost at 3.0% drift (first cycle). The concrete fell out during the second +4.0% cycle (Figure 7(f)). It was during these $\pm 4.0\%$ cycles that the PHZs showed some sign of distress with large sections of cover concrete falling off. The first main longitudinal bar fractured at +3.56% in the second $\pm 4.0\%$ cycle (Figure 7(g)) in the west PHZ in the southern beam with the remaining bars in that PHZ fracturing in the following cycles. A final +5.0% cycle was performed and during this cycle further seat damage was observed along with the main bars and topping mesh fracturing. A photograph of the infill section of the floor at the end of test is shown in Figure 7(h). It was at this stage that life safety became a concern, enough of the hollow-core seat had been damaged to question the stability of the floor diaphragm and nine main bars had fractured in total leading to concern about the stability of the frame elements.



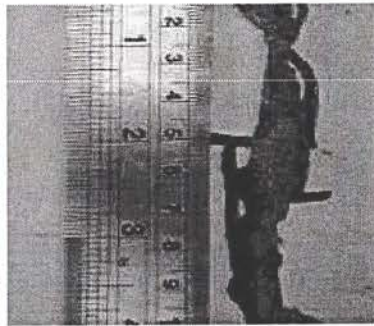
(a) Underside of first hollow-core unit, west end, +3.0% drift.



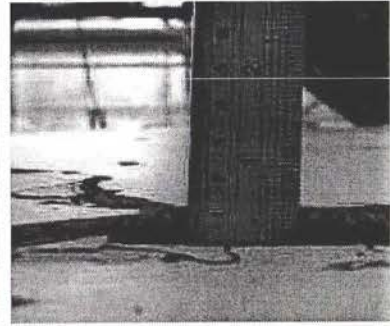
(b) 45-50mm of seat exposed of first unit, west end, +3.0% drift



(c) Crack width of 10mm in places after mesh fractures (+3.0%)



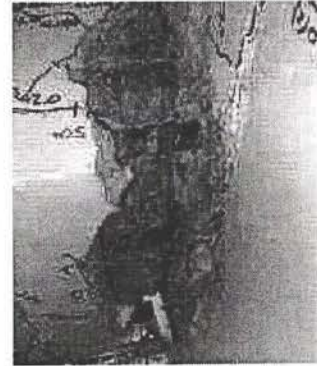
(d) Displacement of 15mm after mesh fractures (+3.0%)



(e) Vertical offset of 10mm after mesh fractures (+3.0%)



(f) Section of unreinforced seat fallen out at +4.0%



(g) Fractured main bar at +3.56% on 2nd cycle to +4%

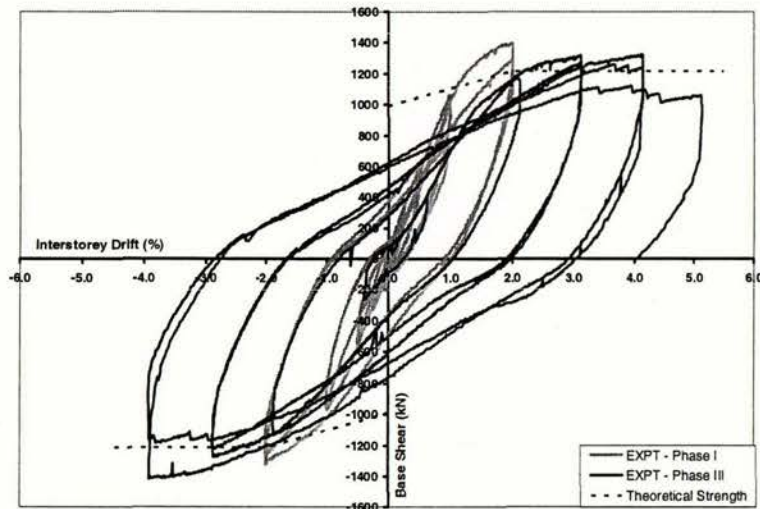


(h) Floor damage at end of test (5.0% drift).

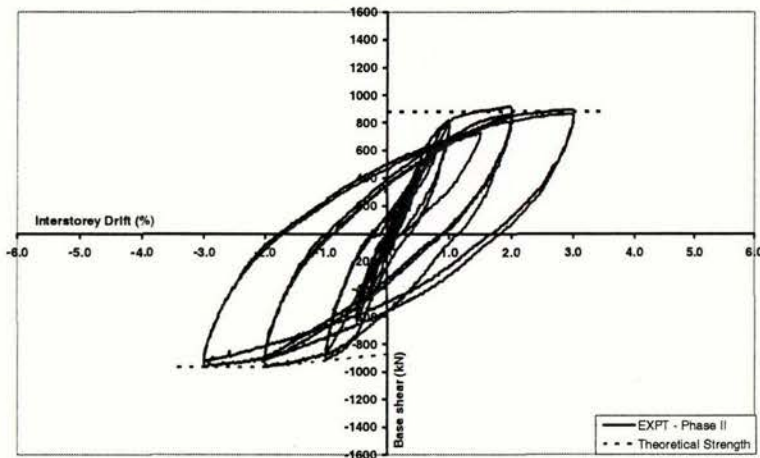
Figure 7. Damage in Phase III testing

HYSTERETIC PERFORMANCE

The base shear versus interstorey drift hysteresis plots for Phase I and III are shown in Figure 8(a) and Phase II in Figure 8(b). In Phase I, the hysteresis loop has a little pinching arising from a self-centring effect due to the PHZ cracks not opening and a large part of the deformation occurring at the beam/column interface which acted almost like a self-centring rocking connection. The maximum positive base shear was 1390kN while the maximum negative was 1320kN which both occurred in the first cycle to $\pm 2.0\%$. It can be seen that in the second cycle of loading very little loss in base shear capacity was observed. The overall theoretical base shear capacity was determined to be 1220kN at 2.0% drift onwards, once the entire floor had been activated. The theoretical mechanism assumes that as the interstorey drift increases more of the starter bars along the transverse beam are activated by flange action and these contribute to the negative moment capacity of the exterior hinges, up to a drift of 2.0% when all of the starters have been activated. The interior hinge capacity is made up of a contribution from the infill slab in the form of a yield line mechanism and activated mesh as well as the longitudinal beam bar capacity.



(a) Hysteresis loop for Phase I and III loading



(b) Hysteresis loop for Phase II loading

Figure 8 Hysteresis loops for the three phases of testing

The reason that the overall calculated base shear in Phase I and III was lower than the experimental one was because, in the theoretical calculations, compensation was made for the effect that the heat treatment had on the bars but the exact effect is not known due to the fact that the bars were heat treated in-situ and not tested. Therefore an assumption was made as to the effectiveness of the heat treatment and the resulting yield stress and hinge locations.

Phase I loading appeared to have no effect on the performance of the super-assembly in Phase II. The hysteresis loop had less pinching than Phase I which is because the transverse beams were reconstructed entirely and therefore there was more distributed cracking and less of a self-centring rocking connection effect at the face of the columns in the hinges as seen in the southern hinges. The maximum positive base shear was 920kN which occurred in the first cycle to +2.0% drift. The maximum negative base shear for Phase II was -970kN which occurred in the first cycle to -3.0% drift. The theoretical mechanism for Phase II assumes that relocated positive moment hinges are at the nominal moments because the hinges are forming in sections of the beams that have not pre-yielded. In the areas where the bars have pre-yielded compensation was made for the effect that the heat treatment had on the bars. Starter bars in the interface between the infill and perimeter beam are also activated in the negative drift direction. This mechanism predicts a positive base shear of 880kN and a negative of -970kN which agree with the experimental data.

The difference in base shear capacities between the positive and negative base shears in Phase II is due, in part, to the non-symmetrical reinforcing layout. On the northern side of the super-assembly the floor is not tied to the tie beam with starters therefore these can not be activated in a negative hinge moment cycle. A crack line also forms at the beam/infill interface through the starter bars. These reasons also account for why the base shear in Phase II is considerably less than Phase I as well as the use of the nominal yield stresses for the positive moment hinges in Phase II due to these hinges forming in steel that was not pre-yielded and subsequently heat treated.

It should also be noted that although hysteresis loops are beneficial in determining the overall capacities of test super-assemblies their usefulness is limited when looking at the performance of individual elements. As can be seen by the graphs in Figure 9, the overall comparison of the two super-assemblies would be that similar overall base shears were observed, the Stage 1 (Matthews [1]) super-assembly was slightly stiffer than Stage 2 (Lindsay) and the Stage 2 super-assembly was loaded to higher drifts and therefore underwent more plastic deformation. What is not known is that the hysteresis loops are dominated by the performance of the perimeter concrete frame, and in Stage 1 the overall performance of the super-assembly was vastly inferior to the Stage 2 testing due to premature failure of the hollow-core flooring system. Therefore hysteresis loops should be used only to determine the overall capacities of systems and the individual performance should be assessed in a different manner.

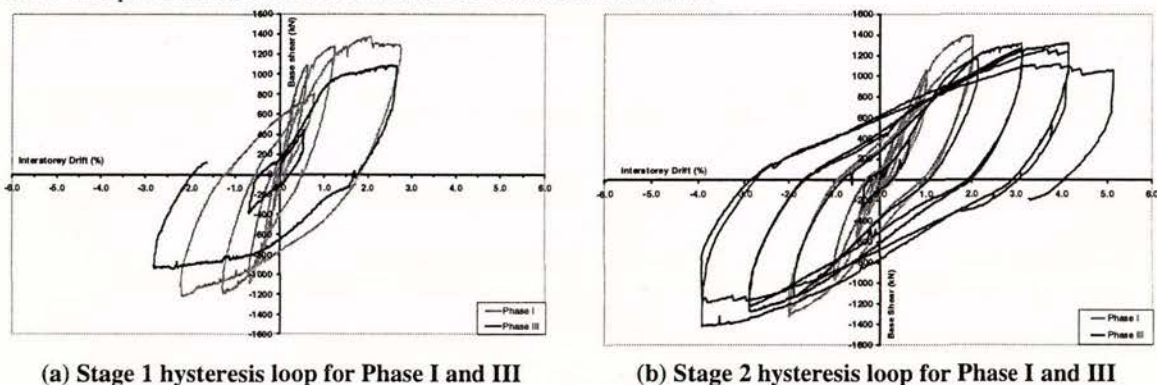


Figure 9. Hysteresis loops for Stage 1 and 2 for comparison of performance.

FRAGILITY ANALYSIS

As was shown above, the use of hysteresis loops in categorising and assessing the performance of a system is not adequate. In Stage 1, there was little evidence to indicate the poor performance of the hollow-core floor system. Assessment of the frame performance alone is not satisfactory in determining the damage state and account needs to be made for the performance of all of the elements in the system.

An investigation has been undertaken by Matthews that determined the expected interstorey drift demand on the class of structure tested in this programme. The findings were, in terms of the expected (median) drift;

$$\tilde{D}_D = 2.0(F_v S_1)_D \quad (1a)$$

or

$$\tilde{D}_D = 2.0(PGA)_D \quad (1b)$$

in which \tilde{D}_D = the median (50th percentile) drift demand as a percentage of the storey height, $(F_v S_1)_D$ = one second spectral acceleration for tall structures (above four stories) and $(PGA)_D$ = peak ground acceleration for low rise structures (up to four stories). From Equation (1a) it follows

$$(F_v S_1)_C = 0.5\tilde{D}_C \quad (2a)$$

or

$$(PGA)_C = 0.5\tilde{D}_C \quad (2b)$$

where \tilde{D}_C = expected drift capacity of the structure. Analysis conducted by Matthews [1] showed that the distribution of drift outcomes is lognormal with a coefficient of variation of $\beta_D = 0.52$. When combining distributions, to give an overall composite distribution, Kennedy et al [5] showed that by using the central limit theorem the coefficient of variation for a lognormal distribution can be found from:

$$\beta_{C/D} = \sqrt{\beta_C^2 + \beta_D^2 + \beta_U^2} \quad (3)$$

where β_C = coefficient of variation of the capacity, taken herein as $\beta_C = 0.2$ (Dutta, [6]); and β_U = dispersion parameter to account for modelling uncertainty, taken here $\beta_U = 0.2$. Applying (3) gives $\beta_{C/D} = 0.60$. By using a lognormal cumulative distribution that can be described by a lognormal variate ξ_β (where the median = 1 and the lognormal coefficient of variation, $\beta_{C/D} = 0.60$), the distribution of ground motion demands needed to produce a given state of damage can be found by

$$F_v S_1 = 0.5\tilde{D}_C (DS)\xi_\beta \quad (4)$$

or

$$PGA = 0.5\tilde{D}_C (DS)\xi_\beta \quad (5)$$

where $\tilde{D}_C(DS)$ = the expected value (in this case, the experimentally observed drift) for a given damage state (DS). The state of damage after an earthquake is typically quantified by a colour-coded or numerical format. Both of these are outlined in Table 1 and Table 2 respectively, along with the drift classification of the test super-assembly under both of these systems.

Table 1. Definition of colour coding used to classify building damage following an earthquake and the interstorey drift classification for the super-assembly investigated by Lindsay.

Tag Colour	Description of damage level	Classification (Interstorey drift)	
		Floor	Frame
Green	No Damage, building occupiable	1.0%	1.0%
Yellow	Moderate levels of damage. Building can be entered to remove belongings.	2.0%	2.0%
Orange	Heavy damage. Building can be entered for brief periods to remove essential items only	2.25%	3.0%
Red	Near collapse. Building can not be entered	4.0%	4.0%

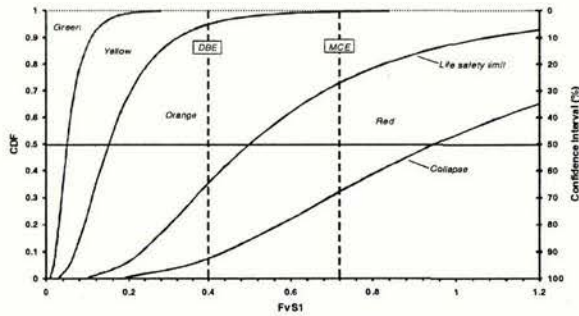
Table 2. Definition of damage states used to classify building damage following an earthquake and the interstorey drift classification for the super-assemblage investigated by Lindsay (Mander, [7]).

Damage State	Description of Damage	Post-earthquake utility of structure	Classification (Interstorey drift)	
			Floor	Frame
1	None (pre-yield)	Normal	-	-
2	Minor/Slight	Slight Damage	1.0%	1.0%
3	Moderate	Repairable Damage	2.0%	2.0%
4	Major/Extensive	Irreparable Damage	2.25%	4.0%
5	Complete Collapse	Irreparable Damage	-	-

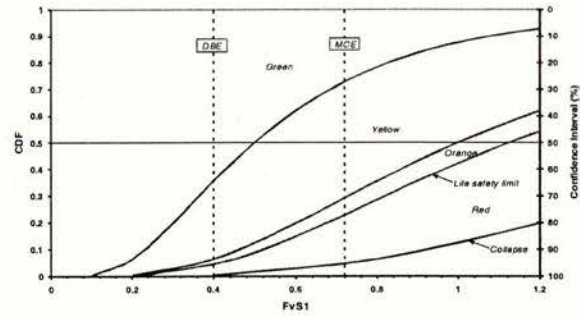
Figure 10 shows the fragility curves for the floor and frame performance when classified under the colour-coded and numerical schemes for the two stages of testing. On each of the graphs the 10% in 50 years, Design Basis Earthquake (DBE), $F_v S_I = 0.40g$ for Wellington, New Zealand is shown, as well as the 2% in 50 years, Maximum Considered Earthquake (MCE), $F_v S_I = 0.72g$, for Wellington, New Zealand. If the structure is classified in terms of the critical element (floor or frame) then it can be seen that if the damage to the two structures (Matthews and Lindsay) was classified in terms of colour-coding under a MCE then in Stage 1 72% of structures would be expected to be red tagged or have collapsed (Figure 10(a)), whereas in Stage 2 only 23% would be expected to sustain damage such that the building could not be entered (Figure 10(b)). Both of these performances are dictated by the performance of the floor. Under a DBE, in Stage 1, every building would still sustain some form of damage to the floors whether it be moderate (5%), heavy (60%), near collapse (27%) or total collapse (8%) (Figure 10(a) and (c)). In Stage 2, 65% would sustain no damage allowing immediate occupancy and 29% would sustain moderate damage to the floors while only 5% of floors would be red tagged. No buildings would collapse from inferior floor or frame performance (Figure 10(b) and (d)).

If the damage is classified in terms of different damage states, then for a MCE, in existing structures with conventional precast floor seating details (Stage 1), only 2% of structures would be expected to sustain slight or repairable damage. The remaining 98% of the structures would be demolished due to irreparable damage or collapse, of these some 32% of floors would be expected to partially or entirely collapse leading to possible loss of life (Figure 10(e)). Even under a DBE, 92% of structures would sustain irreparable damage with 8% leading to possible loss of life (Figure 10(e) and (g)). In this research, testing a structure with the proposed seating details (Stage 2), under a MCE, 71% of the buildings would sustain repairable damage to the frame or floor, of the remaining 29% irreparable damage, 23% of floors and 5% of frames would sustain major damage (Figure 10(f) and (h)). Under a DBE, 94% of buildings would sustain repairable damage to the floor and frame with 5% of the remaining 6% of floors sustaining heavy irreparable damage while none of the remaining 6% of frames sustains heavy irreparable damage (Figure 10(f) and (h)). This is almost a complete reversal of the damage states identified during Stage 1 testing and shows the improved performance due to the enhanced details.

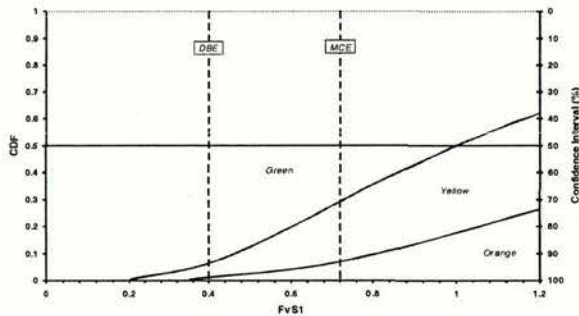
As can be seen, in Stage 2, the performance of both the frame and floor are very similar whereas in Stage 1 the performance of the floor is vastly inferior to the performance of the frame and therefore the overall performance is dictated by the poor performance of the floor. The findings from Stage 2 adhere to the expectations of ductile structures designed and detailed in accordance with the principles of capacity design as well as meeting the target objective that the confidence interval at the onset of irreparable damage under a DBE exceeds 90%. It is clear that similar conclusions can be drawn whether the building damage is rated by the colour-coded or damage state format.



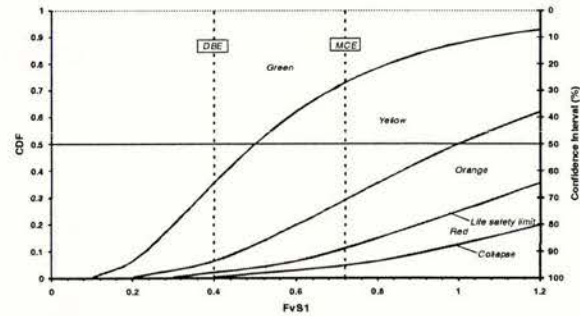
(a) Matthews' fragility curve for the floor performance when rated according to colour coding



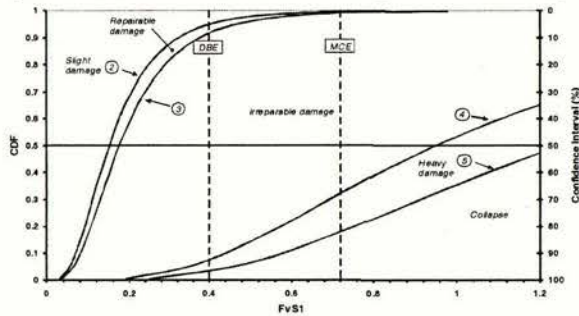
(b) Stage 2 fragility curve for the floor performance when rated according to colour coding



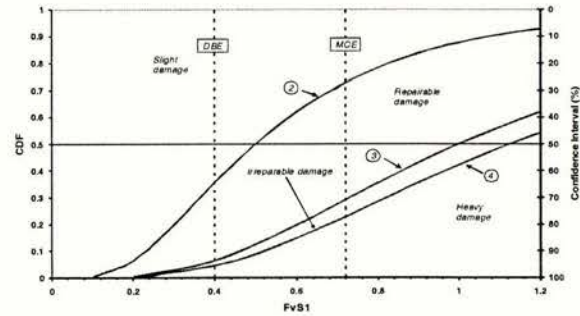
(c) Matthews' fragility curve for the frame performance when rated according to colour coding



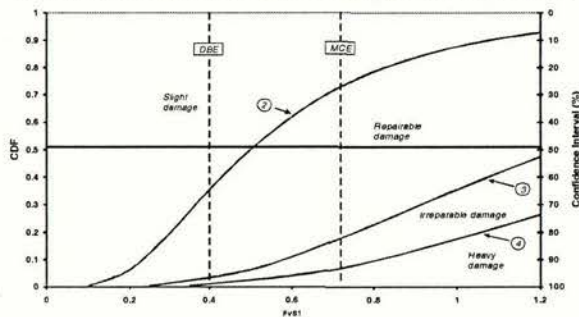
(d) Stage 2 fragility curve for the frame performance when rated according to colour coding



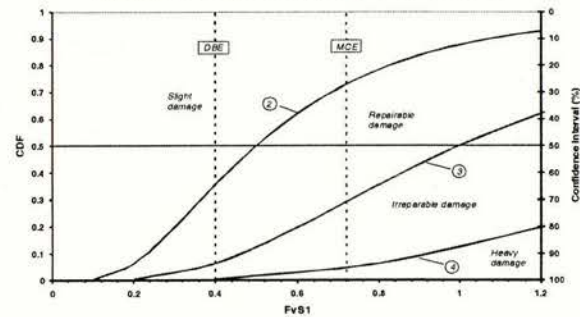
(e) Matthews' fragility curve for the floor performance when rated according to damage states



(f) Stage 2 fragility curve for the floor performance when rated according to damage states



(g) Matthews' fragility curve for the frame performance when rated according to damage states



(h) Stage 2 fragility curve for the frame performance when rated according to damage states

Figure 10 Fragility curves for both stages of testing using both colour-coded and numbered format for quantifying building damage.

DISCUSSION AND RECOMMENDATIONS

The performance of the hollow-core unit was significantly better than the test by Matthews (Stage 1) [1] who investigated existing construction practice that was found to perform at a level far below expectations. This follow-up investigation by Lindsay (Stage 2) demonstrated satisfactory overall performance with the structure maintaining life safety throughout the test.

Performance of Hollow-core Seat Connection

It is clear from the photos (Figure 5(b) and Figure 7(a & b)) that the low friction bearing strip did not perform how it was designed to. The bearing strip has teeth on one side and is smooth on the other allowing the hollow-core unit to slide on the smooth surface. In this case there was not enough bond/friction between the toothed surface and the floor supporting seat and in some places the bearing strip slid with the floor unit instead. By designing a bearing strip that has bigger teeth, to grip the beam better, or bonding the underside of the bearing strip to the beam should stop this movement.

From the initial analysis of the results it is evident that the compressible backing board did not actually compress much more than approximately 1mm. This is because in the early stages of testing the compression strut and rotation of the beam and hollow-core are small as well as the occurrence of elastic elongation of the perimeter beams and therefore the backing board will not compress. After yielding of the super-assembly, beam elongation of the longitudinal beams has occurred meaning that the rotation of the hollow-core unit, which would cause compression of the backing board in simplified two-dimensional tests that do not consider beam elongation, does not compress the backing board. However, a baffle of some sort is required to stop concrete from entering the cores and therefore isolate the floor units from the beam. The authors recommend a thinner and not necessarily compressible backing board but one that is still robust enough to resist the pressure of fresh concrete. The need to reinforce the seat of the hollow-core has become evident (Figure 7(a) and (f)). Reinforcing the seat with an additional longitudinal bar and stirrups would prevent large sections of the unreinforced seat from spalling off.

Performance of Infill Slab between Perimeter Frame and First Hollow-core Unit.

This element performed very well. Damage to the infill section was always anticipated but as can be seen from the photos the rest of the floor was essentially uncracked. Ductile reinforcing mesh was used in the topping to try and stop the fracture of the reinforcing crossing the damaged interface between the infill and first hollow-core unit. This ductile reinforcement did not perform as well as hoped. The reinforcing mesh fractured at an interstorey drift of 0.35% above that when it fractured in the Matthews test (2.25% vs. 1.9% drift). However, at that time the super-assembly had undergone more than six times the plastic rotation than when the mesh fractured in the Matthews test. The authors recommend, however, that the mesh be substituted for simple deformed reinforcing bars (e.g. HD10 at 300 crs both ways: 5th percentile yield stress of 500MPa) and the starter bars from the perimeter beams run over this interface to lap with the topping reinforcement. This will increase the ductility of the damaged interface and lower the risk of fracture of the reinforcing across this joint.

Global Performance Issues

The failure of the longitudinal reinforcing bars can be predicted by low cycle fatigue theory (Dutta and Mander, [8]). As this failure is a function of material properties and overall plastic rotation it is not a parameter that can be altered and therefore becomes the defining failure point for the super-assembly.

The damage to the corners of the first and fourth hollow-core units and cracking of the soffit of the units could be avoided. If the hollow-core units are not seated in the plastic hinge zones (PHZ) of the supporting beams they would not be forced to undergo the large deformations of the PHZ of the beams. Cracking of the soffit of the units should not occur and large sections of the corners of the units should not fracture.

By using the detail shown in Figure 11 on either side of all columns, the plastic hinge zones are forced into the area under the infill rather than underneath the hollow-core unit. The extra bar cast into the beams achieves this. The starter bars extend across the hollow-core/infill interface and are lapped with the HD10 topping reinforcement at 300 centres each way.

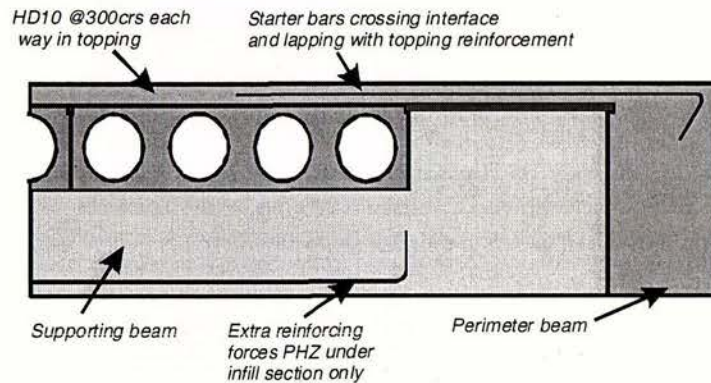


Figure 11. Recommended detail to reduce damage to hollow-core units

Overall System Performance

The hysteresis loops showed a small amount of pinching in the longitudinal loading cycles due to a rocking type connection that formed at the interface between the old and new concrete at the beam/column joint. The theoretical mechanism for the longitudinal loading assumes a progressive yield of the starter bars up to 2.0% drift when all of the starter bars are activated. The effect of the heat treatment on the reinforcing bars is not accurately known, this is because the bars were heat treated in-situ and were unable to be tested, and therefore a yield stress value was assumed. The performance of these bars could have implications on the overall performance of the super-assembly.

The hysteresis loops appeared to be well-formed and dissipated a reasonable amount of energy. However, as previously discussed, this can be misleading. Hysteresis loops are a good indicator of overall system capacities but the performance of the individual elements of the system needs to be investigated in order to assess system performance accurately.

Fragility Analysis Implications

By using fragility curves to assess individual elements of a system it is possible to determine the implications of the drift damage on New Zealand constructed buildings of this type. The analysis shows a vast improvement in performance of Stage 2 testing compared with Stage 1 and this is entirely due to the improved detailing. The results show that following a DBE (10% in 50 years) in Wellington, New Zealand, 94% of buildings would sustain damage to the floors that would be considered repairable and under a MCE (2% in 50 years) 71% of buildings would sustain damage, due to damage to the floors, that would probably be repairable. This is a vast improvement on the expected near total devastation of precast buildings of this type under a MCE following Stage 1 testing. The improved details mean that the floor system performs at a level not inferior to that of the frame. However, in both testing stages the performance of the super-assembly is governed by the performance of the floor system. Therefore by using the detail in Figure 11 further improvements to the performance of the floor system can be made and the ultimate limit of the structure can then be accurately determined by low cycle fatigue of the longitudinal reinforcing. Fragility analysis allows comparisons to be made between separate elements and drift limits to be placed on different performance levels.

CONCLUSIONS

The experiment conducted as part of this research has ensured that new precast concrete moment resisting frame buildings with precast, prestressed hollow-core floors can be expected to perform satisfactorily up to interstorey drifts well in excess of 3.0% with the details outlined above. These details also ensure only moderate economic consequences to the owner of the building under a 10% in 50 years; design basis earthquake, and that life safety is maintained under a 2% in 50 years: maximum considered event. The target objective that the confidence interval at the onset of irreparable damage under a DBE exceeds 90% is also achieved with the new details. The superior performance of the proposed future detailing practice when compared to existing practice was clearly demonstrated when the damage states are compared in a fragility analysis.

This research has also shown the necessity to test structures in the three-dimensional format to fully understand certain elusive secondary, three-dimensional effects that are present. It is concluded that further work is required to test the design recommendations outlined above in Figure 11. Further work also needs to be undertaken to develop retrofit measures for existing structures and to test further seating details for other classes of precast concrete floor systems in order to determine their performance under three-dimensional conditions.

ACKNOWLEDGEMENTS

This project would not be possible without the support from the following organisations: University of Canterbury, Earthquake Commission, Cement and Concrete Association of New Zealand, BRANZ, Foundation for Research Science and Technology – Tūāpapa Pūtaiao Maori Fellowships, C. Lund & Son Ltd, Firth Industries Ltd, Stresscrete, Pacific Steel, Stahlton Prestressed Flooring, Construction Techniques, Precast Components, The Maori Education Trust, Fulton Hogan Ltd, Holmes Consulting Group, Hylton Parker Fasteners and Hilti (NZ) Ltd.

REFERENCES

1. Matthews J.G. "Hollow-core floor slab performance following a severe earthquake." Ph.D Thesis, Christchurch, New Zealand: Department of Civil Engineering, University of Canterbury, 2004.
2. Oberg E, Jones F.D, Horton H.L and Ryffell H.H. "26th Edition Machinery's Handbook." New York: Industrial Press Inc., 2000.
3. Standards New Zealand. "Draft Amendment No. 3 to NZS 3101:1995." Wellington: Standards New Zealand, 2003.
4. Standards New Zealand. "Concrete Structures Standard, NZS 3101, Parts 1& 2." Wellington: Standards New Zealand, 1995.
5. Kennedy R.P, Cornell C.A, Campbell R.D, Kaplan S, Perla H. F. "Probabilistic Seismic Safety Study of an Existing Nuclear Power Plant." Nuclear Engineering and Design, 1980; No. 59: 315-338
6. Dutta A. "On Energy-Based Seismic Analysis and Design of Highway Bridges." Ph.D Thesis, Buffalo, NY: Science and Engineering Library, State Univeristy of New York at Buffalo, 1999.
7. Mander J.B. "Beyond Ductility: The Quest Goes On." Symposium to Celebrate the Lifetime Contributions of Professors Emeriti Tom Paulay and Bob Park. Christchurch, 2003: 75-86.
8. Dutta A and Mander J.B. "Energy Based Methodology for Ductile Design of Concrete Columns." Journal of Structural Engineering, ASCE, 2001; Vol. 127(12): 1374-1381.

Reinforced concrete seating details of hollow-core floor systems

C.J. MacPherson

*Department of Civil Engineering, University of Canterbury, Christchurch.
Holmes Consulting Group, Christchurch.*

J.B. Mander

Department of Civil Engineering, University of Canterbury, Christchurch.

D.K. Bull

*Department of Civil Engineering, University of Canterbury, Christchurch.
Holmes Consulting Group, Christchurch.*



2005 NZSEE
Conference

ABSTRACT: Recent earthquake engineering research has raised concerns of the seismic performance of precast prestressed concrete hollow-core floor systems. Experimental research showed that with simple detailing enhancements, significant improvement in the seismic performance of hollow-core floor systems can be expected. The present experimental research aims at validating several new detailing enhancements. Based on previous research findings, the present super-assembly experiment included the following details: (i) a reinforced connection that rigidly ties the floor into the supporting beam, (ii) an articulated topping slab portion cast onto a timber infill solution that runs parallel to the hollow-core units and edge beams; (iii) specially detailed supporting beam plastic hinge zones reducing potential damage to the hollow-core units; (iv) Grade 500E reinforcing steel used in the main frame elements; and (v) mild steel deformed bars in the concrete topping in lieu of the customary welded wire mesh. The full-scale structure was cyclically tested in both the longitudinal and transverse directions to inter-storey drifts of $\pm 5\%$. Observations show extremely positive results with minor damage incurred by the hollow-core flooring and the overall performance dictated by the performance of the moment resisting frame. Recommendations for the forthcoming revision of the New Zealand Concrete Standard, NZS 3101, are also made.

1 INTRODUCTION

The collapse of the hollow-core units during testing by Matthews (2004) and Matthews et al (2003a,b) flagged issues over the performance of existing precast concrete frame structures with hollowcore flooring structural systems. A continuation of that research by Lindsay (2004) and Lindsay et al (2004a,b) demonstrated that different structural details could be implemented in new structures and these could be expected to behave adequately in a seismic event. This research project is a further continuation of previous work done by Matthews (2004) and Matthews et al (2003a,b) on existing structures and Lindsay (2004) and Lindsay et al (2004a,b) on new structures.

The popularity and widespread use of precast concrete is recognised in New Zealand design standards where there is specific reference to precast concrete flooring support conditions. Amendment No. 3 to the current New Zealand Concrete Design Code NZS3101:1995 provides two details for the connection of hollowcore floor units to reinforced concrete frame supporting beams. While Lindsay (2004) reported on the performance of the first of these, the second solution specifies a reinforced connection that rigidly ties the floor into the supporting beam, but to this point remains untested in any large-scale three-dimensional experiments. This research experimentally investigates the effectiveness of this solution and its adequacy for inclusion into the upcoming revised New Zealand Concrete Standard and use in New Zealand construction practice.

This paper initially provides an overview of the test specimen details and experimental set-up. The second part of this paper provides the visual and instrumental observations of the testing. The results and overall effectiveness of the design changes and new features are discussed and concluding remarks are made.

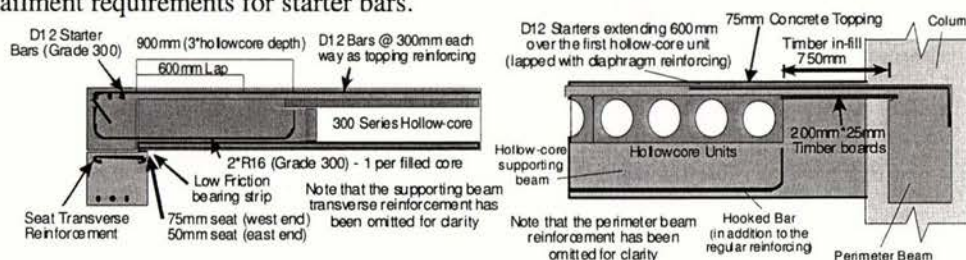
2 SUPER-ASSEMBLAGE DESIGN DETAILS AND CONSTRUCTION

2.1 Hollow-core seating details

The seated connection detail used for this experiment is the second detail prescribed in Amendment No. 3, NZS 3101:2004. The connection features two of the four hollow cores reinforced and filled with concrete, and is diagrammatically shown in Figure 1(a). Grade 300 D12 reinforcing was used at 300mm centres for the starter bars, which is lapped with the diaphragm reinforcing. In the two reinforced cores, Grade 300 R16 bars were placed close to the bottom of the cores. To prevent concrete entering the two non-filled cores of each hollow-core unit, a stiff backing board was used in place of the more conventional end plug. This is to help ensure that the rotation of the floor units relative to the beam occurs at the critical section at the beam-to-floor interface and that the relatively brittle hollow-core unit does not experience high rotational demands. This substitutes for the conventional use of end plugs, which create a concrete key part way into the cores, which, under relative rotations, causes prying and splitting forces within the unreinforced webs of the hollowcore. The hollow-core unit was seated on a low friction bearing strip and the seat widths were 50mm and 75mm at the east and west ends of the test structure respectively. The code amendment prescribes a 75mm seating, but it was decided to investigate the effect of a shorter seat width for cases when hollow-core units arrive on site short, due to drying or elastic shrinkage, indicative of real construction practice.

2.2 Lateral connection and diaphragm reinforcing

The infill detail used in this testing is shown in Figure 1(b). A 75mm thick concrete topping was cast on a 750mm wide timber plank infill running between the first hollowcore unit and the perimeter beams. The starter bars from the perimeter beams extended 600mm into the topping above the first hollowcore unit. It was hoped that the longer starter bars and use of individual reinforcing bars instead of mesh would increase the ductility capacity at the infill-hollowcore interface and reduce the risk of fracture from occurring. The reinforcement used in the diaphragm topping slab was individual reinforcing bars (instead of cold drawn or ductile mesh) which was used to provide a higher level of ductility in areas of high deformation and ensure that the topping reinforcement did not fracture. For this experiment, Grade 300 D12 reinforcement was used at 300mm centres in both directions. The use of D12 bars is beneficial for the fact that it is the same as the starter bars used, and all lapping is between the same reinforcing. The current standards as stipulated in the amendment to NZS 3101:1995, state that starter bars should extend to the larger of either 20% of the hollowcore span, or the development length (l_d) plus an additional 400mm, which in some cases can be a considerable length. In the experiment, the starter bars and diaphragm bars were the same, in effect satisfying the curtailment requirements for starter bars.



(a) Hollow-core seated connection detail.

(b) Perimeter beam-to-hollow-core connection.

Figure 1. Hollow-core connection details.

2.3 Super-assembly construction

The full-scale super-assembly specimen was a two-bay by one-bay structure designed as a lower storey corner section of a multi-storey precast concrete moment resisting frame building. The pretensioned flooring system ran parallel to the longitudinal perimeter beams (east-west), past the central column, and were seated on the transverse beams. The frame dimensions were identical to the original Matthews rig to maintain the same loading set-up and to be able to compare results. The columns were 750mm square in section and spaced at 6.1m centres with an inter-storey height of 3.5m. The perimeter beams were 750mm deep by 400mm wide, and the transverse seating beams were 750mm deep by 475mm wide. The super-assembly was constructed in a similar fashion as it would be done on a construction site. Plan and elevation layouts of the super-assembly are shown in Figure 2.

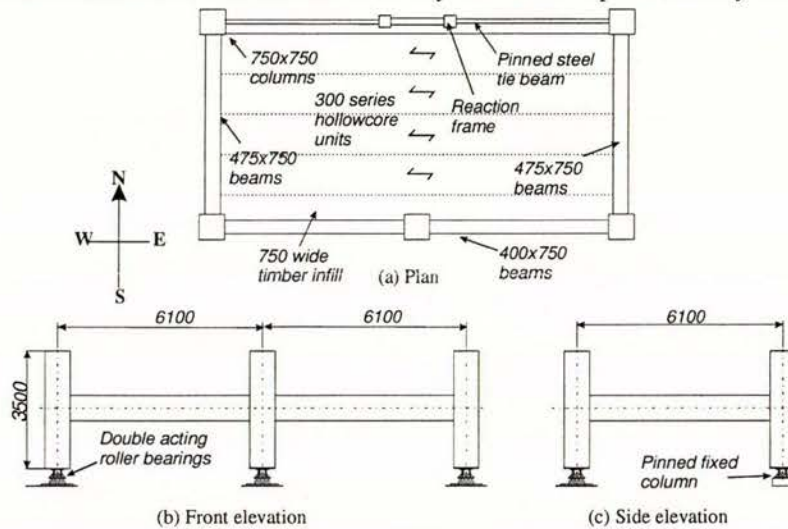


Figure 2. Details and geometry of the super-assembly

The original testing (Matthews, 2004) was, in part, a retrospective look at the structural details of existing buildings whereas this experiment was aimed at validating new construction solutions. With this in mind, it was decided to use Grade 500E seismic steel throughout the frame, which is currently the most commonly used grade of steel in New Zealand construction practice. During previous testing (Lindsay, 2004), the hollowcore units seated on the potential plastic hinge zones of the supporting beams suffered damage due to the high deformation occurring in these zones. To restrain the deformation demand on the floor units, a hooked bar was placed adjacent to the longitudinal steel (as shown in Figure 1) within the beam to force the hinge to occur close to the column face. Another negative feature from the performance of the previous experiments was the spalling of the ledges that supported the precast floor units, sometimes called the “seat”. To overcome this, transverse reinforcement was placed within the seat to tie the seat concrete back into the transverse beams. Part of the support detail was a low friction bearing strip between the bottom of the precast unit and the top of the ledge. A second generation of low-friction bearing strip was used which featured longer ‘teeth’ to both ensure the strip stayed fixed to the ledge and reduce the effects of seat surface roughness.

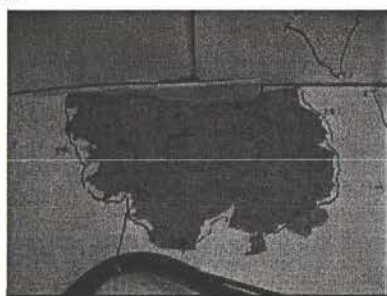
3 TEST SET-UP

Loading of the super-assembly was undertaken by inter-storey drift control. A self-equilibrating primary loading frame was used to apply equal and opposite shear forces to the top and bottom of the columns. A secondary loading frame was used to ensure the columns displaced parallel to each other and in a realistic manner. A full account of the test loading configuration can be found in Matthews (2004). The experiment consisted of three phases comprising: (i) longitudinal loading of two completely reversing cycles to inter-storey drifts of $\pm 0.5\%$, $\pm 1\%$ and $\pm 2\%$; (ii) transverse loading of two completely reversing cycles to $\pm 0.5\%$, $\pm 1\%$, $\pm 2\%$ and $\pm 3\%$; and (iii) longitudinal re-loading of an initial reversing cycle to $\pm 2\%$ followed by two completely reversing cycles of $\pm 3\%$, $\pm 4\%$ and $\pm 5\%$.

4 EXPERIMENTAL RESULTS.

4.1 Phase I: longitudinal loading

Photographs of the key damage sustained are shown in Figure 3. From the early stages of the experiment, diagonal torsional cracks appeared at the ends of the transverse beams and continued to extend and widen throughout this phase of testing. Cracking propagating diagonally outwards from the longitudinal beams appeared over the infill slab from the onset of testing and continued to extend into the second hollowcore unit, arching towards the south central column. Damage in the plastic hinges was confined to one major crack at the beam to column interface, and another significant crack around 300mm from the column. Some instances of spalling of seat cover concrete were evident at +1%. Following the 2% cycles, the spalling had not extended but had worsened in a few areas, as can be seen in Figure 3(a). The damage to the hollow-core floor units themselves was minimal. Damage was confined to a single crack at the beam to floor interface, as shown in Figure 3(b), hairline hollow-core soffit cracks, and a web crack across the side and bottom of the hollow-core unit immediately next to the infill strip was observed at +2% propagating at 45 degrees from the seat to the topping. Beam elongation was illustrated both by the residual crack openings and by the sliding of the floor units out from the supporting beams, as could be seen by the exposure of the unpainted sections of the soffit of the precast floor units. It also showed that the bearing strips were working as intended: the strip staying fixed to the ledges while the hollow-core units slide across the top of the strips. The residual drift after the $\pm 2\%$ cycles was around $\pm 1.1\%$ and the structure had suffered moderate, but repairable damage.



(a) Spalling of seat concrete after Phase I loading.



(b) Continuity crack after Phase I.

Figure 3. Damage to the super-assembly from Phase I longitudinal loading.

4.2 Phase II: transverse loading

A selection of photographs showing the behaviour of the test specimen under transverse Phase 2 loading is shown in Figure 4. During the early stages of testing, the structure exhibited very little new damage with only the cracks caused by Phase 1 loading opening wider. In a similar fashion to the longitudinal beams, the rotation experienced by the transverse beams was concentrated at or near the column face rather than being distributed over a conventional plastic hinge zone length (due to a different reinforcement configuration). Figure 4(a) and (b) show the damage in these zones, where crack widths were approximately 15mm at 3% drift. There was little new damage to the floor and topping slab in general, although elongation of the transverse frames was clearly apparent with large openings between the column and topping slab and the top of beams under negative moments. At -3% drift, the topping slab was pulling away from the corner columns approximately 25mm. Vertical deformations of the floor also became apparent through vertical displacement of the supporting beams. This movement can be accounted for by shear deformations at the ends of the transverse beams. The large deformation occurring at the northern end of the east transverse beam resulted in a crack propagating from the seat through the northernmost filled core of the northernmost hollow-core unit and into the topping slab, as shown in Figure 4(c). This damage did not worsen during the rest of the experiment. At the completion of the transverse Phase II loading to $\pm 3\%$ the residual drifts were roughly $\pm 1.6\%$ and the structure had suffered moderate damage but was still in a repairable state.

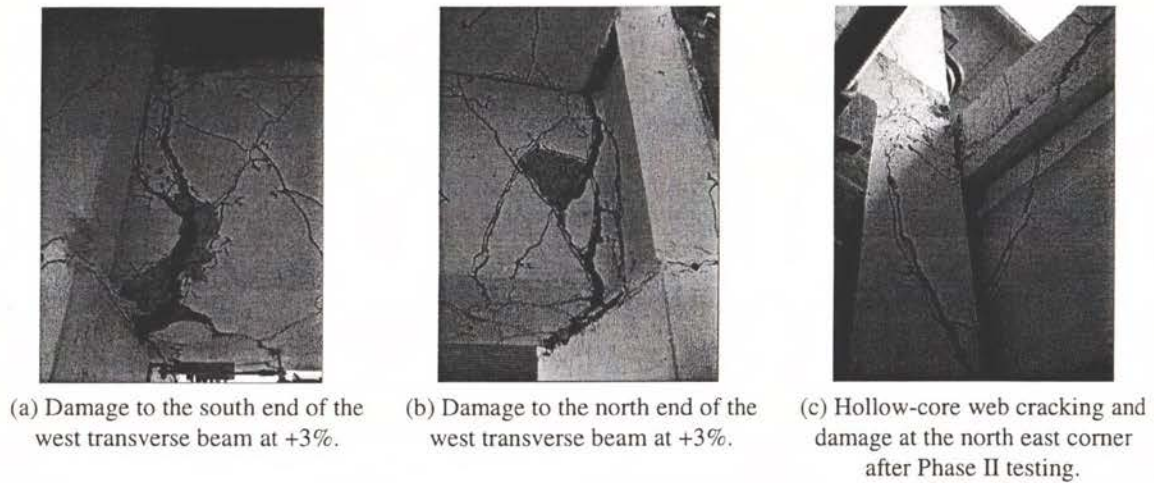


Figure 4 Notable damage from Phase II transverse testing.

4.3 Phase III longitudinal re-loading

Figure 5 shows some key photographs of the Phase III longitudinal re-loading of the test specimen. During the initial stages of loading, no major new damage occurred. A 1m long soffit crack, 1-2mm wide, running along the unit, appeared at the west end of the southernmost unit underneath one of the filled cores. However no more damage to the hollow-core or beam seats was witnessed throughout the remaining testing. At -2.4% drift, compression crushing of the top concrete of the south centre column occurred. The torsional response of the transverse beams was worth noting. While the front frame and north columns were inclined (east-west), the transverse beams appeared to remain vertical, acting to minimise the relative rotation imposed on the seating connection. Cracking at the ends of the transverse beams showed between 2mm and 5mm of lateral movement and evidence of torsional hinging. At $\pm 4\%$ drifts, significant amounts of concrete had become loose and fallen from the plastic hinge zones of these beams, exposing several of the reinforcing bars. Figure 5(b) is indicative of the damage in the plastic hinges and although the structure was still stable and maintained load carrying capacity, the damage in some areas became irreparable and major components would need to be replaced for further structural use. Prior to the first cycle to -4% drift, buckling of the compression bars at the bottom of the western beam of the south frame was observed, as illustrated in Figure 5(c). On the accompanying cycles with an opposite bending moment the bars, now in tension, did not straighten completely. During the final cycle of loading to $\pm 5\%$ drift (at -1.14% and then at -0.36% , unloading from -5%) the inside and outside top reinforcing bars respectively in the eastern beam of the south frame fractured. Although, the future load-carrying capacity of the structural system was jeopardised, life-safety of the structure was still maintained at the $\pm 5\%$ drift limit; only two reinforcing bars had fractured ensuring that the frame remained stable and the lack of damage to the hollowcore units and seating support mitigated the major life safety concerns.

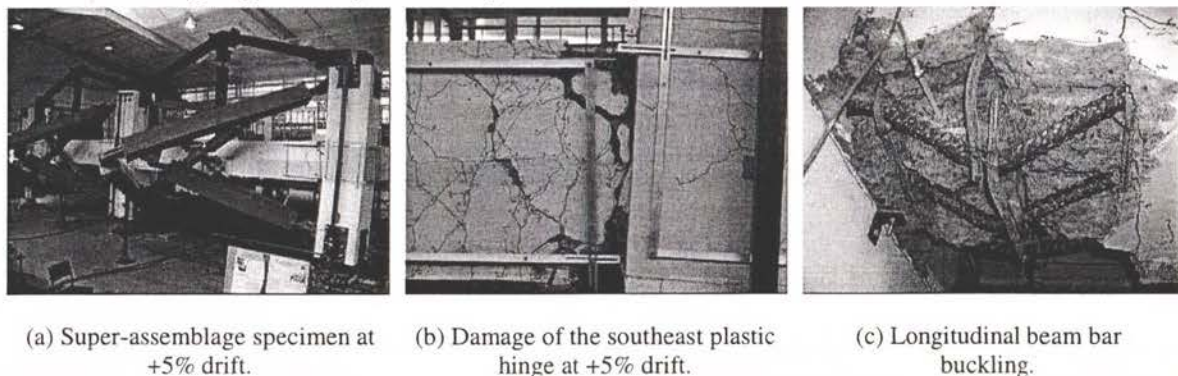


Figure 5. Damage during and after Phase III loading.

5 DISCUSSION OF RESULTS

The overall behaviour of the super-assembly was positive and the specimen performed well up to inter-storey drifts of $\pm 5\%$ when the longitudinal reinforcing bars in one of the beams fractured due to low cycle fatigue. The hollow-core flooring sustained little damage and the overall performance was dictated by the behaviour of the frame, as against the failure of the floor (Matthews, 2004). The following provides comments on the primary areas of interest and significant features of the test.

5.1 Hollow-core seated connection

The beam-to-floor connection detail performed well and the super-assembly structure was able to sustain inter-storey drifts up to $\pm 5\%$ without loss of support of the floor. At the conclusion of testing, there was minor diagonal web cracking in the hollow-core units at the eastern end. A camera that could be placed into four of the hollow-core units could not detect any internal cracking of the particular cores observed and only minor soffit cracking was observed under the filled reinforced cores. The single crack that formed along the beam-to-floor interface in the timber infill link slab concrete and lack of any other cracking demonstrated the objective to centre the rotation on this plane and restrict the rotational demand on the floor units themselves. The bearing strip was also adequate and allowed the floor units to slide whilst staying on the seat. The improved friction resistance and better grip associated with the newer generation of bearing strip seems to have greatly improved the performance of the bearing strip. The minimal amount of spalling of the edge of the seats was also a very positive feature of the experiment owing to the beneficial effects of torsion of the supporting beams, the improved bearing strip performance and the transverse reinforcement of the seat. It must also be noted that there was no difference in behaviour between the 50mm and 75mm seating ends of the structure. However, the specification of a minimum of 75mm seat allows for elastic and drying shortening of the hollow-core units that occur and specifications should adhere to minimum seat widths of 75mm or more. Consideration of the construction tolerances are in addition to the minimum 75 mm seat width.

5.2 Timber infill connection and diaphragm performance

The inclusion of the timber infill connection isolating the longitudinal beams from the floor system performed well during the Lindsay (2004) and Lindsay et al (2004) experiment but it did suffer from a few shortcomings. The provision of longer starter bars and use of conventional reinforcing instead of ductile mesh for this investigation proved to be successful. The presence of the longer starter bars, which were terminated 600mm over the first floor unit ensured that a longitudinal crack or tear did not form at the interfaces between perimeter beam and infill slab, and the infill slab and first hollow-core floor unit. The cracking in the infill only showed very small signs of vertical displacement at the higher drifts during Phase III loading. The crack pattern extended through the topping concrete over the first floor unit and into that above the second floor unit indicating that the longer starter bars were more suitable and able to distribute the forces over a larger area. Figure 6 illustrates the cracking pattern and damage to the infill following the completion of testing. The use of conventional reinforcing within the diaphragm also proved to be successful. The combination of the longer starter bars and conventional reinforcement throughout the topping concrete ensured that no major cracks appeared, and therefore the diaphragm steel was not exposed to high ductility demands.

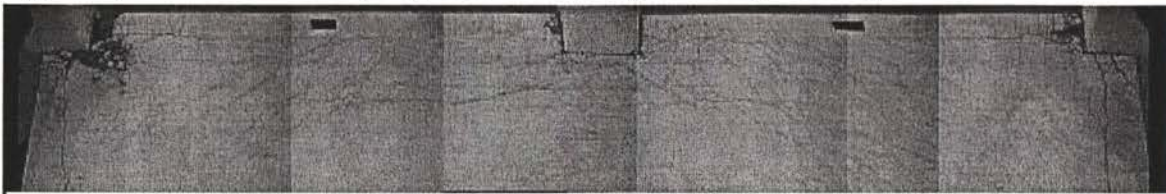


Figure 6. Floor damage after the completion of testing.

5.3 Supporting beam detailing enhancements

To overcome some of the deficiencies observed during the previous experiments (Matthews, 2004; Matthews et al, 2003; Lindsay, 2004; Lindsay et al, 2004), detailing improvements including a hooked

bar to promote column face hinging and seat transverse reinforcement were implemented. The minor damage that occurred within the hollow-core units at the southern corners of the structure, point to the added hooked bar performing as designed – restricting the plastic hinge in the beams to the column faces, inhibiting plastic deformations from progressing under the first hollow-core unit. That action was detrimental in the previous work (Matthews 2003, Lindsay 2004). The hinging in this current investigation was confined to a small area, approximately within half the beam depth from the column face for all of the plastic hinges within the structure, so it is difficult to say that the hooked bar was solely responsible. However, the unit seated on the northeastern corner plastic hinge did experience web cracking, which can be seen in Figure 4(c), which further emphasises the fact that it is preferable to seat hollow-core floor units away from areas of high deformation, and infill-type isolation details should be used over plastic hinge zones of beams.

5.4 Transverse beam torsion

One of the significant features of the present experiment was the degree of torsional twist evident under longitudinal loading on the two transverse beams. Figure 7 shows diagrammatically the behaviour observed. Five inclinometers were installed on the western transverse beam as a means of gauging the amount of torsion experienced. Figure 8 presents the torsion, in terms of percentage drift as a function of time for both Phases I and III loading. It can be seen that during early stages of testing, the rotation of the beam followed that of the corner columns - rigid rotation, which would be expected. In the latter stages of Phase I the beam rotation was similar to the columns for positive drifts but less for negative drifts, which shows the effect of the eccentric loading of the flooring units that rotate the beam in a positive direction. Figure 8 also shows that the transverse Phase II loading had had a marked effect in that beam rotations for Phase III were noticeably reduced with respect to the column signifying that the beams were remaining essentially upright and the flooring horizontal. There is an apparent tendency towards positive drifts accounting for the eccentric floor support. For example, at the first cycle to +4% the beam was at an average +1% inclination, and the first cycle to -4%, the beam rotation remained at around +0.1%. The fact that all five of the inclinometers, which were distributed evenly along the beam, show similar behaviour indicates that the torsion was occurring at the ends of the beams and that torsional hinges were present. The presence of torsional hinges had important effects on the behaviour of the structure. The positive implication of the torsional hinging was that the relative rotation between the flooring units and supporting beam was small and this can help explain the excellent performance of the seated connection and lack of damage.

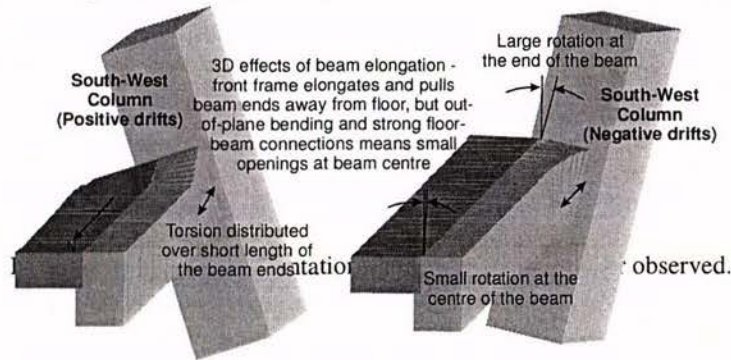


Figure 7. Schematic representation of the torsional behaviour observed

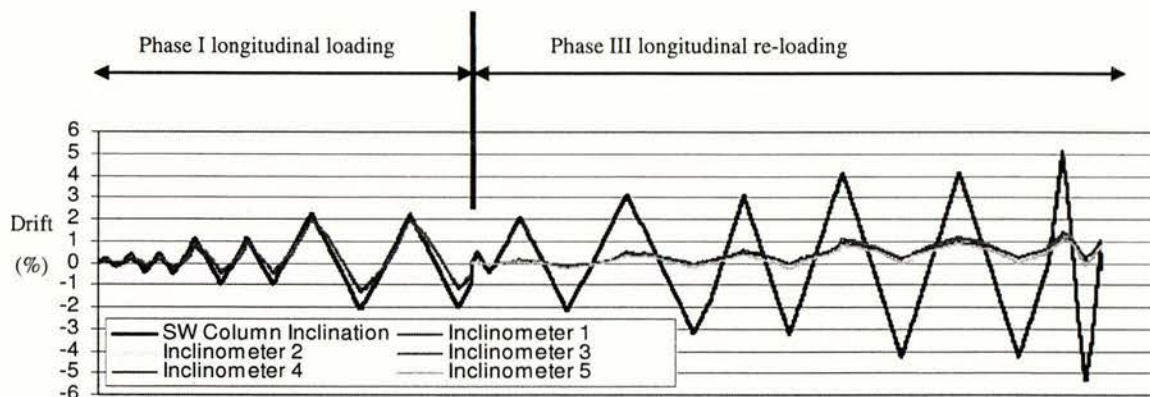


Figure 8. Torsion rotations during Phase I and III longitudinal loading.

6 CONCLUSIONS

The rigid floor-to-supporting beam connection behaved well up to structural inter-storey drifts of $\pm 5\%$, where damage to the hollow-core units and seating support was minimal. Previously, the details investigated herein were untested, and for that reason Amendment No. 3 to the current New Zealand Concrete Design Code NZS3101:1995 limited inter-storey drifts of this class of construction to 1.2% . In light of the good performance, this restriction should be removed. The use of longer starter bars and conventional reinforcing with the articulated timber infill slab connection performed well with no major cracking and tearing experienced. The displacement incompatibility that occurs between the floor units and the beams of the parallel frame was able to be accommodated and diaphragm action was maintained. This research has shown that new concrete frame structures with hollow-core flooring can be expected to perform well in an earthquake event and that life-safety would be maintained under a 2% probability seismic event in 50 years (a 2500 year return period event).

This research has successfully validated several detailing enhancements for hollow-core floor systems in new concrete structures. However, more research at both a sub-assembly level and in full-scale three-dimensional test rigs needs to be done to examine retrofit measures for existing buildings, and more broadly, to investigate the seismic adequacy of other precast flooring systems.

7 ACKNOWLEDGEMENTS

Financial support has been made for this research by a grant from the EQC Research Foundation. Products and support were provided by the following organisations: University of Canterbury, Firth Industries Ltd, Stresscrete, Pacific Steel and Fletcher Reinforcing, Construction Techniques and McDowels Concrete Accessories. All of this financial and in-kind support is gratefully acknowledged.

REFERENCES:

- Lindsay R.A, 2004, *Experiments on the seismic performance of hollow-core floor systems in precast concrete building*, Masters Thesis, Department of Civil Engineering, University of Canterbury, Christchurch, NZ.
- Lindsay R.A, Mander J.B, and Bull D.K, 2004a, *Preliminary results from experiments on hollow-core floor systems in precast concrete buildings*, 2004 NZSEE Conference, Rotorua, NZ, Paper 33, 8 pp.
- Lindsay R.A, Mander J.B, and Bull D.K, 2004b, *Experiments of the Seismic Performance of Hollow-core Floor Systems in Precast concrete Buildings*, 13th World conference on Earthquake Engineering, Vancouver, Canada, CD ROM paper No. 585.
- Matthews J.G, 2004, *Hollow-core floor slab performance following a severe earthquake*, PhD Thesis, Department of Civil Engineering, University of Canterbury, Christchurch, New Zealand.

Matthews J.G, Bull D.K, and Mander J.B, 2003a, *Background to the Testing of a Precast Concrete Hollowcore Floor Slab Building*, 2003, Pacific Conference on Earthquake Engineering, February, Christchurch, NZ, CD ROM paper 170.

Matthews J.G, Bull D.K, and Mander J.B, 2003b, *Preliminary Experimental Results and Seismic Performance Implications of Precast Floor Systems with Detailing and Load Path Deficiencies*, 2003 Pacific Conference on Earthquake Engineering, February, Christchurch, NZ. CD ROM paper 077.

NZS3101, 1995, *Concrete Structures Standard, NZS3101*, Parts 1 & 2, Standards New Zealand, Wellington, NZ.

NZS3101, 2004, *Amendment No. 3 to 1995 Standard (NZS3101)*, Standards New Zealand, Wellington, NZ.

The seismic fragility of precast concrete buildings

J. Matthews

Holmes Consulting Group, Auckland, New Zealand (formerly University of Canterbury)

R. Lindsay

Holmes Consulting Group, Christchurch, New Zealand (formerly University of Canterbury)

J. B Mander

Department of Civil Engineering, University of Canterbury, Christchurch, New Zealand

D. Bull

Holmes Consulting Group, and University of Canterbury, Christchurch, New Zealand

Keywords: Seismic resistance, precast concrete, fragility curves

ABSTRACT: Recent earthquake engineering research undertaken at the University of Canterbury has aimed at determining whether New Zealand designed and built precast concrete structures, which incorporate precast concrete hollow-core floor slabs, possess inadequate seating support details. First, an extensive study that examines the seismic demands on a variety of precast concrete multi-storey buildings is described. Next, to determine the inter-storey drift capacities of precast buildings is determined experimentally. A full scale precast concrete super-assembly was constructed in the laboratory and tested in two stages. The first stage investigated existing construction and demonstrated major shortcomings in construction practice that would lead to very poor seismic performance. Stage 2 investigates the efficiency of improved construction details on seismic performance. Test results show a marked increase in performance between the new connection detail and the existing standard construction details, with relatively small amounts of damage to both the frame and flooring system at high lateral drift levels. The results show that inter-storey drifts in excess of 3.0% can be sustained without loss of support of the floor units with the improved detailing. Finally, the overall performance of precast concrete buildings is assessed by balancing capacity versus demand and developing fragility curves that relate to damage that may affect post-earthquake utility or life-safety. Recommendations for future design and construction are made based on the performance of the super-assembly test specimen and the probabilistic fragility analysis.

1 INTRODUCTION

Precast concrete buildings that use prestressed hollow-core floor units have been the dominant form of construction used in New Zealand (NZ) over the last two decades. Failures observed after the 1994 Northridge (USA) earthquake have raised some concern regarding the performance of NZ's precast concrete multi-storey moment resisting frame buildings. This is because NZ construction methods are similar to that used in the US and many of their buildings did not perform adequately during the Northridge earthquake.

Several buildings in Northridge collapsed as a result of the hollow-core flooring units losing their seating from the supporting beams (Norton et al; 1994). Once the beam support was lost, the units collapsed onto the floor below causing a cascade failure. When the floor units lost their support they failed in one of three manners. First, collapse of a complete unit occurred due to shear failure and the floor unit and topping collapsed in one piece. Second, when support from the beam was lost, the hollow-core floor unit delaminated from the topping

concrete and the units dropped. Third, a failure mechanism occurred when the webs of a hollow-core unit split once the support was lost (Figure 1). This meant that part of the hollow-core unit and all the topping was left suspended by the beam while the remainder of the unit collapsed onto the floor below.

After observing the failures in Northridge a multi-stage study has been undertaken at the University of Canterbury, to determine whether NZ designed and built structures have similar problems, and if so, to what extent these problem exists and what can be done about them.

This paper first describes the assessment of seismic demands that are to be experienced by typical multi-storey precast concrete buildings—particularly those in moderate to high seismic regions, such as Wellington, NZ.

Secondly, the paper describes a series of large scale experiments that were conducted on a full-scale super-assembly specimen in order to ascertain the inter-storey drift capacities at various damage states. Stage 1 of the experimental study examined the past precast concrete detailing practice in accordance with the governing codes and standards of the day for the period of 1985 to 2003. The results obtained

from the *Stage 1* experiment were not encouraging, as the laboratory specimen effectively reproduced the field observed failure shown in Figure 1. Thus a *Stage 2* experiment was conducted where a new precast concrete floor system was implemented that incorporated improved detailing based on lessons learned from the field and the *Stage 1* experiment.

Thirdly the paper integrates aspects of capacity versus demand by developing a series of probabilistic based fragility curves. From these curves conclusions regarding several performance trends can be drawn, and the efficacy of improved detailing practice quantified.



Figure 1 Photograph of precast hollow core floor collapse after the 1994 Northridge earthquake

2 PROBABILISTIC ASSESSMENT OF DRIFT DEMAND

2.1 Background

For a given spectral acceleration (S_a) Cornell et al (2002) stated it is possible to predict the drift demand by the following general relationship:

$$D' = a(S_a)^b \quad (1)$$

in which D' = drift demand; a = coefficient determined by non-linear time history analyses; and b = an exponent.

For moment frames, Luco and Cornell (2000) recommend $b = 1$. The assumption is consistent with the well-known equal displacement rule that suggests for moderate period structures the inelastic displacement demands are similar to the demands imposed on a linear structure.

It is inevitable that equation (1) will not provide an exact prediction of response—there will be a measure of variability in the predicted outcomes. For example, in a study undertaken on steel moment resisting frame structures, the results of Luco and Connell (2000) showed an increase between the median result and the 1-sigma value (84th percentile value) was approximately 2.0. Similarly, Lee and Foutch (2002) for steel moment frame structures

showed multipliers ranging from 1.5 to 2 for the 84th percentile and more than 2.0 for the 95th percentile results.

When determining realistic drift demands on structures, rather than using median or expected values of drift, Cornell et al (2002) suggest that due to the inherent variability, a 90 percent confidence interval be adopted. This ensures that there is only a ten percent chance that a design demand drift will not be exceeded during an earthquake.

Based on the aforementioned probabilistic method of assessing steel structures developed by Cornell et al (2002), Lupoi et al (2002) have gone on and examined this approach for the seismic design of reinforced concrete structures.

The work presented herein is another attempt at using the approach, but applied to a family of seismically vulnerable precast concrete multi-storey buildings designed and constructed during the period from 1985 to 2003.

To assess the expected seismic demands on a precast concrete structure, nonlinear time history studies were undertaken. These studies investigated a number of variables in order to determine the principal structure dependent parameters; principally drift amplitude and cyclic demand.

2.2 Earthquake records studied

In order to simulate the likely seismic performance of the test buildings, a suite of earthquake records was chosen for the time history analysis. These records included both near and far field effects, since earthquakes of both of these natures are expected within highly active seismic regions, including Wellington, NZ. Listed in Table 1 are the various earthquakes along with their peak ground acceleration (PGA), spectral acceleration at the one-second period ($F_v S_1$), and location of the earthquake and whether it is a near or far field event.

2.3 Prototype buildings

The dimensions of the “prototype buildings” investigated herein were based on a representative sample of buildings idealized from professional practice as constructed principally in NZ from the 1980's through 1990's. Four different height buildings were studied; namely 3, 6, 9 and 12 stories, as shown in Figure 2. For the purposes of the study, the buildings were assumed rectangular and torsionally stable.

Each building had the following dimensions: storey height = 3.5m; bay length = 6.1m; number of bays = 4; column dimensions = 750mm×750mm; beam dimensions = 750mm×400mm; basic live load = 2.5kPa; superimposed dead load = 0.75kPa; hollow-core unit used = 300mm deep; and concrete topping slab thickness = 75mm.

The “prototype buildings” shown in Figure 3 were designed as typical NZ precast concrete structures in

accordance with the New Zealand Concrete Structures Standard (NZS3101:1995). The member sizes were based on typical dimensions used during the 1980's and 1990's and were associated with a maximum allowable inter-storey drift of two percent. The resulting perimeter beam reinforcement ratios were typically in the order of 0.01. Capacity design for the reinforcement details of the frame members was used throughout.

Table1 The suite of earthquakes used for the time history studies.

Location	Near or far field	PGA (g)	F _v S ₁
El Centro USA 1940	Far	0.35	0.52
Kern County USA 1952	Far	0.16	0.13
Sylmar Northridge USA 1994	Near	0.84	1.05
Sylmar Northridge USA 1994	Near	0.8	0.93
Kobe Japan 1995	Near	0.84	1.23
Kobe Japan 1995	Near	0.64	1.53
El Centro USA 1940	Far	0.338	0.42*
El Centro USA 1940	Far	0.362	0.51*
Olympia Puget Sound USA	Far	0.433	0.49*
Olympia Puget Sound USA	Far	0.414	0.5*
Kern County USA 1952	Far	0.433	0.49*
Kern County USA 1952	Far	0.364	0.5*
El Centro USA 1940	Far	0.683	1.0
San Fernando USA 1971	Far	0.959	1.0
San Fernando USA 1971	Far	1.344	1.0
Imperial Valley USA 1999	Far	1.729	0.83
Kobe Japan 1995	Near	0.55	0.38
Kobe Japan 1995	Near	0.517	0.54
Northridge USA 1994	Near	0.552	0.78
Northridge USA 1994	Near	0.777	0.57

* These records have been scaled to match the design spectrum for NZS4203:1992

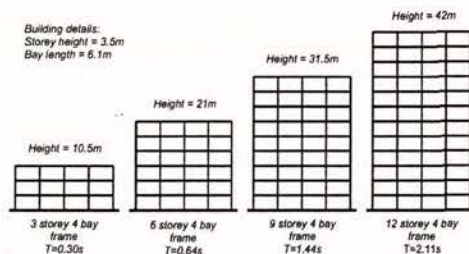


Figure 2 Design test buildings and fundamental periods

2.4 Results of time-history analysis

Results showed the difference between the inter-storey drift at the first storey are of the order of 100 percent greater than the overall structural drift. This is attributed to a combination of factors including higher mode effects and high shears causing greater deformations in the lower stories. By examining all the time history results it became clear that there was no common trend between all the various results. A sample of the typical variability for one earthquake for the four different buildings along with near and far filed variability is shown in Figure 3. The near

field events typically had one large pulse and resulted in some measure of residual displacement.

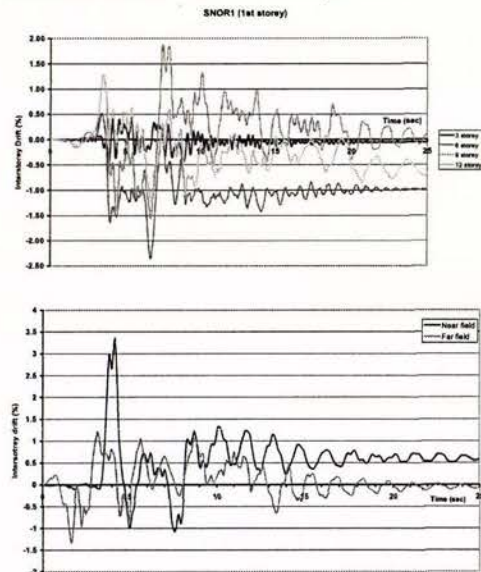


Figure 3 Comparison between localised storey performance (top) and results for near and far-field earthquakes (bottom).

2.5 Probabilistic assessment of drift demand variability

Because no common trend (in terms of the magnitude of the inter-storey drift) could be obtained from the response outcomes, the results were normalized so that all the various forms of earthquake motions had a common variable. First, the results were plotted with the maximum inter-storey drift for each structure height and earthquake versus an acceleration intensity measure $F_v S_1$ (the spectral acceleration at 1 second) as shown in Figure 4. Once plotted it was possible to determine the median values for the spread of results (line of best fit). It should be noted that for the three-storey structure the inter-storey drift was plotted against PGA rather than $F_v S_1$. This was because for low period structures (0.3 seconds in the case of the three storey structure) the amount of variability in the 1 second spectral acceleration is large, therefore more meaningful results were obtained if the three storey structures results were obtained when PGA was used as the intensity measure.

The variability of the data can be better understood by plotting the results in an alternative form. By assuming $b = 1$ in Equation (1), then rearranging gives

$$a = D / S_a \quad (2)$$

in which a = drift index proportionality parameter.

If the data is ranked from smallest to largest and then plotted in the form of a cumulative distribution the median value (50th percentile) can be found. These results are plotted as data points in Figure 4 along with a continuous curve that is a best fit to a lognormal probability distribution. Only two parameters are needed to describe this distribution, the median (50th percentile), \tilde{a} , and the lognormal coefficient of variation, β (sometimes called the dispersion factor). From the plot it is evident that the results conform quite well to a cumulative lognormal probability distribution.

Individual results show values of $\beta = 0.60, 0.45, 0.40$ and 0.45 for the respective 3, 6, 9 and 12 storey buildings considered. These values of β agree well with the results of Lupoi et al (2002) whose β values ranged between 0.44 and 0.58. From the results, it is evident that to ensure a 90th percentile confidence interval, the observed drifts should be amplified by a factor of least 1.9 above their expected (median) values. It is therefore contended that for dependable seismic performance any experimental assessment of seismic capacity should have a factor of some two times the expected value of the drift demand.

The composite cumulative distribution has a median of $\tilde{a}=2.0$ and a dispersion factor of $\beta=0.52$. Interestingly, the value for β falls in midrange of the aforementioned findings of Lupoi et al (2002), presumably for a completely different suite of earthquake ground motions. Although the median line is plotted on the inter-storey drift versus $F_v S_1$ (or PGA) plot a more meaningful line is the 90th percentile value. This gives a dependable upper limit to the inter-storey drift for a given $F_v S_1$ (or PGA) there is a probability of 10% in exceeding this value. Figure 4 (b) shows that a 90th percentile value of 1.95 (times the median value) is obtained. These results justify the use of a 2.0 multiplier when assigning dependable (confidence) limits.

Once the 90th percentile lines have been generated for the overall response, it is then possible to determine the expected inter-storey drifts for the different height structures for both a 10% in 50 years, "Design Basis Earthquake" (DBE) and a 2% in 50 years, "Maximum Considered Earthquake" (MCE). The DBE is based on Wellington NZ conditions where there is a design PGA = 0.4g whereas the MCE has PGA = 0.72g (1.8xDBE). The multiplier of 1.8 used to convert a DBE to a MCE is determined from the relationship between the structural risk factor and the earthquake return period as set out in NZS4203:1992. Table 2 summarizes these results.

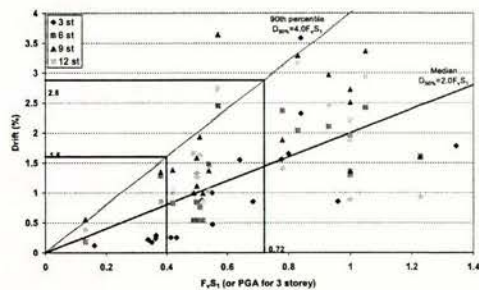
It is proposed that the drift index parameter, a , (from Equation (2)) should be taken as 2.5 and the DBE and MCE values are calculated as follows:

$$DBE \Rightarrow \tilde{D} = 2.5 \times 0.4 = 1.0\% \quad (3)$$

$$DBE \Rightarrow D_{90\%} = 2 \tilde{D} = 2 \times 1.0 = 2.0\% \quad (4)$$

$$MCE \Rightarrow D_{90\%} = 1.8 D_{90\%,DBE} = 1.8 \times 2.0 = 3.6\% \quad (5)$$

These values for the DBE and MCE have been added to Table 2 as the adopted nominal outcomes.



(a) Inter-storey drift based on applied $F_v S_1$ (and PGA)

(b) cumulative distribution as a function parameter "a"

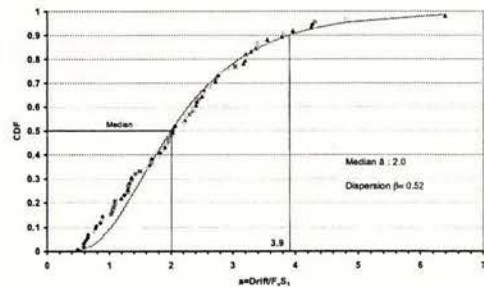


Figure 4. Combined results for the four different building heights examined

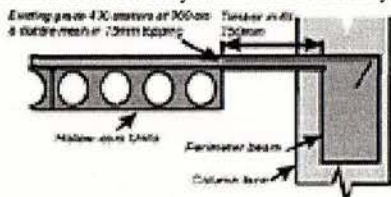
Table 2 The 90th percentile inter-storey drifts that correspond to a Design Basis Earthquake (DBE=10% in 50 years) and Maximum Considered Earthquake (MCE=2% in 50 years) for the various height structures

Number of Stories	DBE Drift	MCE Drift
3	1.4%	2.5%
6	1.5%	2.8%
9	2.1%	3.8%
12	1.9%	3.5%
Nominal Outcome	2.0%	3.6%

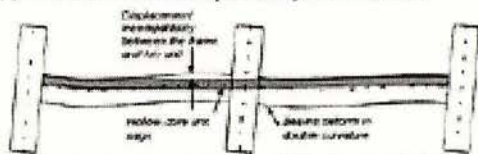
edge of the perimeter beam, when hollow-core units are not designed for such displacement profiles (Figure 7).

The seating connection between the hollow-core unit and the supporting beam consisted of replacing the plastic dam plug in the ends of the unit with 10mm of compressible material fully across the end of the unit and seating the unit on a low friction bearing strip. This detail is shown in Figure 6(b) along with how the floor unit is expected to rotate relative to the beam. The low friction bearing strip allows the floor unit to slide as designers had previously assumed it would. The compressible material is assumed to reduce the compression forces applied at the bottom of the unit under negative moments as well as restricting concrete from entering the cores of the units. If the large compression force forms between the bottom of the unit and the face of the supporting beam it is transferred at a relatively flat angle to the topping concrete. A perpendicular principal tensile force then forms, causing splitting of the webs at very early stages of the test.

The lateral connection to the perimeter frame consisted of moving the first unit away from the perimeter beam and replacing it with a 750mm timber infill with 75mm in-situ concrete topping (Figure 7(a)). The infill allows a more flexible interface between the frame and southern hollow-core unit. Some cracking is expected in this interface due to the displacement incompatibility but it is anticipated that the more flexible interface will accommodate this while allowing the beam to deform in double curvature and the hollow-core unit in single curvature, (Figure 7(b)) leaving the floor essentially undamaged. Ductile reinforcing mesh was used in the topping to aid in the performance of the floor by helping to ensure that any damage and cracking would not result in such an early failure of the floor system.



(a) First hollow-core unit to perimeter frame connection.



(b) Expected displacement incompatibility between the hollow-core floor units and the perimeter frame.

Figure 7. Accommodation of the displacement incompatibilities between the perimeter frame and the precast concrete floor system.

3.1 Classification of observed building damage

A common form of damage classification is to use a numerical indicator format as adopted by HAZUS (1999). A number between one and five that also refers to the level of damage is used, as given in Table 3.

Table 3 Definition of the damage states used to classify the level of damage to a structure following an earthquake (Mander, 2003)

Damage State	Damage Descriptor	Post-earthquake Utility of Structure
1	None (pre-yield)	Normal
2	Minor/Slight	Slight Damage
3	Moderate	Repairable damage
4	Major/Extensive	Irreparable damage
5	Complete collapse	Irreparable damage

Following the completion of the experimental testing program it was possible to classify the super-assemblage according to the two classification methods. Based on the two experiments, and related back to past (pre-2004) and current (post-2004) code requirements (Amendment 3 to NZS3101,1995) the results are summarized in Table 4. It should be noted that since the classification of performance between the reinforced concrete moment resisting frame and the hollow-core floor slab was so different, the two components were classified separately.

A marked difference in performance between the reinforced concrete moment resisting frame and the precast hollow-core floor slabs is evident in Table 4. If the global classification of the structure were required, then the floor performance values would be stated, as these are critical to the overall structure. In summary, Table 4 gives drift limit states based on post-earthquake utility and life-safety considerations, respectively. In now remains to balance these capacity limits with the seismic demands placed on the structure. The approach to this is described in what follows.

Table 4 Damage state classification for the super-assemblage

Damage State	Inter-storey drift based on:		
	Historical [@] floor detailing practice	Modern [#] detailing practice for floors and their connections	Historical [@] and current [#] frame detailing practice
2	0.3%	1%	1%
3	0.35%	2%	2%
4	1.9%	4%	4%
5	2.5%	-	-

[@] 1985-2003 details to NZS3101
[#] 2004 Amendment 3 to NZS3101-1995

4 BALANCING CAPACITY VERSUS DEMAND: A FRAGILITY APPROACH

In the analysis of drift demand, described above, it was demonstrated that the distribution of drift outcomes was lognormal with a lognormal coefficient of variation of $\beta_D = 0.52$ (note the subscript D stands for demand).

By adopting the aforementioned value of $\bar{a} = 2.0$ in equation 1, and then inverting, the expected value (median or 50th percentile) of the ground motion demand needed to achieve a given median drift capacity can be found such that

$$\bar{F}_v S_1 = 0.5 \bar{D}_c \quad (8)$$

$$PGA = 0.5 \bar{D}_c \quad (9)$$

where \bar{D}_c = expected drift capacity of the structure.

Now the capacity parameter \bar{D}_c is not precisely known, but assuming that the full-scale experiments provide a reliable indicator of the expected drift capacities, and assuming these capacities themselves have a coefficient of variation of $\beta_C = 0.2$ (this is in keeping with the findings from Dutta (1999)), Kennedy et al (1980) have shown that the composite value of the lognormal distribution is found by

$$\beta_{C/D} = \sqrt{\beta_C^2 + \beta_D^2 + \beta_U^2} \quad (10)$$

in which β_C and β_D are as defined above, and β_U is a lognormal dispersion parameter for modelling uncertainty. The latter parameter has been taken as $\beta_U = 0.2$.

Using this data it follows from equation (10) that $\beta_{C/D} = 0.60$. This value is in keeping with results inferred from observed damage to bridge structures in the 1994 Northridge earthquake (Mander and Basöz, 1999).

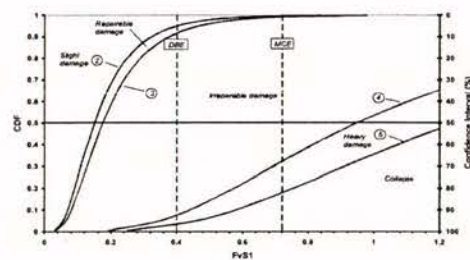
By using a lognormal cumulative distribution that can be described by a unit lognormal variate ξ_β (where the median = 1 and lognormal coefficient of variation $\beta_{C/D} = 0.60$), the distribution of ground motion demands necessary to produce a given damage state outcome can be found by

$$F_v S_1 = 0.5 \bar{D}_c (DS) \xi_\beta \quad (11)$$

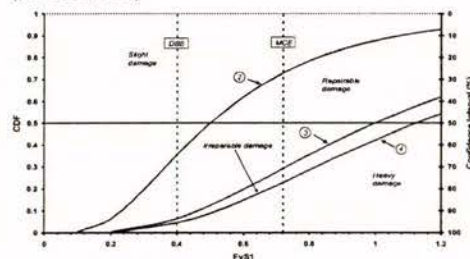
$$PGA = 0.5 \bar{D}_c (DS) \xi_\beta \quad (12)$$

Figure 8 shows the fragility curves for the rating of the floor and frame performance in terms of different numerical damage states. Figure 8(a) shows that for a MCE if the structures performance is clas-

sified in terms of the precast hollow-core floor performance due to the use of historic reinforcing details (1985 to 2003) then 2% of structures would be expected to sustain slight or repairable damage. The remaining 98% of structures would be expected to be demolished as a result of irreparable damage or collapse, of these some 32% of floors would be expected to partially or entirely collapse leading to loss of life. Under a DBE, 92% of structures would sustain excessive damage, with some 8% potentially leading to loss of life. Ironically, some engineers may consider this to be a satisfactory outcome as there is more than 90 percent confidence that loss of life will not occur. However, given that the vast majority of the buildings would be unsafe and need demolishing, this is felt to be unsatisfactory, let alone considering that nearly 10% of structures could collapse, leading to loss of life. Figure 8(b) shows that for a MCE if the structures performance is classified in terms of the frame performance (rather than the floor) then 93% of structures might be expected to sustain damage that is either slight or repairable; only 7% of structures would be expected to require demolition.



(a) Precast concrete buildings with vulnerable precast concrete hollow-core floors built to pre-2004 Standards (NZS3101, 1995)



(b) Concrete buildings built to post-2004 Standards (NZS3101, 1995, Amendment 3)

Figure 8 Fragility curves for New Zealand concrete buildings rated to the HAZUS damage states.

5 CONCLUSIONS

Based on the research described herein, the following conclusions are drawn:

1. For a Design Basis Earthquake (10% in 50 years) structures may be permitted to be designed for a 2.0% inter-storey drift limit. But due to conservatively defined material properties and in-built over-strength, the median (50 percentile) seismic drift demand will be in the order of only 1.0%. However, there is a wide range of possible results, and to be 90 percent confident that all possibilities are captured, a demand drift of 2.0% is realistic. This means that for a Maximum Considered Earthquake of 2% in 50 years (approximately 2500 year return period) and a 90% confidence interval the drift demand is 3.6%.
2. Experiments have shown that precast concrete structures with hollow core floor systems built to pre-2004 Standards possess inadequate capacity to sustain the expected seismic demands. Incipient collapse can occur at drifts in the order of 1.9%.
3. For multi-storey structures with hollow-core floors detailed to pre-2004 Standards significant collapses may be expected for a 2% in 50 years (MCE) event in Wellington, NZ. Under a 10% in 50 year (DBE) event, the situation is also not favourable; some 90% of buildings might be expected to be demolished including 8% that could potentially cause loss of life through collapse.
4. For multi-storey structures with hollow-core floors detailed to post-2004 Standards the number of buildings that would require demolition following a maximum considered earthquake (MCE) for Wellington would be low. This outcome is in keeping with the expectations of capacity design.

ACKNOWLEDGEMENTS

This project would not be possible without the support from the following organizations: University of Canterbury, Earthquake Commission, Cement and Concrete Association of New Zealand, BRANZ, Foundation for Research Science and Technology – Tūāpapa Pūtaiao Maori Fellowships, C. Lund & Son Ltd, Firth Industries Ltd, Stresscrete, Pacific Steel, Stahlton Prestressed Flooring, Construction Techniques, Precast Components, The Maori Education Trust, Fulton Hogan Ltd, Holmes Consulting Group, Hylton Parker Fasteners and Hilti (NZ) Ltd.

REFERENCES

- Cornell C.A., Jalayer F, Hamburger R.O and Foutch D.A, 2002, *Probabilistic Basis for 2000 SAC Federal Emergency Management Agency Steel Moment Frame Guidelines*, ASCE Journal of Structural Engineering, April, pp 526-533
- Dutta A, 1999, *On Energy-Based Seismic Analysis and Design of Highway Bridges*, Ph.D Dissertation, science and Engineering Library, State university of New York at Buffalo, Buffalo, NY
- HAZUS. 1999. *Earthquake Loss Estimation Methodology*. Technical Manual. Prepared by the National Institute of Building Sciences for Federal Emergency Management Agency, Washington, DC.
- Kennedy R.P, Cornell, C.A, Campbell R.D, Kaplan, S and Perla H.F, 1980, *Probabilistic Seismic Safety Study of an Existing Nuclear Power Plant*, Nuclear Engineering and Design No. 59, pp 315-338
- Lee K and Foutch D.A, 2002, Seismic Performance Evaluation of Pre-Northridge Steel Frame Buildings with Brittle Connections, ASCE Journal of Structural Engineering, April, pp 546-555
- Lindsay, R., 2004, "Experiments on the seismic performance of hollow-core floor systems in precast concrete buildings", ME Thesis, University of Canterbury, Christchurch, New Zealand.
- Luco N and Cornell C.A, 2000, Effects of Connection Fractures on SMRF Seismic Drift Demands, ASCE Journal of Structural Engineering, January, pp 127-136
- Lupoi G, Lupoi A and Pinto P.E, 2002, *Seismic Risk Assessment of RC Structures with the "2000 SAC/FEMA" Method*, Journal of Earthquake Engineering, Vol. 6, No 4, pp 499-512
- Mander J.B and Basöz N, 1999, *Seismic fragility curve theory for highway bridges in transportation lifeline loss estimation in Optimising Post-Earthquake Lifeline System Reliability*, TCLEE Monograph No. 16 Eds Elliot and McDonough
- Matthews J.G. 2004, "Hollow-core floor slab performance following a severe earthquake." Ph.D Thesis, University of Canterbury, Christchurch, New Zealand.
- NZS3101:1995, *Concrete Structures Standard-The Design of Concrete Structures*, Standards New Zealand, Wellington New Zealand
- NZS3101: 2004, *Amendment 3 to NZS3101:1995*, Standards New Zealand, Wellington, New Zealand
- Norton, J.A, King, A.B, Bull, D.K, Chapman, H.E, McVerry, G.H, Larkin, T.J, Spring, K.C, 1994, *Northridge Earthquake Reconnaissance Report*, Bulletin of the New Zealand National Society for Earthquake Engineering Vol. 27, No.4, December

The seismic fragility of precast concrete buildings

J. Matthews

Holmes Consulting Group, Auckland, New Zealand (formerly University of Canterbury)

R. Lindsay

Holmes Consulting Group, Christchurch, New Zealand (formerly University of Canterbury)

J. B Mander

Department of Civil Engineering, University of Canterbury, Christchurch, New Zealand

D. Bull

Holmes Consulting Group, and University of Canterbury, Christchurch, New Zealand

Keywords: Seismic resistance, precast concrete, fragility curves

ABSTRACT: Recent earthquake engineering research undertaken at the University of Canterbury has aimed at determining whether New Zealand designed and built precast concrete structures, which incorporate precast concrete hollow-core floor slabs, possess inadequate seating support details. First, an extensive study that examines the seismic demands on a variety of precast concrete multi-storey buildings is described. Next, to determine the inter-storey drift capacities of precast buildings is determined experimentally. A full scale precast concrete super-assembly was constructed in the laboratory and tested in two stages. The first stage investigated existing construction and demonstrated major shortcomings in construction practice that would lead to very poor seismic performance. Stage 2 investigates the efficiency of improved construction details on seismic performance. Test results show a marked increase in performance between the new connection detail and the existing standard construction details, with relatively small amounts of damage to both the frame and flooring system at high lateral drift levels. The results show that inter-storey drifts in excess of 3.0% can be sustained without loss of support of the floor units with the improved detailing. Finally, the overall performance of precast concrete buildings is assessed by balancing capacity versus demand and developing fragility curves that relate to damage that may affect post-earthquake utility or life-safety. Recommendations for future design and construction are made based on the performance of the super-assembly test specimen and the probabilistic fragility analysis.

1 INTRODUCTION

Precast concrete buildings that use prestressed hollow-core floor units have been the dominant form of construction used in New Zealand (NZ) over the last two decades. Failures observed after the 1994 Northridge (USA) earthquake have raised some concern regarding the performance of NZ's precast concrete multi-storey moment resisting frame buildings. This is because NZ construction methods are similar to that used in the US and many of their buildings did not perform adequately during the Northridge earthquake.

Several buildings in Northridge collapsed as a result of the hollow-core flooring units losing their seating from the supporting beams (Norton et al; 1994). Once the beam support was lost, the units collapsed onto the floor below causing a cascade failure. When the floor units lost their support they failed in one of three manners. First, collapse of a complete unit occurred due to shear failure and the floor unit and topping collapsed in one piece. Second, when support from the beam was lost, the hollow-core floor unit delaminated from the topping

concrete and the units dropped. Third, a failure mechanism occurred when the webs of a hollow-core unit split once the support was lost (Figure 1). This meant that part of the hollow-core unit and all the topping was left suspended by the beam while the remainder of the unit collapsed onto the floor below.

After observing the failures in Northridge a multi-stage study has been undertaken at the University of Canterbury, to determine whether NZ designed and built structures have similar problems, and if so, to what extent these problem exists and what can be done about them.

This paper first describes the assessment of seismic demands that are to be experienced by typical multi-storey precast concrete buildings—particularly those in moderate to high seismic regions, such as Wellington, NZ.

Secondly, the paper describes a series of large scale experiments that were conducted on a full-scale super-assembly specimen in order to ascertain the inter-storey drift capacities at various damage states. Stage 1 of the experimental study examined the past precast concrete detailing practice in accordance with the governing codes and standards of the day for the period of 1985 to 2003. The results obtained

from the *Stage 1* experiment were not encouraging, as the laboratory specimen effectively reproduced the field observed failure shown in Figure 1. Thus a *Stage 2* experiment was conducted where a new precast concrete floor system was implemented that incorporated improved detailing based on lessons learned from the field and the *Stage 1* experiment.

Thirdly the paper integrates aspects of capacity versus demand by developing a series of probabilistic based fragility curves. From these curves conclusions regarding several performance trends can be drawn, and the efficacy of improved detailing practice quantified.



Figure 1 Photograph of precast hollow core floor collapse after the 1994 Northridge earthquake

2 PROBABILISTIC ASSESSMENT OF DRIFT DEMAND

2.1 Background

For a given spectral acceleration (S_a) Cornell et al (2002) stated it is possible to predict the drift demand by the following general relationship:

$$D' = a(S_a)^b \quad (1)$$

in which D' = drift demand; a = coefficient determined by non-linear time history analyses; and b = an exponent.

For moment frames, Luco and Cornell (2000) recommend $b = 1$. The assumption is consistent with the well-known equal displacement rule that suggests for moderate period structures the inelastic displacement demands are similar to the demands imposed on a linear structure.

It is inevitable that equation (1) will not provide an exact prediction of response—there will be a measure of variability in the predicted outcomes. For example, in a study undertaken on steel moment resisting frame structures, the results of Luco and Connell (2000) showed an increase between the median result and the 1-sigma value (84th percentile value) was approximately 2.0. Similarly, Lee and Foutch (2002) for steel moment frame structures

showed multipliers ranging from 1.5 to 2 for the 84th percentile and more than 2.0 for the 95th percentile results.

When determining realistic drift demands on structures, rather than using median or expected values of drift, Cornell et al (2002) suggest that due to the inherent variability, a 90 percent confidence interval be adopted. This ensures that there is only a ten percent chance that a design demand drift will not be exceeded during an earthquake.

Based on the aforementioned probabilistic method of assessing steel structures developed by Cornell et al (2002), Lupoi et al (2002) have gone on and examined this approach for the seismic design of reinforced concrete structures.

The work presented herein is another attempt at using the approach, but applied to a family of seismically vulnerable precast concrete multi-storey buildings designed and constructed during the period from 1985 to 2003.

To assess the expected seismic demands on a precast concrete structure, nonlinear time history studies were undertaken. These studies investigated a number of variables in order to determine the principal structure dependent parameters; principally drift amplitude and cyclic demand.

2.2 Earthquake records studied

In order to simulate the likely seismic performance of the test buildings, a suite of earthquake records was chosen for the time history analysis. These records included both near and far field effects, since earthquakes of both of these natures are expected within highly active seismic regions, including Wellington, NZ. Listed in Table 1 are the various earthquakes along with their peak ground acceleration (PGA), spectral acceleration at the one-second period ($F_v S_1$), and location of the earthquake and whether it is a near or far field event.

2.3 Prototype buildings

The dimensions of the "prototype buildings" investigated herein were based on a representative sample of buildings idealized from professional practice as constructed principally in NZ from the 1980's through 1990's. Four different height buildings were studied; namely 3, 6, 9 and 12 stories, as shown in Figure 2. For the purposes of the study, the buildings were assumed rectangular and torsionally stable.

Each building had the following dimensions: storey height = 3.5m; bay length = 6.1m; number of bays = 4; column dimensions = 750mm×750mm; beam dimensions = 750mm×400mm; basic live load = 2.5kPa; superimposed dead load = 0.75kPa; hollow-core unit used = 300mm deep; and concrete topping slab thickness = 75mm.

The "prototype buildings" shown in Figure 3 were designed as typical NZ precast concrete structures in

accordance with the New Zealand Concrete Structures Standard (NZS3101:1995). The member sizes were based on typical dimensions used during the 1980's and 1990's and were associated with a maximum allowable inter-storey drift of two percent. The resulting perimeter beam reinforcement ratios were typically in the order of 0.01. Capacity design for the reinforcement details of the frame members was used throughout.

Table1 The suite of earthquakes used for the time history studies.

Location	Near or far field	PGA (g)	F _v S ₁
El Centro USA 1940	Far	0.35	0.52
Kern County USA 1952	Far	0.16	0.13
Sylmar Northridge USA 1994	Near	0.84	1.05
Sylmar Northridge USA 1994	Near	0.8	0.93
Kobe Japan 1995	Near	0.84	1.23
Kobe Japan 1995	Near	0.64	1.53
El Centro USA 1940	Far	0.338	0.42*
El Centro USA 1940	Far	0.362	0.51*
Olympia Puget Sound USA	Far	0.433	0.49*
Olympia Puget Sound USA	Far	0.414	0.5*
Kern County USA 1952	Far	0.433	0.49*
Kern County USA 1952	Far	0.364	0.5*
El Centro USA 1940	Far	0.683	1.0
San Fernando USA 1971	Far	0.959	1.0
San Fernando USA 1971	Far	1.344	1.0
Imperial Valley USA 1999	Far	1.729	0.83
Kobe Japan 1995	Near	0.55	0.38
Kobe Japan 1995	Near	0.517	0.54
Northridge USA 1994	Near	0.552	0.78
Northridge USA 1994	Near	0.777	0.57

* These records have been scaled to match the design spectrum for NZS4203:1992.

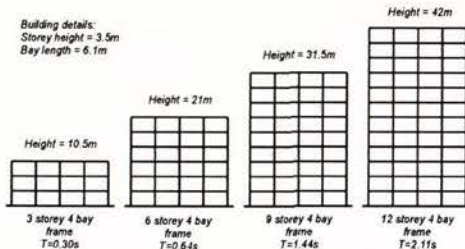


Figure 2 Design test buildings and fundamental periods

2.4 Results of time-history analysis

Results showed the difference between the inter-storey drift at the first storey are of the order of 100 percent greater than the overall structural drift. This is attributed to a combination of factors including higher mode effects and high shears causing greater deformations in the lower stories. By examining all the time history results it became clear that there was no common trend between all the various results. A sample of the typical variability for one earthquake for the four different buildings along with near and far filed variability is shown in Figure 3. The near

field events typically had one large pulse and resulted in some measure of residual displacement.

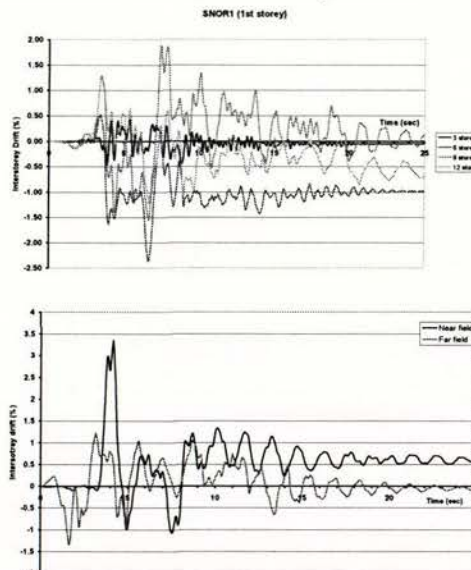


Figure 3 Comparison between localised storey performance (top) and results for near and far-field earthquakes (bottom).

2.5 Probabilistic assessment of drift demand variability

Because no common trend (in terms of the magnitude of the inter-storey drift) could be obtained from the response outcomes, the results were normalized so that all the various forms of earthquake motions had a common variable. First, the results were plotted with the maximum inter-storey drift for each structure height and earthquake versus an acceleration intensity measure $F_v S_1$ (the spectral acceleration at 1 second) as shown in Figure 4. Once plotted it was possible to determine the median values for the spread of results (line of best fit). It should be noted that for the three-storey structure the inter-storey drift was plotted against PGA rather than $F_v S_1$. This was because for low period structures (0.3 seconds in the case of the three storey structure) the amount of variability in the 1 second spectral acceleration is large, therefore more meaningful results were obtained if the three storey structures results were obtained when PGA was used as the intensity measure.

The variability of the data can be better understood by plotting the results in an alternative form. By assuming $b = 1$ in Equation (1), then rearranging gives

$$a = D' / S_a \quad (2)$$

in which a = drift index proportionality parameter.

If the data is ranked from smallest to largest and then plotted in the form of a cumulative distribution the median value (50th percentile) can be found. These results are plotted as data points in Figure 4 along with a continuous curve that is a best fit to a lognormal probability distribution. Only two parameters are needed to describe this distribution, the median (50th percentile), \tilde{a} , and the lognormal coefficient of variation, β (sometimes called the dispersion factor). From the plot it is evident that the results conform quite well to a cumulative lognormal probability distribution.

Individual results show values of $\beta = 0.60, 0.45, 0.40$ and 0.45 for the respective 3, 6, 9 and 12 storey buildings considered. These values of β agree well with the results of Lupoi et al (2002) whose β values ranged between 0.44 and 0.58. From the results, it is evident that to ensure a 90th percentile confidence interval, the observed drifts should be amplified by a factor of least 1.9 above their expected (median) values. It is therefore contended that for dependable seismic performance any experimental assessment of seismic capacity should have a factor of some two times the expected value of the drift demand.

The composite cumulative distribution has a median of $\tilde{a}=2.0$ and a dispersion factor of $\beta=0.52$. Interestingly, the value for β falls in midrange of the aforementioned findings of Lupoi et al (2002), presumably for a completely different suite of earthquake ground motions. Although the median line is plotted on the inter-storey drift versus $F_v S_1$ (or PGA) plot a more meaningful line is the 90th percentile value. This gives a dependable upper limit to the inter-storey drift for a given $F_v S_1$ (or PGA) there is a probability of 10% in exceeding this value. Figure 4 (b) shows that a 90th percentile value of 1.95 (times the median value) is obtained. These results justify the use of a 2.0 multiplier when assigning dependable (confidence) limits.

Once the 90th percentile lines have been generated for the overall response, it is then possible to determine the expected inter-storey drifts for the different height structures for both a 10% in 50 years, "Design Basis Earthquake" (DBE) and a 2% in 50 years, "Maximum Considered Earthquake" (MCE). The DBE is based on Wellington NZ conditions where there is a design PGA = 0.4g whereas the MCE has PGA = 0.72g (1.8xDBE). The multiplier of 1.8 used to convert a DBE to a MCE is determined from the relationship between the structural risk factor and the earthquake return period as set out in NZS4203:1992. Table 2 summarizes these results.

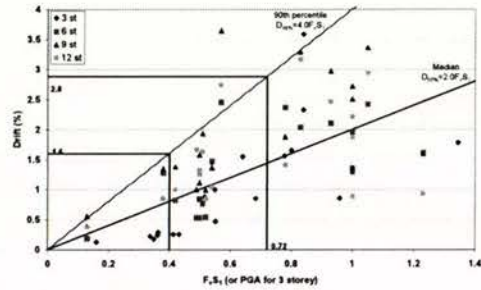
It is proposed that the drift index parameter, a , (from Equation (2)) should be taken as 2.5 and the DBE and MCE values are calculated as follows:

$$DBE \Rightarrow \tilde{D} = 2.5 \times 0.4 = 1.0\% \quad (3)$$

$$DBE \Rightarrow D_{90\%} = 2 \tilde{D} = 2 \times 1.0 = 2.0\% \quad (4)$$

$$MCE \Rightarrow D_{90\%} = 1.8 D_{90\%, DBE} = 1.8 \times 2.0 = 3.6\% \quad (5)$$

These values for the DBE and MCE have been added to Table 2 as the adopted nominal outcomes.



(a) Inter-storey drift based on applied $F_v S_1$ (and PGA)

(b) cumulative distribution as a function parameter "a"

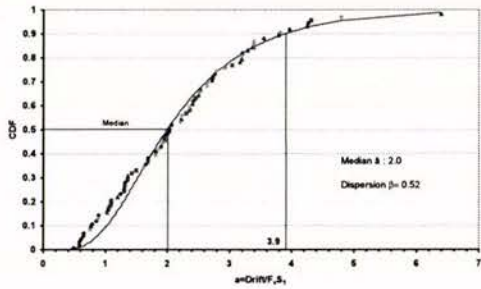


Figure 4. Combined results for the four different building heights examined

Table 2 The 90th percentile inter-storey drifts that correspond to a Design Basis Earthquake (DBE=10% in 50 years) and Maximum Considered Earthquake (MCE=2% in 50 years) for the various height structures

Number of Stories	DBE Drift	MCE Drift
3	1.4%	2.5%
6	1.5%	2.8%
9	2.1%	3.8%
12	1.9%	3.5%
Nominal Outcome	2.0%	3.6%

3 EXPERIMENTAL ASSESSMENT OF DRIFT CAPACITY

A full scale super-assembly experimental set-up was conceived and a new testing methodology developed to investigate the 3D seismic performance of precast concrete frames. The super-assembly specimen was a two-bay by one-bay section of a lower storey in a multi-storey precast concrete moment resisting frame. The floor units were pre-tensioned prestressed precast hollow-core units that were orientated so that they ran parallel with the long edge of the building, past a central column. The buildings origin along with the layout and dimensions are shown in Figure 5.

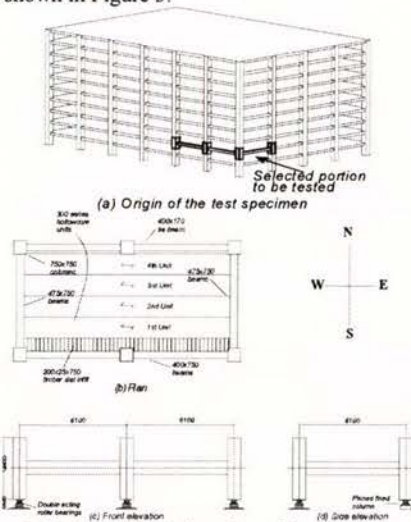
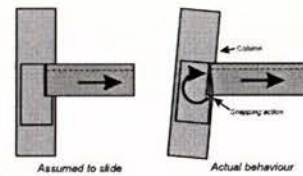


Figure 5 Origin, layout and dimensions of the super-assembly experiment.

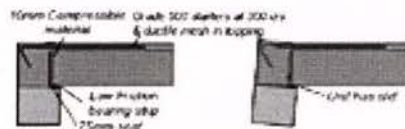
The super-assembly was tested in two stages as follows:

Stage 1: Matthews (2004) first tested the super-assembly specimen, emulating the 1980's and 1990's construction practice that has historically become the norm in NZ. The reinforcing details were in accordance with the current Standard, NZS3101 (1995). Although the perimeter moment resisting frame behaved well in the experiment, the overall performance of the precast, prestressed concrete hollow-core floor system was quite poor. Due to inadequate seating details, in particular, as well as displacement incompatibilities between the frame and floor, the Matthews (2004) experiment showed premature failure of the flooring system can be expected for design basis earthquakes in NZ. The *Stage 1* experiment demonstrated that the floor-to-beam seat connections of existing precast concrete construction are particularly vulnerable. As shown in Figure 6(a)

their behavior was quite different than what would be implicitly assumed by design. In the experiment, the floors failed and collapsed at drifts considered to be unacceptably low. The supporting frame, although damaged, remained in good condition and was repairable. Thus, at the conclusion of the *Stage 1* work completed by Matthews (2004) there were several areas highlighted for future research. These issues were addressed in *Stage 2* of the program by Lindsay (2004).



(a) Behavior assumed by design versus actual behavior of hollow core seats observed in the 1994 Northridge earthquake (Norton et al.; 1994) and laboratory experiments (Matthews; 2004)



(b) Modified connection detail tested by Lindsay (2004) and now recommended as one of two acceptable solutions by Amendment 3 to NZS3101 (1995).

Figure 6. Connection details of the precast concrete hollow-core units at their seats showing expected and observed performance.

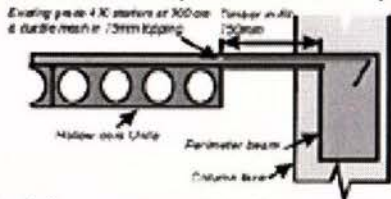
Stage 2: Lindsay (2004) repaired the damaged plastic hinge zones in the frame, and then reconstructed the floor by using modified seating details, these included the following three specific structural detailing aspects:

1. Improving the seating connection detail between the precast, prestressed hollow-core floor diaphragm and the perimeter reinforced concrete moment resisting frame (Figure 6b)
2. Stopping the central column from displacing laterally out of the building due to an insufficient lateral tie into the building. It was because of this lack of interconnection that the floor slab tore longitudinally due to displacement incompatibility in the Matthews test. The central column was therefore no longer restrained and was able to translate freely outwards
3. Isolating the first hollow-core unit spanning parallel with the perimeter beams from the frame due to displacement incompatibility. This displacement incompatibility was caused by the units being forced to displace in a double curvature manner due to being effectively connected to the

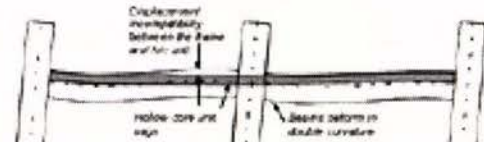
edge of the perimeter beam, when hollow-core units are not designed for such displacement profiles (Figure 7).

The seating connection between the hollow-core unit and the supporting beam consisted of replacing the plastic dam plug in the ends of the unit with 10mm of compressible material fully across the end of the unit and seating the unit on a low friction bearing strip. This detail is shown in Figure 6(b) along with how the floor unit is expected to rotate relative to the beam. The low friction bearing strip allows the floor unit to slide as designers had previously assumed it would. The compressible material is assumed to reduce the compression forces applied at the bottom of the unit under negative moments as well as restricting concrete from entering the cores of the units. If the large compression force forms between the bottom of the unit and the face of the supporting beam it is transferred at a relatively flat angle to the topping concrete. A perpendicular principal tensile force then forms, causing splitting of the webs at very early stages of the test.

The lateral connection to the perimeter frame consisted of moving the first unit away from the perimeter beam and replacing it with a 750mm timber infill with 75mm in-situ concrete topping (Figure 7(a)). The infill allows a more flexible interface between the frame and southern hollow-core unit. Some cracking is expected in this interface due to the displacement incompatibility but it is anticipated that the more flexible interface will accommodate this while allowing the beam to deform in double curvature and the hollow-core unit in single curvature, (Figure 7(b)) leaving the floor essentially undamaged. Ductile reinforcing mesh was used in the topping to aid in the performance of the floor by helping to ensure that any damage and cracking would not result in such an early failure of the floor system.



(a) First hollow-core unit to perimeter frame connection.



(b) Expected displacement incompatibility between the hollow-core floor units and the perimeter frame.

Figure 7. Accommodation of the displacement incompatibilities between the perimeter frame and the precast concrete floor system.

3.1 Classification of observed building damage

A common form of damage classification is to use a numerical indicator format as adopted by HAZUS (1999). A number between one and five that also refers to the level of damage is used, as given in Table 3.

Table 3 Definition of the damage states used to classify the level of damage to a structure following an earthquake (Mander, 2003)

Damage State	Damage Descriptor	Post-earthquake Utility of Structure
1	None (pre-yield)	Normal
2	Minor/Slight	Slight Damage
3	Moderate	Repairable damage
4	Major/Extensive	Irreparable damage
5	Complete collapse	Irreparable damage

Following the completion of the experimental testing program it was possible to classify the super-assembly according to the two classification methods. Based on the two experiments, and related back to past (pre-2004) and current (post-2004) code requirements (Amendment 3 to NZS3101,1995) the results are summarized in Table 4. It should be noted that since the classification of performance between the reinforced concrete moment resisting frame and the hollow-core floor slab was so different, the two components were classified separately.

A marked difference in performance between the reinforced concrete moment resisting frame and the precast hollow-core floor slabs is evident in Table 4. If the global classification of the structure were required, then the floor performance values would be stated, as these are critical to the overall structure. In summary, Table 4 gives drift limit states based on post-earthquake utility and life-safety considerations, respectively. In now remains to balance these capacity limits with the seismic demands placed on the structure. The approach to this is described in what follows.

Table 4 Damage state classification for the super-assembly

Damage State	Inter-storey drift based on:		
	Historical [@] floor detailing practice	Modern [#] detailing practice for floors and their connections	Historical [@] and current [#] frame detailing practice
2	0.3%	1%	1%
3	0.35%	2%	2%
4	1.9%	4%	4%
5	2.5%	-	-

[@] 1985-2003 details to NZS3101

[#] 2004 Amendment 3 to NZS3101-1995

4 BALANCING CAPACITY VERSUS DEMAND: A FRAGILITY APPROACH

In the analysis of drift demand, described above, it was demonstrated that the distribution of drift outcomes was lognormal with a lognormal coefficient of variation of $\beta_D = 0.52$ (note the subscript D stands for demand).

By adopting the aforementioned value of $\bar{a} = 2.0$ in equation 1, and then inverting, the expected value (median or 50th percentile) of the ground motion demand needed to achieve a given median drift capacity can be found such that

$$\tilde{F}_v S_1 = 0.5 \tilde{D}_c \quad (8)$$

$$P\tilde{G}A = 0.5 \tilde{D}_c \quad (9)$$

where \tilde{D}_c = expected drift capacity of the structure.

Now the capacity parameter \tilde{D}_c is not precisely known, but assuming that the full-scale experiments provide a reliable indicator of the expected drift capacities, and assuming these capacities themselves have a coefficient of variation of $\beta_C = 0.2$ (this is in keeping with the findings from Dutta (1999)), Kennedy et al (1980) have shown that the composite value of the lognormal distribution is found by

$$\beta_{C/D} = \sqrt{\beta_C^2 + \beta_D^2 + \beta_U^2} \quad (10)$$

in which β_C and β_D are as defined above, and β_U is a lognormal dispersion parameter for modelling uncertainty. The latter parameter has been taken as $\beta_U = 0.2$.

Using this data it follows from equation (10) that $\beta_{C/D} = 0.60$. This value is in keeping with results inferred from observed damage to bridge structures in the 1994 Northridge earthquake (Mander and Basöz, 1999).

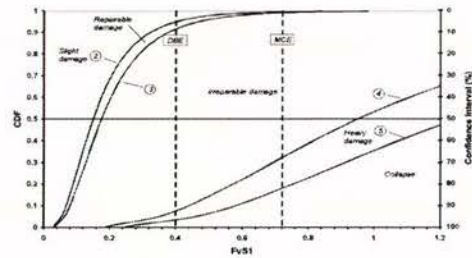
By using a lognormal cumulative distribution that can be described by a unit lognormal variate ξ_β (where the median = 1 and lognormal coefficient of variation $\beta_{C/D} = 0.60$), the distribution of ground motion demands necessary to produce a given damage state outcome can be found by

$$F_v S_1 = 0.5 \tilde{D}_c (DS) \xi_\beta \quad (11)$$

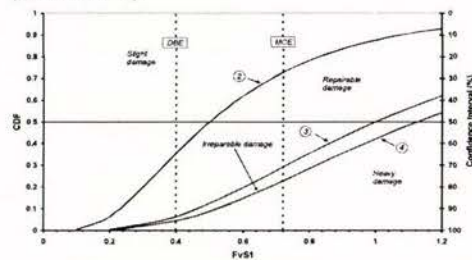
$$P\tilde{G}A = 0.5 \tilde{D}_c (DS) \xi_\beta \quad (12)$$

Figure 8 shows the fragility curves for the rating of the floor and frame performance in terms of different numerical damage states. Figure 8(a) shows that for a MCE if the structures performance is clas-

sified in terms of the precast hollow-core floor performance due to the use of historic reinforcing details (1985 to 2003) then 2% of structures would be expected to sustain slight or repairable damage. The remaining 98% of structures would be expected to be demolished as a result of irreparable damage or collapse, of these some 32% of floors would be expected to partially or entirely collapse leading to loss of life. Under a DBE, 92% of structures would sustain excessive damage, with some 8% potentially leading to loss of life. Ironically, some engineers may consider this to be a satisfactory outcome as there is more than 90 percent confidence that loss of life will not occur. However, given that the vast majority of the buildings would be unsafe and need demolishing, this is felt to be unsatisfactory, let alone considering that nearly 10% of structures could collapse, leading to loss of life. Figure 8(b) shows that for a MCE if the structures performance is classified in terms of the frame performance (rather than the floor) then 93% of structures might be expected to sustain damage that is either slight or repairable; only 7% of structures would be expected to require demolition.



(a) Precast concrete buildings with vulnerable precast concrete hollow-core floors built to pre-2004 Standards (NZS3101, 1995)



(b) Concrete buildings built to post-2004 Standards (NZS3101, 1995, Amendment 3)

Figure 8 Fragility curves for New Zealand concrete buildings rated to the HAZUS damage states.

5 CONCLUSIONS

Based on the research described herein, the following conclusions are drawn:

1. For a Design Basis Earthquake (10% in 50 years) structures may be permitted to be designed for a 2.0% inter-storey drift limit. But due to conservatively defined material properties and in-built over-strength, the median (50 percentile) seismic drift demand will be in the order of only 1.0%. However, there is a wide range of possible results, and to be 90 percent confident that all possibilities are captured, a demand drift of 2.0% is realistic. This means that for a Maximum Considered Earthquake of 2% in 50 years (approximately 2500 year return period) and a 90% confidence interval the drift demand is 3.6%.
2. Experiments have shown that precast concrete structures with hollow core floor systems built to pre-2004 Standards possess inadequate capacity to sustain the expected seismic demands. Incipient collapse can occur at drifts in the order of 1.9%.
3. For multi-storey structures with hollow-core floors detailed to pre-2004 Standards significant collapses may be expected for a 2% in 50 years (MCE) event in Wellington, NZ. Under a 10% in 50 year (DBE) event, the situation is also not favourable; some 90% of buildings might be expected to be demolished including 8% that could potentially cause loss of life through collapse.
4. For multi-storey structures with hollow-core floors detailed to post-2004 Standards the number of buildings that would require demolition following a maximum considered earthquake (MCE) for Wellington would be low. This outcome is in keeping with the expectations of capacity design.

ACKNOWLEDGEMENTS

This project would not be possible without the support from the following organizations: University of Canterbury, Earthquake Commission, Cement and Concrete Association of New Zealand, BRANZ, Foundation for Research Science and Technology – Tūāpapa Pūtaiao Maori Fellowships, C. Lund & Son Ltd, Firth Industries Ltd, Stresscrete, Pacific Steel, Stahlton Prestressed Flooring, Construction Techniques, Precast Components, The Maori Education Trust, Fulton Hogan Ltd, Holmes Consulting Group, Hylton Parker Fasteners and Hilti (NZ) Ltd.

REFERENCES

- Cornell C.A, Jalayer F, Hamburger R.O and Foutch D.A, 2002, *Probabilistic Basis for 2000 SAC Federal Emergency Management Agency Steel Moment Frame Guidelines*, ASCE Journal of Structural Engineering, April, pp 526-533
- Dutta A, 1999, *On Energy-Based Seismic Analysis and Design of Highway Bridges*, Ph.D Dissertation, science and Engineering Library, State university of New York at Buffalo, Buffalo, NY
- HAZUS. 1999. *Earthquake Loss Estimation Methodology*. Technical Manual. Prepared by the National Institute of Building Sciences for Federal Emergency Management Agency, Washington, DC.
- Kennedy R.P, Cornell, C.A, Campbell R.D, Kaplan, S and Perla H.F, 1980, *Probabilistic Seismic Safety Study of an Existing Nuclear Power Plant*, Nuclear Engineering and Design No. 59, pp 315-338
- Lee K and Foutch D.A, 2002, Seismic Performance Evaluation of Pre-Northridge Steel Frame Buildings with Brittle Connections, ASCE Journal of Structural Engineering, April, pp 546-555
- Lindsay, R., 2004, "Experiments on the seismic performance of hollow-core floor systems in precast concrete buildings", ME Thesis, University of Canterbury, Christchurch, New Zealand.
- Luco N and Cornell C.A, 2000, Effects of Connection Fractures on SMRF Seismic Drift Demands, ASCE Journal of Structural Engineering, January, pp 127-136
- Lupoi G, Lupoi A and Pinto P.E, 2002, *Seismic Risk Assessment of RC Structures with the "2000 SAC/FEMA" Method*, Journal of Earthquake Engineering, Vol. 6, No 4, pp 499-512
- Mander J.B and Basöz N, 1999, *Seismic fragility curve theory for highway bridges in transportation lifeline loss estimation in Optimising Post-Earthquake Lifeline System Reliability*, TCLEE Monograph No. 16 Eds Elliot and McDonough
- Matthews J.G. 2004, "Hollow-core floor slab performance following a severe earthquake." Ph.D Thesis, University of Canterbury, Christchurch, New Zealand.
- NZS3101:1995, *Concrete Structures Standard-The Design of Concrete Structures*, Standards New Zealand, Wellington New Zealand
- NZS3101: 2004, *Amendment 3 to NZS3101:1995*, Standards New Zealand, Wellington, New Zealand
- Norton, J.A, King, A.B, Bull, D.K, Chapman, H.E, McVerry, G.H, Larkin, T.J, Spring, K.C, 1994, *Northridge Earthquake Reconnaissance Report*, Bulletin of the New Zealand National Society for Earthquake Engineering Vol. 27, No.4, December